

**Reactivity of Cationic (π -allyl)Pd(II) Complexes
with Olefins and Dienes**

Stephanie A. Urbin

A dissertation submitted to the faculty of the University of North Carolina at Chapel Hill
in partial fulfillment of the requirements for the degree of Doctor of Philosophy in the
Department of Chemistry

Chapel Hill
2009

Approved by:

Advisor: Professor M. Brookhart

Reader: Professor J. L. Templeton

Reader: Professor C. K. Schauer

Professor M. D. E. Forbes

Professor W. Lin

© 2009
Stephanie A. Urbin
ALL RIGHTS RESERVED

ABSTRACT

STEPHANIE A. URBIN: Reactivity of Cationic (π -allyl)Palladium(II) Complexes with Olefins and Dienes.

(Under the direction of Professor Maurice Brookhart)

The use of transition metal catalysts for 1,3-diene polymerization is desirable due to the ability to control the microstructure, polydispersity, and molecular weight of the resulting polymer by easily tuning the ligand and metal used. Previously, progress has been made through the development of highly active, nickel(II) “ligand-free” catalysts for 1,3-diene polymerizations, which has also provided significant insight into the mechanism for these reactions. While highly active, these catalysts are relatively unstable and difficult to generate, and hence development of stable, initiator-free complexes is desirable. This dissertation focuses on the synthesis of (allyl)Pd(II) catalysts and their reactivity with olefins and 1,3-dienes. Particular attention is given towards the observation and, in some cases, isolation of intermediates for the mechanism of 1,3-diene polymerizations.

Chapter 2 describes the successful synthesis of [(allyl)Pd(arene)][SbF₆] complexes with highly labile arene ligands. The reactivity of these complexes with α -olefins and alkynes results in formation of bis-olefin and bis-alkyne Pd(II) species at low temperatures and is thoroughly discussed. A comparison of the reactivity of these Pd(II) complexes with the analogous [(allyl)Ni(arene)][B(Ar_F)₄] complexes is a feature of this work.

Chapter 3 presents the reactivity of the [(allyl)Pd(arene)][SbF₆] complexes with a variety of dienes. For the first time, a diene complex exhibiting an *s-trans*- η^4 -binding mode to a d⁸ metal center has been synthesized and characterized. Additionally, a variety of [(allyl)Pd(η^4 -diene)]⁺ species have been spectroscopically observed at low temperatures. This chapter also focuses on the direct observation of insertion intermediates as models for the polymerization of 1,3-butadiene, including an η^3, η^2 -wrap-around species.

Chapter 4 describes the synthesis of stable η^3, η^2 -wrap-around complexes as models for the first insertion product in the polymerization of 1,3-dienes. The binding affinity of the η^2 -olefin can be quantitatively measured and controlled by tuning different electronic factors of the wrap-around complexes. Furthermore, reactions of the Pd(II) wrap-around complexes with 1,3-dienes were explored with the goal of gaining further insight into the chain transfer and polymerization mechanism for (allyl)Pd(II) complexes.

ACKNOWLEDGEMENTS

First and foremost, I have to thank my advisor Brook for all of his guidance and support over the past five years. I will fondly remember our time together, looking over vast amounts of NMR spectra and going over kinetics. I am eternally grateful for everything I've learned from you in and out of the lab, and feel so fortunate to have been able to complete my graduate degree under such a well-balanced and talented individual. Additionally, thank you so much for helping me with my job search, and I am very excited to start working at Proctor & Gamble.¹ I am honored to be one of your last graduate students.

This dissertation, and really all of the work we graduate students accomplish in our time here at UNC-CH, would not be possible without the superb support of our wonderful faculty and staff. I am particularly fortunate that my committee members were very much a part of my life and graduate work, from taking classes to teaching classes to helping run conferences. Many thanks to Joe Templeton, Cindy Schauer, Wenbin Lin, and particularly to Malcolm Forbes for providing me with a “well-rounded” education.² I also owe a great deal to Dave Harris and Marc ter Horst in the NMR facility, who have patiently helped me with many NMR studies and often provided me with a great deal of entertainment while I was collecting spectra. Again, getting all my research results would not be possible without the efforts of Peter White and Matt Crowe, who always provided assistance with a smile. I would also like to thank Ann Jeremiah, because

without her superb efforts as our administrative assistant, I sincerely doubt our group would function as efficiently as it does. Additionally, all of the staff who seldom get mentioned, including Paul Tulowiecki, Walt Boger, Peaches, John Beres, Harlan Mangum, Karen Gilliam, Lars Sahl, Student Service members, and others, are a very integral part to our department functioning like a well-oiled machine, and I greatly appreciate their efforts to support our research.

Easily the best part about joining the Brookhart Lab was the group of people I have had the great fortune to work with. A big shout-out goes to some former group members, Abby O'Connor,³ Tomislav Pintauer, Alison Sykes, Mark Doherty, Emily Carson, Amy Roy MacArthur,⁴ and Jian Yang, all of whose scientific expertise has helped me immensely and whose sense of humor has made our lab such a great environment to work in. I feel very fortunate to have Zheng Huang as my fellow last-Brookhart-graduate-student, as he always has a kind word and warm smile to offer, particularly when writing our dissertations. As our lab has dwindled down in numbers, we have managed to procure three excellent post-docs, Marc Walter, Wes Bernskoetter, and Michael Findlater, who really keep our lab going strong and all of whom I respect and admire greatly. I especially thank Marc,⁵ who is not only a great asset to this lab with his wide and versatile knowledge, but also is a wonderful friend willing to help out in the toughest of times (this has meant a great deal to me). Many thanks to Wes for being a fantastic desk-mate, and I really value all of our random, hilarious conversations, some of which were actually very useful! Thanks also to Michael for being himself; I really can think of no better (or appropriate) way to describe this, but trust me, it is a very big compliment.⁶ Of course, the Brookhart group couldn't be complete without our

counterparts, the Templeton group, which, when combined, form “The Brookleton Force” or “The Templehart Bears”. Thanks especially to Templetonians Andrew Garrett, Andy Jackson, Margaret MacDonald, Chetna Khosla, Bryan Frauhiger, and Ned West for making the 4th floor a fun and exciting place to work.

One of the best parts of grad school in Chapel Hill is that you get to meet some really fantastic people, and I feel so fortunate to have made the friends I have in my time here. A good deal of gratitude goes to one of my closest friends, Andy Satterfield, who has a huge heart and always makes me laugh. And thanks especially to Alessandra Ferzoco, who not only has been a brilliant friend and running partner, but also spent many countless hours in coffee shops with me writing; I seriously doubt my dissertation would have been finished on time without having someone to commiserate with. To all my soccer peeps (UNC Rams ladies (and Chris and Lars), Pioneers ladies, and Milltown guys); I’m so glad to have such a great group of people to play soccer and hang out with as it is always nice to have a life outside of the chemistry lab. To so many others, thank you for all the memorable times and experiences, which I wish I could recount but will not do so here due to the large number and hilarious⁷ nature of said times. Instead, I will just say thanks to Becky (Wolfe) Stiles, Cory Bausch, Frank Sun, Ben Harrison, Liz Austin, Abby O’Connor, Matt Crowe, Pete Coneski, Julie Sullivan, and Rachel Lieberman, who have all been wonderfully entertaining and great friends over the years.

Finally, and most importantly, I would like to thank my family. My mom and dad have been so supportive of me and have always encouraged me to pursue my dreams. All of this they have done while providing me with everything I could possibly need throughout my life, including a good “work ethic.”⁸ They’ve helped me through so many

situations⁹ and I am so fortunate to have such marvelous role models as parents. My favorite sister and best friend, Stacey, is such an important influence on my life, and I don't think we could be closer unless we were twins. True, our similar mannerisms sometimes¹⁰ freak people out, but we treasure and celebrate them. Anyway, countless thanks go to Stacey for always being there for me and for being an awesome sister in general, as the specifics would take much too long to acknowledge. I would be remiss without mentioning my cat Hailey, aka "little muffin," as this white furball has often been a great comfort. Last, but certainly not least, I owe a great deal of appreciation to my fiancé, Travis Falconer, for all of his love and support.¹¹ I could not imagine or hope for a better person to share my life with, and am very much looking forward to our future together.

¹Buy Tide, it's the best detergent ever!!

²<smile>

³The "Golden Child!"

⁴Poor you! –Amy's favorite saying.

⁵AKA the German Robot.

⁶By the way, I'd like to apologize for saying that your Mom's name was Cabertoss. Honest mistake. P.S. You rock at chemistry, despite your love of group 13!

⁷And definitely inappropriate.

⁸Because no one considers stacking cut wood a fun Saturday activity; I'm looking at you, Dad.

⁹Especially Mom, although I'm still not sure that laughing at me and my predicaments is helping... but at least after the laughter comes a lot of good advice. ☺

¹⁰Always.

¹¹And for putting up with me while I was writing; this was no easy task!

TABLE OF CONTENTS

	Page
LIST OF TABLES.....	xiii
LIST OF SCHEMES.....	xiv
LIST OF FIGURES.....	xvi
LIST OF ABBREVIATIONS AND SYMBOLS.....	xviii
 Chapter	
I. 1,3-Diene Polymerizations Catalyzed by Transition Metal Complexes.....	1
A) Methods of Production of Poly-1,3-Dienes.....	2
B) Mechanism of 1,3-Diene Polymerization by (Allyl) Transition Metal Catalysts.....	3
C) Nickel(II) Catalyzed Polymerization of 1,3-Dienes.....	5
D) Research Goals and Achievements.....	8
E) References.....	11
II. Synthesis and Reactivity of (Allyl)Nickel(Arene) ⁺ and (Allyl)Palladium(Arene) ⁺ Complexes with Olefins and Alkynes.....	13
A) Introduction.....	13
B) Results and Discussion.....	15
1) Synthesis of (2-R-Allyl)M(Arene) ⁺ Salts.....	15
2) Ligand Substitution Reactions of (Allyl)Pd(Arene) ⁺ Complexes.....	19
(a) Reactions with Diethyl Ether.....	19

(b) Exchange Reaction with Free Mesitylene.....	19
(c) Reactions with Olefins and Alkynes.....	20
3) Reactions of (Allyl)Ni(Arene) ⁺ Complexes.....	28
(a) Reactions with Diethyl Ether.....	28
(b) Arene Exchange Reactions.....	29
(c) Reactions with Olefins.....	29
4) Mechanism of Hydrogen Transfer.....	32
C) Conclusions.....	34
D) Experimental Section.....	35
1) General Considerations.....	35
2) Materials.....	36
3) General Procedure for the Synthesis of [(Allyl)Pd(Arene)][SbF ₆] Complexes.....	37
4) Synthesis of (Allyl)Pd(II) Bis-Olefin Complexes.....	39
5) Dynamic Measurements using ¹ H Line Broadening.....	46
6) Synthesis of (2-R-Allyl)Ni(Arene) ⁺ Complexes.....	49
7) Reaction of Olefins with Complexes 5 or 6	52
8) Crystal Structure Determination of 5 and 7	54
E) References.....	55
III. Reactivity of [(Allyl)Palladium(Arene)] ⁺ Complexes with Dienes.....	57
A) Introduction.....	57
B) Results and Discussion.....	59
1) Synthesis of [(cyclohexenyl)Pd(arene)][SbF ₆], 4	59

2) <i>In Situ</i> Generation of [(allyl)Pd(<i>s-trans</i> - η^4 -2,3-dimethyl-1,3-butadiene)][SbF ₆], and [(2-methallyl)Pd(<i>s-trans</i> - η^4 -2,3-dimethyl-1,3-butadiene)][SbF ₆]	60
3) Isolation and Independent Synthesis of <i>s-trans</i> [(allyl)Pd(η^4 -DMBD)][SbF ₆] and <i>s-trans</i> [(2-methallyl)Pd(η^4 -DMBD)][SbF ₆]	63
4) <i>In Situ</i> Generation of s-cis/s-trans-6-Cl with Isoprene	65
5) <i>In Situ</i> Generation of 7-H and 7-Cl with 1,3-Butadiene	67
6) <i>In Situ</i> Reaction of 3-H with Cyclohexa-1,3-diene to Form a <i>s-cis</i> η^4 -bound Diene Complex	70
7) <i>In Situ</i> Reactivity of 3-H with Cyclopentadiene	72
8) <i>In Situ</i> Reactions of 3-H and 3-Me with Hexa-1,5-diene	76
9) Synthesis of [(allyl)Pd(η^4 -hexa-1,5-diene)][SbF ₆] and [(2-methallyl)Pd(η^4 -hexa-1,5-diene)][SbF ₆]	76
C) Summary	77
D) Experimental Section	79
1) General Considerations	79
2) Materials	79
E) References	94
IV. Synthesis, Characterization, and Reactivity of (π -Allyl)Palladium(II) Wrap-Around Complexes with 1,3-Dienes	97
A) Introduction	97
B) Results and Discussion	100
1) Synthesis of Wrap-Around Complexes	100
2) Determination of Olefin Binding Affinities by Reaction of Wrap-Around Complexes with Nitriles	104
3) Polymerization of Isoprene and Butadiene by Wrap-Around Catalysts	111

4) Chain Transfer with Wrap-Around Catalysts.....	112
C) Summary.....	115
D) Experimental Section.....	116
1) General Considerations.....	116
2) Materials.....	116
3) (Allyl)Pd(II) Complex Synthesis.....	117
4) Characterization of the Organic Chain Transfer Product.....	122
5) Polymerization Procedures.....	125
6) General Procedure for Titration Experiments.....	125
E) References and Notes.....	127
APPENDIX I.....	129
APPENDIX II.....	143

LIST OF TABLES

Table 4.1	Equilibrium constants for titration of wrap-around complexes with 3,5-bis(trifluoromethyl)benzonitrile.....	110
Table 4.2	Influence of [BD] on the rate of chain transfer.....	114
Table I.1	X-Ray crystallographic data for complexes 7-H and 8-Me	131
Table I.2	Selected bond lengths (Å) for complex 7-H	131
Table I.3	Selected bond angles (°) for complex 7-H	134
Table I.4	Selected bond lengths (Å) for complex 8-Me	138
Table I.5	Selected bond angles (°) for complex 8-Me	140
Table II.1	X-ray crystallographic data for complexes 1a and 2a	143
Table II.2	Selected bond lengths (Å) and angles (°) for complex 1a	144
Table II.3	Selected bond lengths (Å) and angles (°) for complex 2a	146

LIST OF SCHEMES

Scheme 1.1	Highly active (allyl)Ni(II) catalysts for 1,3-diene polymerization.....	6
Scheme 1.2	Generation of [(allyl)Ni(arene)] ⁺ species <i>in situ</i> and further reactivity with 1,3-butadiene.....	7
Scheme 1.3	Cationic palladium(II) wrap-around complex.....	9
Scheme 2.1	Active 1,3-diene polymerization catalysts.....	15
Scheme 2.2	Synthesis of (allyl)M(arene) ⁺ complexes.....	17
Scheme 2.3	Formation of Pd(II) bis-ethylene adducts 10-H and 10-Cl	22
Scheme 2.4	Synthesis of (2-R-allyl)Pd(cyclopentene) ₂ ⁺ adducts, 12-H and 12-Cl , at low temperature.....	25
Scheme 2.5	Synthesis of Pd(II) bis-alkyne complexes 15-H and 15-Cl and Pd(II) mixed ligand complexes 16-H and 16-Cl	27
Scheme 2.6	Reaction of complexes 7-H and 7-Me with 1-hexene at room temperature.....	30
Scheme 2.7	Intramolecular hydrogen atom transfer with complex 7-H and 1-octene.....	32
Scheme 2.8	Proposed mechanism of hydrogen atom transfer in the reaction of 1-hexene with (allyl)Ni(mes) ⁺ complexes.....	33
Scheme 3.1	<i>In situ</i> generation of (cyclohexenyl)Ni(η ⁴ -dimethylbutadiene) ⁺	58
Scheme 3.2	Typical coordination modes observed for mononuclear η ⁴ -1,3-diene complexes.....	59
Scheme 3.3	Cationic Pd(arene) complexes.....	60
Scheme 3.4	<i>In situ</i> generation of s-trans-5-H	61
Scheme 3.5	Possible isomers for the η ⁴ -coordination of DMBD to palladium(II).....	62
Scheme 3.6	Synthetic routes to obtain s-trans-5-H and s-trans-5-Me	64
Scheme 3.7	Generation of several η ⁴ -diene isomer adducts.....	65
Scheme 3.8	Reactivity of 3-H and 3-Cl with 1,3-butadiene.....	68

Scheme 3.9	Formation of the η^3, η^2 -wrap-around complex 8-Cl <i>in situ</i>	69
Scheme 3.10	Trapping with PPh ₃ to form 9-Cl , a known complex.....	70
Scheme 3.11	Generation of 10-H	71
Scheme 3.12	Generation of [(allyl)Pd(η^4 -cyclopentadiene)] ⁺ , 11-H	72
Scheme 3.13	Reaction with dicyclopentadiene to form a mononuclear and dinuclear species.....	73
Scheme 3.14	Possible isomers for the dinuclear species 13-H	75
Scheme 3.15	Reactivity with hexa-1,5-diene.....	76
Scheme 4.1	Insertion of 1,3-butadiene into allyl moiety of Pd(II) halide dimer.....	98
Scheme 4.2	Known wrap-around complexes.....	98
Scheme 4.3	Displacement of η^2 -olefin chelate by nitrile.....	99
Scheme 4.4	General synthetic route for Pd(II) wrap-around complexes.....	100
Scheme 4.5	Wrap-around Pd(II) complexes prepared.....	101
Scheme 4.6	Titration of wrap-around complexes with nitrile.....	104
Scheme 4.7	Wrap-around equilibrium with 3,5-bis(trifluoromethyl)benzonitrile.....	110
Scheme 4.8	Chain transfer and trapping of the new Pd(II) complex.....	113

LIST OF FIGURES

Figure 1.1	Enchainment modes for poly-1,3-dienes.....	2
Figure 1.2	Structurally different coordination modes of butadiene to the metal M and their respective nomenclature.....	4
Figure 1.3	Different configurations of the substituted allyl (R = organic group, e.g. the growing polymer chain) via <i>syn-anti</i> isomerization.....	4
Figure 2.1	ORTEP diagram of (allyl)Ni(mes) ⁺ , 7-H	18
Figure 2.2	ORTEP diagram of (2-methallyl)Ni(hmb) ⁺ , 8-Me	18
Figure 2.3	Variable temperature ¹ H NMR overlay of the addition of 4 equiv mesitylene to 5-H	20
Figure 2.4	¹ H NMR variable temperature overlay showing the formation of (2-Cl-allyl)Pd(ethylene) ₂ ⁺ , 10-Cl , and exchange with free ethylene at higher temperatures.....	22
Figure 2.5	¹ H NMR overlay showing the formation of (2-Cl-allyl)Pd(cyclopentene) ₂ ⁺ , 12-Cl , and exchange with free cyclopentene at higher temperatures in CD ₂ Cl ₂	25
Figure 3.1	Variable temperature ¹ H NMR spectra of the <i>in situ</i> reaction of DMBD with [(allyl)Pd(mes)][SbF ₆], 3-H , to form the <i>s-trans</i> [(allyl)Pd(η ⁴ -DMBD)][SbF ₆] species s-trans-5-H	62
Figure 3.2	Room temperature ¹ H NMR spectrum of wrap-around complex 8-Cl generated <i>in situ</i> in CD ₂ Cl ₂	69
Figure 3.3	¹ H NMR spectrum of the <i>in situ</i> reaction of 1,3-cyclohexadiene with [(allyl)Pd(mes)][SbF ₆], 3-H , to form the <i>s-cis</i> [(allyl)Pd(η ⁴ -CHD)][SbF ₆] species 10-H at -100 °C in CDCl ₂ F.....	71
Figure 3.4	Room temperature ¹ H NMR spectrum of the reaction of [(allyl)Pd(mes)][SbF ₆] 3-H with one equivalent of dicyclopentadiene in CD ₂ Cl ₂	74
Figure 4.1	ORTEP diagram of 1a	102
Figure 4.2	ORTEP diagram of 2a	102
Figure 4.3	Sample ¹ H NMR spectra of several <i>syn</i> wrap-around complexes.....	103

Figure 4.4	Titration of wrap-around complexes with nitrile.....	106
Figure 4.5	Variable temperature ^{31}P NMR spectra of 3a with five equivalents of benzonitrile in CD_2Cl_2	108
Figure 4.6	Kinetic plot of disappearance of the wrap-around complex 1b over time upon addition of 10 equivalents of 1,3-butadiene.....	114

LIST OF ABBREVIATIONS AND SYMBOLS

δ	chemical shift
Å	angstroms
ΔG	change in Gibbs' free energy
°C	degrees Celsius
‡	denotes transition state
ω	spectral linewidth
Ar	aryl
Ar _F	3,5-(CF ₃) ₂ C ₆ H ₃
BD	butadiene
br	broad
COSY	correlated spectroscopy
d	doublet
DFT	density functional theory
DMBD	2,3-dimethyl-1,3-butadiene
equiv	equivalents
g	grams
GPC	gel permeation chromatography
h	hours
Hz	hertz
hmb	hexamethyl benzene
HMQC	heteronuclear multiple quantum coherence
IP	isoprene

J	scalar coupling constant, in Hz
K	Kelvin (in NMR data)
K	equilibrium constant
k	rate constant
k_p	rate constant for chain propagation
k_{ct}	rate constant for chain transfer
kcal	kilocalorie
L	ligand
M	molar
m	multiplet
m	meta
Me	methyl, -CH ₃
Mes	mesitylene
MHz	megahertz
min	minutes
mL	milliliters
M_n	number average molecular weight
mmol	millimole
mol	moles
M_w	weight average molecular weight
NMR	nuclear magnetic resonance
o	ortho
p	para

PBD	polybutadiene
PDI	polydispersity index, M_w/M_n
ppm	parts per million
q	quartet
RT	room temperature
s	seconds
s	singlet (in NMR data)
solv	solvent
t	triplet
T_g	glass transition temperature
VT	variable temperature

CHAPTER ONE

1,3-Diene Polymerizations Catalyzed by Transition Metal Complexes

Introduction and Background

Introduction

Polybutadiene is a material that has a wide range of applications from elastic rubber tires to hard coatings for golf balls.¹ Each year, over two million metric tons of polybutadiene are consumed worldwide. Butadiene is typically copolymerized with styrene in a 3:1 ratio to produce polybutadiene-polystyrene rubber (SBR), which is also used in the production of car tires.² Other noteworthy polymers of 1,3-dienes that are produced on a large scale include polyisoprene, poly-2,3-dimethyl-1,3-butadiene, and polychloroprene.³ Polychloroprene is a commodity polymer, commonly known as Neoprene (DuPont), and is used in the production of wet suits, laptop sleeves, and car fan belts. Polyisoprene is similar to polybutadiene, and is used in the production of erasers, rubber bands, and adhesives.⁴

The properties of polybutadiene depend greatly upon the microstructure of the polymer backbone. Monomer enchainments can range from highly *cis*-1,4, producing elastic and rubbery materials, to highly *trans*-1,4, producing hard and brittle materials. 1,2 and 3,4, for substituted diene enchainments, give rise to chiral polymers with unsaturated vinyl groups (Figure 1.1).^{1,5} The most industrially relevant of these

microstructures are the *cis*-1,4 enchainment polydienes (*cis*-polybutadiene and *cis*-polyisoprene) since these natural-rubberlike polymers constitute the largest portion of commodity polydienes. In particular, over 70% of polybutadiene produced is used in the manufacture of car tires.³

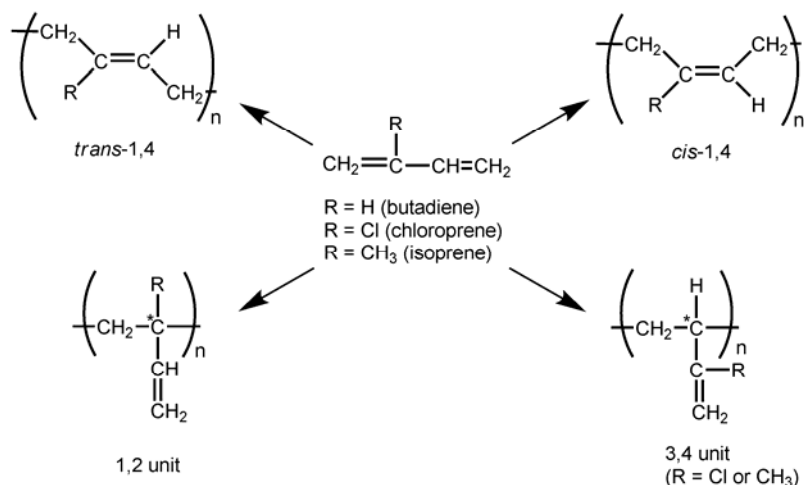


Figure 1.1. Enchainment modes for poly-1,3-dienes.

Methods of Production of Poly-1,3-Dienes

Radical, anionic, and transition metal complex-mediated methods are used for inducing polymerization of butadiene. Each gives polymers with different microstructures and thus different physical properties. Radical polymerization of butadiene yields amorphous, highly branched polymers.⁶ Anionic butadiene polymerization can yield random *cis/trans* mixtures or, when in the presence of coordinating Lewis bases, up to 92% vinyl 1,2-polymer.⁶ Transition metal-mediated polymerizations of 1,3-butadiene are the most successful methods for the production of highly *cis*-1,4-enchainment polymer. In the late 1950's, Ziegler and coworkers⁷ and Natta and coworkers^{8,9} employed TiCl₄/AlR₃ systems for polymerization of ethylene. Shortly

following this work, Ti,¹⁰ Co,¹¹ and Ni¹² complexes were discovered that yielded up to 94% 1,4-*cis*-enchained polybutadiene. These Ziegler-Natta type catalysts are very active and are still widely used for the industrial production of highly *cis*-enchained polybutadiene.

While the Ziegler-Natta catalysts are highly active for production of 1,4-*cis*-polybutadiene, there are several limitations for these systems. The molecular weight distributions and composition distributions of the resulting polymers are broad (PDI 3-4), due to incomplete activation of the catalyst and the presence of multiple catalytically active sites.¹ This results in poor control of the polymerization process. Well-defined, homogeneous, single-site catalysts offer more precise control over polymer properties. In addition, these systems provide the ability to garner insight into the polymerization mechanism. Well-studied examples that are known to polymerize 1,3-dienes are those derived from (allyl)Ni(II) complexes.⁵ Using late transition metals increases the tolerance for functional groups on the dienes, and thus could result in the discovery of new polymers.

Mechanism of 1,3-Diene Polymerization by (Allyl)Transition Metal Catalysts

Two general mechanisms have been proposed for the insertion of butadiene into allyl-metal bonds. Cossee and Arlman proposed that the η^2 - or η^4 -coordinated butadiene can undergo nucleophilic attack by the σ -bonded structure of the allyl unit, commonly referred to as the σ -allyl insertion mechanism.^{13,14} Alternatively, the second mechanism involves direct coupling of coordinated butadiene with the η^3 -allyl group, which is known as the direct allyl-insertion mechanism.¹ This is the generally accepted mechanism for these systems, and is supported by both experimental¹⁵⁻¹⁷ and theoretical evidence.¹⁸⁻²⁰

When discussing the mechanism for these allyl-based systems, several key terms are commonly employed. Coordination of the allyl unit and 1,3-diene moiety can occur in several different ways (Figure 1.2). Butadiene can coordinate in either an η^2 or η^4 fashion, and in either the η^2 or η^4 -coordination mode the diene may be in either the *s-cis* or *s-trans* geometry.^{21,22} The allyl and diene moieties may also be prone or supine relative to one another. Additionally, a substituted allyl moiety or an allyl unit possessing a growing polymer chain may undergo *syn/anti* isomerization, where the R group is either *syn* or *anti* with respect to the central allylic hydrogen. This can occur via a σ - π mechanism (Figure 1.3).¹

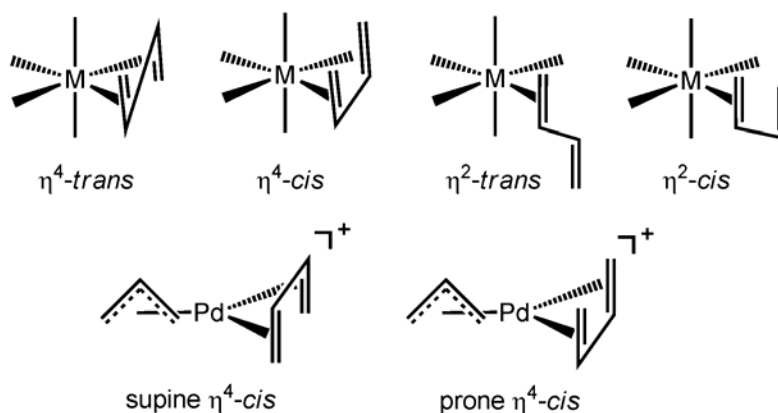


Figure 1.2. Structurally different coordination modes of butadiene to the metal M and their respective nomenclature.

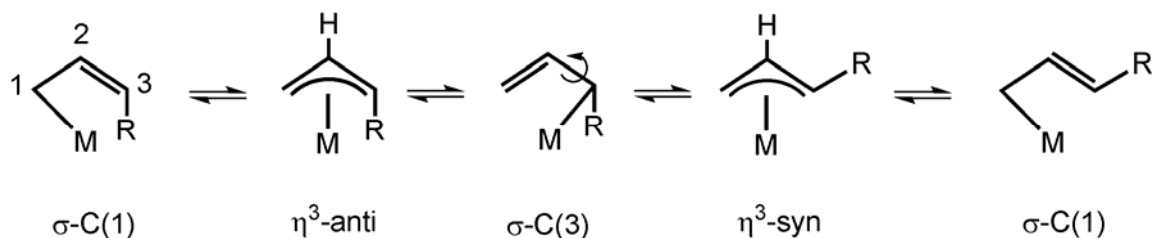


Figure 1.3. Different configurations of the substituted allyl (R = organic group, e.g. the growing polymer chain) via *syn-anti* isomerization.

It is well known that *syn-anti* isomerization controls the *cis-trans* stereochemistry of the resulting polymer for the metal-catalyzed polymerizations. Controlling the rate of equilibration between the *syn* and *anti* isomers relative to their rates of insertion has been proposed to be a key influence in regulating the resulting microstructure of the poly-1,3-dienes.^{19,23,24} While the prone and supine η^4 -isomers do not seem to influence the polymer enchainment, the prone η^4 -isomer for the nickel analogue of that in Figure 1.2 is calculated to be thermodynamically favored over the supine isomer by 7.0 kcal/mol.¹⁸

Nickel(II) Catalyzed Polymerization of 1,3-Dienes

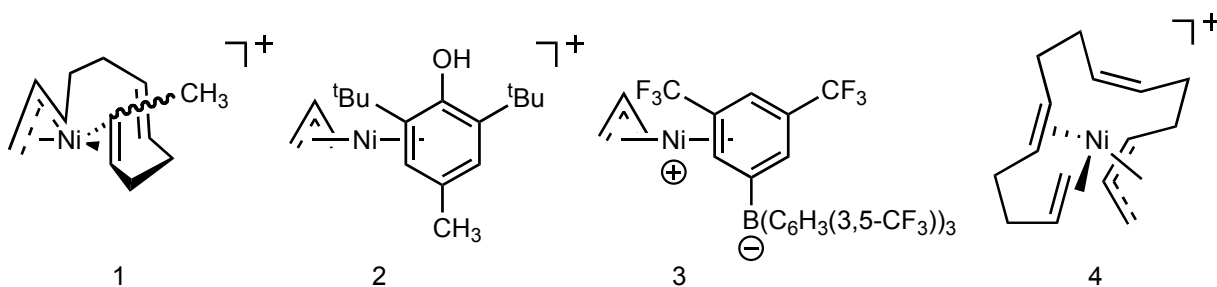
In the 1960's, Porri and Natta,²⁵ as well as Dolgoplosk,²⁶ independently developed the first examples of (allyl)nickel catalysts for 1,3-diene polymerizations. The [(allyl)NiX]₂ dimers (X = Cl, Br, I) that they prepared are capable of polymerizing butadiene, albeit with very low activities. The analogous [(2-R-allyl)PdX]₂ dimers do not polymerize 1,3-dienes, however the insertion of one equivalent of isoprene or butadiene into the substituted allyl complexes (R = H, Cl, Me) has been demonstrated and the kinetics of diene insertion studied.^{27,28}

In the late 1970s and early 1980s another (allyl)Ni dimer, [(allyl)Ni(trifluoroacetato)]₂ was reported by Teyssié to polymerize butadiene.²⁹ Interestingly, this system exhibits an amazing stereoselective control over the enchainment of the resulting polymer ranging from 99% *cis* to 99% *trans* polybutadiene, based solely upon the choice of added ligands and kinetic conditions employed.^{30,31} For example, when the dimer is used by itself, highly *cis*-enchained polymer results, whereas addition of a ligand such as triphenyl phosphite to this system instead favors the *trans*-enchained polymer. Teyssié claimed that the selectivity of the catalyst to favor various

enchainments is dictated by the environment surrounding the metal center. Either blocking a metal coordination site with a bulky ligand or building a sterically congested environment around the metal center results in more *trans*-enchained polymer.³¹

Taube came to a similar conclusion in the mid 1980s after developing the first examples of isolated, cationic (allyl)Ni(II) complexes for 1,3-diene polymerization. These complexes were of the type [(allyl)NiL₂][X] (X = non-coordinating anion), with the ancillary ligands being aryl phosphite, aryl phosphines, aryl arsines, acetonitrile, stibines, or COD.³² Again, complexes with bulky ligands, e.g. triphenyl phosphine, *t*-butylisonitrile, and tri-*o*-tolyl phosphite, are either inactive or favor the *trans* enchainment in the resulting polymer. However, in observations similar to those of Teyssié, the use of weakly coordinating ligands, e.g. triphenyl stibine and triphenyl arsine, resulted in production of a more *cis* enriched polymer.³³ These catalytic systems exhibit moderate activity towards 1,3-diene polymerizations.

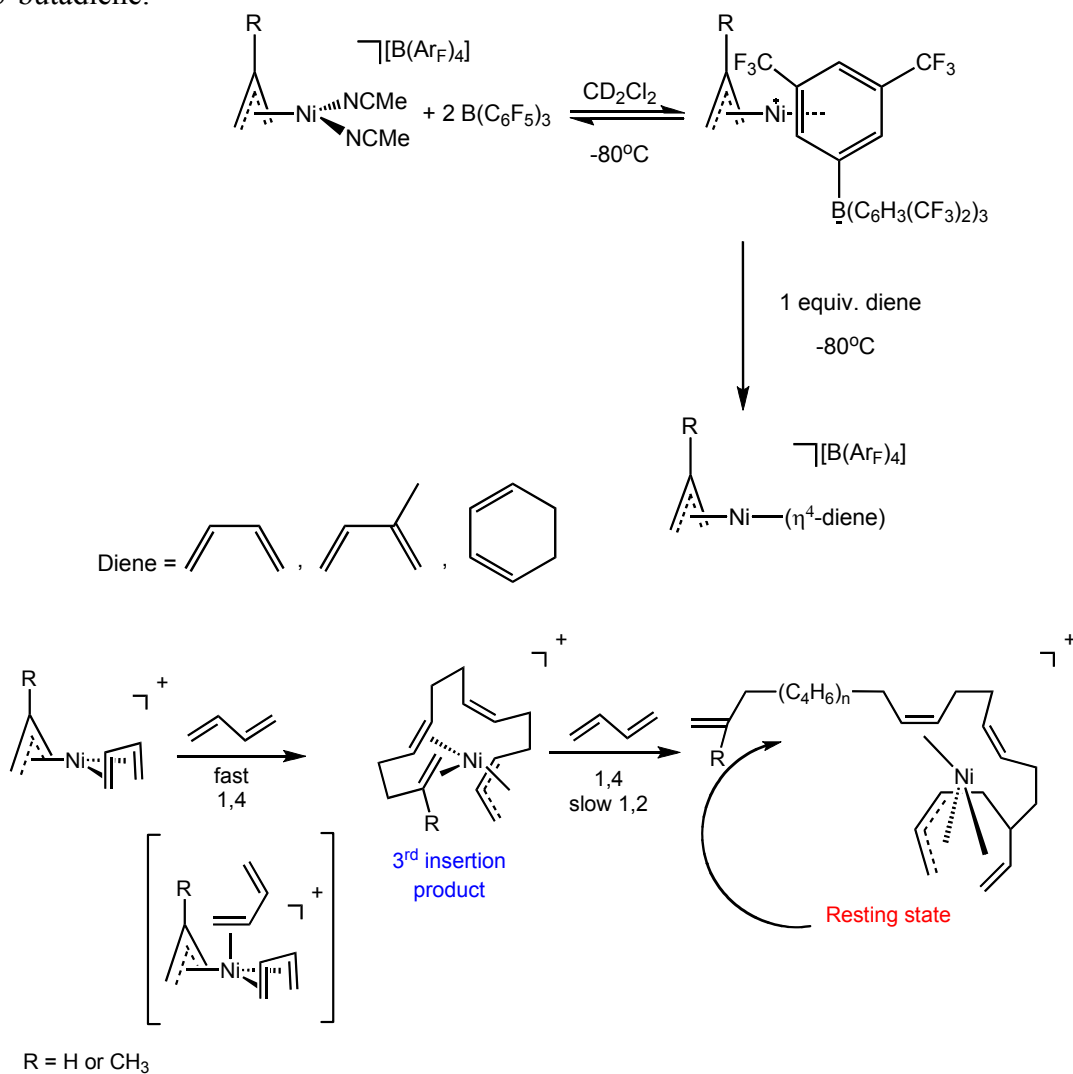
Scheme 1.1. Highly active (allyl)Ni(II) catalysts for 1,3-diene polymerization.



Currently, well-defined, highly active Ni(II) complexes for the polymerization of butadiene either possess labile ligands (**2** and **3**, Scheme 1.1)³⁴⁻³⁶ or are classified as “ligand free” (**1** and **4**, Scheme 1.1); all yield highly *cis*-enchained polybutadiene.^{36,37} The “ligand free” species **4** observed by O’Connor and Brookhart is accessed via addition

of butadiene to **3**, which is generated *in situ* (Scheme 1.2). Through this method, details of the polymerization mechanism, including the identity of the catalyst resting state, have been elucidated. Additionally, the elusive η^4 -butadiene adduct has been observed before it undergoes three fast insertions of butadiene to yield the “ligand free” Ni(II) complex **4**.³⁶

Scheme 1.2. Generation of $[(\text{allyl})\text{Ni}(\text{arene})]^+$ species *in situ* and further reactivity with 1,3-butadiene.



Surprisingly, the exploration of analogous (allyl)Pd(II) systems for 1,3-diene polymerization is limited, especially since these 2nd row analogues could tender other observable intermediates in the polymerization of 1,3-dienes. Reaction rates of palladium systems are typically slower than those for nickel. One example of a [(allyl)Pd(arene)]⁺ exists, and was reported by Maitlis and coworkers.³⁸ While Maitlis and coworkers were able to synthesize several derivatives of the type [(allyl)Pd(1,5-diene)]⁺, reactions of these Pd(II) complexes with 1,3-dienes such as cyclo-octa-1,3-diene and cyclohexa-1,3-diene remain unexplored.

Research Goals and Achievements

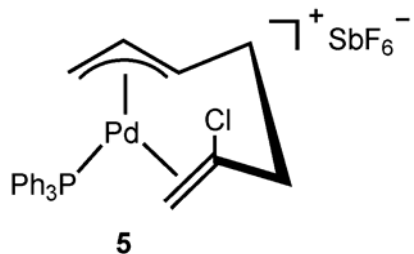
Previously the Brookhart lab has made significant progress in the development of highly active, late transition-metal catalysts for α -olefin polymerizations, primarily based on nickel and palladium.³⁹ However, none of these complexes show activity for polymerization of 1,3-dienes and substituted 1,3-dienes. Recent progress has been made through the development of highly active, nickel(II) “ligand-free” catalysts for 1,3-diene polymerizations, which has also provided significant insight into the mechanism for these reactions.³⁶ While highly active, these catalysts are relatively unstable and difficult to generate, and hence development of initiator-free complexes is desirable. Since reaction rates of palladium systems are typically slower than those for nickel, cationic palladium complexes may tender other observable intermediates in the polymerization of 1,3-dienes. The goals of this research include (1) development of synthetic routes to (allyl)Pd(II) complexes with highly labile arene ligands; (2) exploration of the reactivity of these complexes with olefins and dienes and comparison of the chemistry of the Pd(II)

systems to the parallel chemistry of the Ni(II) systems; and (3) elucidation of the mechanism of insertion, chain growth, and chain transfer in reactions of these (allyl)Pd(II) systems with dienes.

Chapter 2 describes the successful synthesis of [(allyl)Pd(arene)][SbF₆] complexes with highly labile arene ligands. The reactivity of these complexes with α -olefins and alkynes results in formation of bis-olefin and bis-alkyne Pd(II) species at low temperatures and is thoroughly discussed. A comparison of the reactivity of these Pd(II) complexes with the analogous [(allyl)Ni(arene)][B(Ar_F)₄] complexes investigated by Abby R. O'Connor, is also presented.

Chapter 3 outlines the reactivity of the [(allyl)Pd(arene)][SbF₆] complexes with a variety of dienes. For the first time, a diene complex exhibiting an *s-trans*- η^4 -binding mode to a d⁸ metal center has been synthesized and characterized. Additionally, a variety of [(allyl)Pd(η^4 -diene)]⁺ species have been spectroscopically observed at low temperatures. This chapter also focuses on the direct observation of insertion intermediates as models for the polymerization of 1,3-butadiene, including an η^3, η^2 -wrap-around species such as **5** (Scheme 1.3).

Scheme 1.3. Cationic palladium(II) wrap-around complex.



Chapter 4 describes the synthesis of stable η^3, η^2 -wrap-around complexes as models for the first insertion product in the polymerization of 1,3-dienes. The binding affinity of the η^2 -olefin can be measured and controlled by tuning different electronic factors of the wrap-around complexes. Furthermore, reactions of the Pd(II) wrap-around complexes with 1,3-dienes were explored with the goal of gaining further insight into the chain transfer and polymerization mechanism for (allyl)Pd(II) complexes.

References and Notes

- (1) Thiele, S. K. H.; Wilson, D. R. *J. Macromol. Sci.* **2003**, *C43*, 581.
- (2) <http://www.britannica.com/eb/article-76457>.
- (3) Kaminsky, W.; Hinrichs, B. *Handbook of polymer synthesis, 2nd ed.*; Marcel Dekker: New York, 2005.
- (4) <http://en.wikipedia.org/wiki/Neoprene#Applications>.
- (5) Taube, R.; Sylvester, G. *Applied Homogeneous Catalysis with Organometallic Complexes*; VCH: Weinheim, Germany, 1996.
- (6) Binder, J. L. *Ind. Eng. Chem.* **1954**, *46*, 1727.
- (7) Ziegler, K.; Holzkamp, E.; Breil, H.; Martin, H. *Angew. Chem.* **1955**, *67*, 541.
- (8) Natta, G. *Angew. Chem.* **1956**, *68*, 393.
- (9) Natta, G.; Porri, L.; Mazzanti, G. *Chem. Abstr.* **1959**, *53*, 3756.
- (10) Phillips Petroleum Co. (R. Zelinski, D. S., GB 848.065 (1956) *Chem. Abstr.* **1961**, *55*, 15982.
- (11) Goodrich-Gulf Chemicals, I. C. E. B., A. F. Ecker), US 2.977.349 (1955) *Chem. Abstr.* **1961**, *55*, 16012.
- (12) Bridgestone Tire Co. (K. Ueda, A. O., T. Yoshimoto, J. Hosono, K. Maeda), DE-AS 1.213.120 (1959).
- (13) Cossee, P. *Stereochemistry of Macromolecules*; Marcel Dekker: New York, 1967; Vol. 1.
- (14) Arlman, E. J. *J. Catal.* **1966**, *5*, 178.
- (15) Taube, R.; Gehrke, J. P. *J. Organomet. Chem.* **1985**, *291*, 101.
- (16) Taube, R.; Gehrke, J. P.; Böhme, P. *Wiss. Z. Tech. Leuna-Merseburg* **1987**, *29*, 310.
- (17) Wache, S.; Taube, R. *J. Organomet. Chem.* **1993**, *456*, 137.
- (18) Tobisch, S.; Bögel, H.; Taube, R. *Organometallics* **1996**, *15*, 3563.
- (19) Tobisch, S.; Bögel, H. *Organometallics* **1998**, *17*, 1177.

- (20) Tobisch, S.; Taube, R. *Organometallics* **1999**, *18*, 5204.
- (21) Benn, R.; Jolly, P. W.; Joswig, T.; Mynott, R.; Schick, K. P. *Z. Naturforsch., Teil B* **1986**, *41*, 680.
- (22) Yasuda, H.; Nakamura, A. *Angew. Chem., Int. Ed. Engl.* **1987**, *26*, 723.
- (23) Dolgoplosk, B. A. *Sov. Sci. Rev. Sect. B.* **1980**, *2*, 203.
- (24) Jolly, P. W.; Wilke, G. *The Organic Chemistry of Nickel, Vol. 2, Organic Synthesis*; Academic Press: New York, 1975.
- (25) Porri, L.; Natta, G.; Gallazzi, M. C. *J. Polym. Sci., Part C* **1967**, 2525.
- (26) Babitskii, B. D.; Dolgoplosk, B. A.; Kormer, V. A.; Lobach, M. I.; Tinyakova, E. I.; Yakovlev, V. A. *Isv. Akad. Nauk SSSR Ser. Chem.* **1965**, 1507.
- (27) Takahashi, Y.; Sakai, S.; Ishii, Y. *J. Organomet. Chem.* **1969**, *16*, 177.
- (28) Hughes, R. P.; Powell, J. *J. Am. Chem. Soc.* **1972**, 7723.
- (29) Hadjiandreou, P.; Julemont, M.; Teyssié, P. H. *Macromolecules* **1984**, *17*, 2455.
- (30) Durand, J. P.; Dawans, F.; Teyssié, P. *J. Polym. Sci., Part A-1* **1970**, *8*, 1993.
- (31) Marechal, J. C.; Dawans, F.; Teyssié, P. *J. Polym. Sci., Part A-1* **1970**, *8*, 979.
- (32) Taube, R.; Gehrke, J. P.; Schmidt, U. *J. Organomet. Chem.* **1985**, 292, 287.
- (33) Taube, R.; Schmidt, U.; Gehrke, J. P.; Anacker, U. *J. Prakt. Chem.* **1984**, 326, 1.
- (34) Cámpora, P. J.; Carmona, G. E.; Conejo Argandona, M. M. 2004; Vol. ES Patent 2200698.
- (35) Cámpora, P. J.; Conejo, M. D. M.; Reyes, M. L.; Mereiter, K.; Passaglia, E. *Chem. Commun.* **2003**, 78.
- (36) O'Connor, A. R.; White, P. S.; Brookhart, M. *J. Am. Chem. Soc.* **2007**, *129*, 4142.
- (37) Taube, R.; Wache, S. *J. Organomet. Chem.* **1992**, 428, 431.
- (38) Mabbott, D. J.; Mann, B. E.; Maitlis, P. M. *J. Chem. Soc. Dalton Trans.* **1977**, 294.
- (39) Ittel, S. D.; Johnson, L. K.; Brookhart, M. *Chem. Rev.* **2000**, *100*, 1169.

CHAPTER TWO

Synthesis and Reactivity of (Allyl)Nickel(Arene)⁺ and (Allyl)Palladium(Arene)⁺ Complexes with Olefins and Alkynes

All of the experiments with the [(2-R-allyl)Ni(arene)][B(Ar_F)₄] derivatives were performed by Abby R. O'Connor, and most of the experiments conducted with [(2-Cl-allyl)Pd(mes)][SbF₆] were performed by Rebecca A. Moorhouse

(This chapter has been published as an *Organometallics* paper, with permission, from

O'Connor, A. R.; Urbin, S. A.; Moorhouse, R.; White, P.; Brookhart, M.

Organometallics **2009**, 28, 2372. Copyright 2009, American Chemical Society.)

Introduction

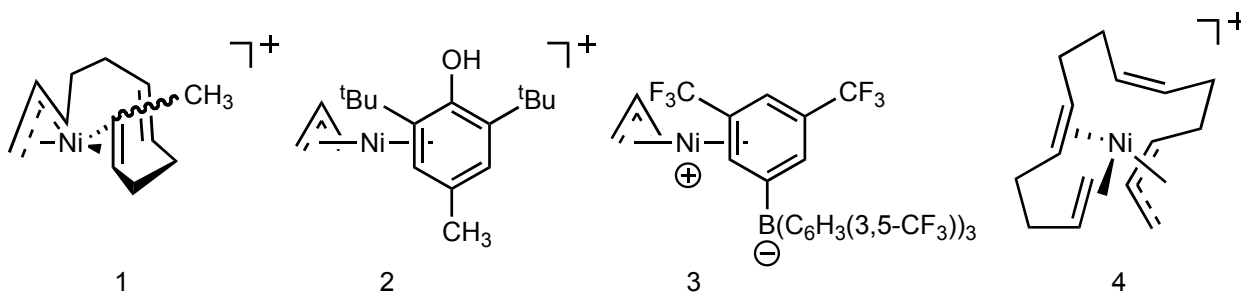
Pd(II) and Ni(II) allyl complexes occupy a prominent position in structural, synthetic, and catalytic organometallic chemistry.^{1, 2} Cationic (allyl)ML₂⁺ complexes bearing highly labile ligands which can be easily displaced via ligand substitution serve as useful precursors to an array of new allyl Pd or Ni species.² For example, Lloyd-Jones has used (allyl)Pd(NCCH₃)₂⁺ as a convenient precursor to a series of phosphine-substituted complexes, useful for synthetic and mechanistic studies of asymmetric allylic alkylation reactions.^{3, 4}

Our interests are focused on the use of (allyl)ML₂⁺ (M = Ni or Pd) systems for polymerization and oligomerization of 1,3-dienes⁵ and strained olefins. The ligand L

must be highly labile in order to be displaced by dienes or alkenes and effect rapid initiation of polymerization. If initiation is slow relative to propagation, then only a fraction of the Pd or Ni complex is activated, molecular weights cannot be controlled, and living polymerizations cannot be achieved. The problem of slow initiation relative to propagation using such species is illustrated by the work of Goodall, who employed readily available (allyl)Pd(COD)⁺ (COD = 1,5-cyclooctadiene) complexes⁶ for norbornene polymerization.⁷ While these are highly active catalysts, in the absence of chain transfer agents, the molecular weights of the polymers could not be controlled and far exceed values expected for a living polymerization.

Polymerizations of butadiene using cationic (allyl)Ni(II) complexes containing highly labile ligands have been reported by Taube,⁸⁻¹⁸ Cámpora,^{19, 20} and our laboratory (Scheme 2.1).⁵ Taube pioneered the use of “ligand free” complex **1**, while Cámpora reported use of arene complex **2** for butadiene polymerization, illustrating the lability of the arene ligand. We have used the B(3,5-(CF₃)₂C₆H₃)₄⁻ complex **3** as an initiator and shown it reacts quite rapidly with butadiene at -80 °C to yield the highly reactive and observable (allyl)Ni(η⁴-1,3-butadiene)⁺ complex, a key and previously unobserved intermediate. Chain growth from this species yielded initially wrap-around complex **4** and monitoring further chain growth by NMR spectroscopy yielded additional mechanistic details of the chain growth process including the nature of the catalyst resting state.^{5, 21}

Scheme 2.1. Active 1,3-Diene Polymerization Catalysts



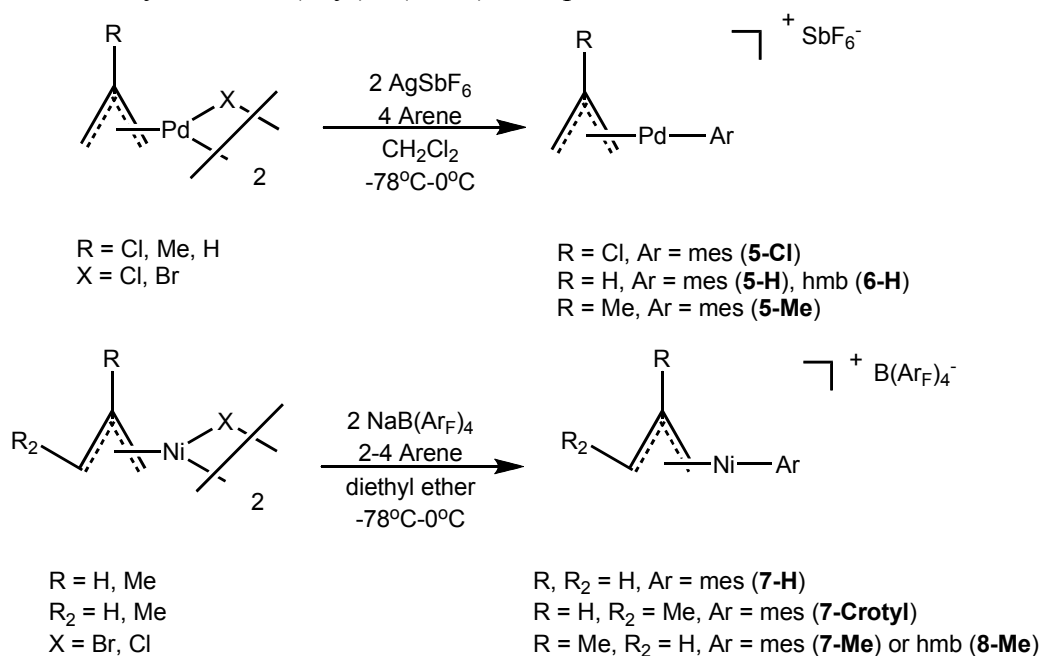
Complexes **1**, **3**, and **4** are not readily accessed and thus Ni arene complexes of type **2**, described by Campora, are the most practical “ligand free” initiators for use on preparative scales. In addition, given the high lability of the arene ligands, allyl complexes of the type $(\text{allyl})\text{M}(\text{arene})^+$ are not only attractive as initiators for polymerization reactions, but also as precursors for a wide variety of new cationic (or neutral) allyl Ni(II) and Pd(II) complexes through displacement of the labile arene ligand. We describe in this chapter the synthesis and characterization of several $(\text{allyl})\text{M}(\text{arene})^+$ ($\text{M} = \text{Pd}, \text{Ni}$) complexes, the kinetics of exchange reactions with arenes, and their reactions with diethyl ether, olefins, and alkynes, all of which demonstrate the high lability of the arene ring and the utility of these complexes as useful precursors to $(\text{allyl})\text{M}(\text{L})(\text{L}')^+$ type complexes.

Results and Discussion

Synthesis of $(2\text{-R-C}_3\text{H}_4)\text{M}(\text{Arene})^+$ Salts ($\text{M} = \text{Pd}$, Arene = mesitylene (mes), $\text{R} = \text{H}$ (5-H), $\text{R} = \text{Me}$ (5-Me), $\text{R} = \text{Cl}$ (5-Cl); $\text{M} = \text{Pd}$, Arene = hexamethylbenzene (hmb), $\text{R} = \text{H}$ (6-H); $\text{M} = \text{Ni}$, Arene = mes, $\text{R} = \text{H}$ (7-H), $\text{R} = \text{Me}$ (7-Me), $\text{R} = \text{H}$, $\text{R}' = \text{Me}$, (7-Crotyl)²²; $\text{M} = \text{Ni}$, Arene = hmb, $\text{R} = \text{Me}$ (8-Me)). Synthesis of the $(\text{allyl})\text{M}(\text{arene})^+$ complexes was achieved by salt metathesis of the well-known allyl halide $[\text{allyl}(\text{M})\text{X}]_2$ dimers²³⁻²⁶ in the presence of a slight excess of arene. Maitlis and

coworkers previously reported the synthesis of (2-methallyl)Pd(hmb)⁺ with the PF₆⁻ counteranion.⁶ Scheme 2.2 summarizes the complexes prepared and the general methods used. NaB(Ar_F)₄ (Ar_F = 3,5-(CF₃)₂C₆H₃) was used for preparation of the Ni complexes, while AgSbF₆ was required for synthesis of the Pd complexes. The Ni complexes are quite robust and can be handled at room temperature, while the Pd derivatives need to be isolated and stored at low temperatures. ¹H and ¹³C{¹H} NMR spectroscopy was used to characterize the complexes. As representative for these systems, allyl ¹H resonances of Ni complex **7-H** in CD₂Cl₂ appear at δ 5.85 (m), 3.69 (d, ³J_{H-H} = 6.6 Hz), and 2.45 (d, ³J_{H-H} = 12.6 Hz) for the central, *syn*, and *anti* protons, respectively; while those of the Pd analog, **5-H**, appear at δ 5.65 (m), 4.54 (d, ³J_{H-H} = 4.8 Hz), 3.30 (d, ³J_{H-H} = 11.4 Hz) for the central, *syn*, and *anti* protons, respectively. The mesitylene signals for the aromatic hydrogens (δ 6.66) of **7-H** are shifted upfield relative to free mesitylene (δ 6.79) in the Ni complex, while in Pd complex **5-H** the signals are shifted downfield to δ 7.03 relative to free mesitylene (see Experimental Section and Supporting Information for complete characterization of complexes **5-8**). The (2-Cl-allyl)Pd(mes)⁺ complex is used for the explored reactivity studies because the NMR spectrum is easily interpreted (2 singlets for the *syn* and *anti* protons).

Scheme 2.2. Synthesis of (allyl)M(arene)⁺ complexes.



Single crystal X-ray analysis provided structural details for complexes **7-H** and **8-Me** and confirmed the η^6 -coordination mode of the arene. The crystallographic information is collected in Appendix I. ORTEP drawings for **7-H** and **8-Me** appear in Figures 1 and 2, respectively. The Ni-C arene bond lengths in complex **7-H** range from 2.12 to 2.19 Å indicating the ring is coordinated nearly symmetrically to the Ni center (Figure 2.1). This is in good agreement with the arene coordination in the crystal structure reported by Cámpora for the analogous [(allyl)Ni(2,6-di-*tert*-butyl-4-methylphenol)][B(Ar_F)₄].²⁰ The angle between the mesitylene plane and the allyl plane is 17.2°. The arene bond lengths for complex **8-Me** vary from 2.12 to 2.26 Å (Figure 2.2), similar to those obtained for compound **7-H**, indicating once again a symmetrically bound arene ring. The angle between the hexamethylbenzene and allyl planes is 15.4°. The arene ring is tilted slightly away from the methyl group of the 2-methallyl moiety.

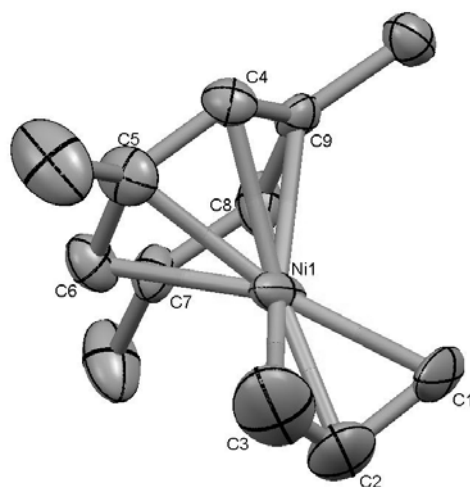


Figure 2.1. ORTEP diagram of (allyl)Ni(mes)⁺, **7-H**. Thermal ellipsoids drawn at 50% probability, [B(Ar_F)₄]⁻ omitted for clarity. Selected bond lengths (Å): Ni(1)-C(2) = 1.962(4), Ni(1)-C(1) = 1.994(4), Ni(1)-C(3) = 2.061 (6), Ni(1)-C(6) = 2.121(4), Ni(1)-C(8) = 2.130(4), Ni(1)-C(5) = 2.142(4), Ni(1)-C(9) = 2.157(3), Ni(1)-C(4) = 2.176(4), Ni(1)-C(7) = 2.192(4).

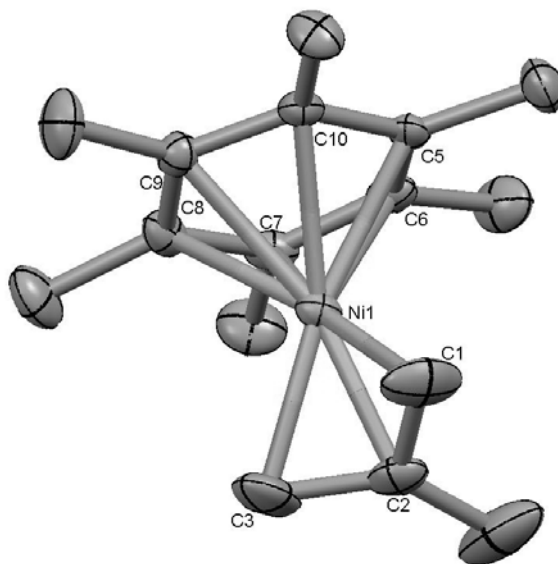
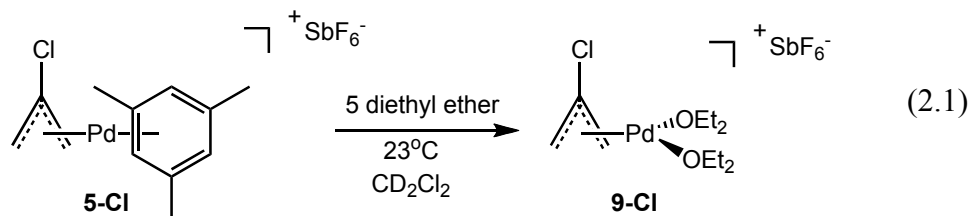


Figure 2.2. ORTEP diagram of (2-methallyl)Ni(hmb)⁺, **8-Me**. Thermal ellipsoids drawn at 50% probability, [B(Ar_F)₄]⁻ is omitted for clarity. Selected bond lengths (Å): Ni(1)-C(2) = 1.978(2), Ni(1)-C(1) = 2.001(2), Ni(1)-C(3) = 2.007(2), Ni(1)-C(8) = 2.1205(19), Ni(1)-C(5) = 2.1392(18), Ni(1)-C(10) = 2.1426(18), Ni(1)-C(7) = 2.1857(19), Ni(1)-C(9) = 2.1901(19), Ni(1)-C(6) = 2.2563(18).

Ligand Substitution Reactions of (Allyl)Pd(II)(Mes)⁺ Complexes.

Reactions with Diethyl Ether. The rapid reaction of **5-Cl** with diethyl ether illustrates the high lability and weak binding affinity of the bound arene. Upon mixing at room temperature in CD₂Cl₂, 5 equivalents of diethyl ether displace the mesitylene ligand of **5-Cl** to yield a diethyl ether complex **9-Cl** as shown in eq 2.1.



Free mesitylene is generated (δ 6.80) and a new allyl signal appears for H_{syn} at δ 4.43 (s), while the signal for H_{anti} overlaps with the methylene signal of diethyl ether. The bound ether ligands exchange rapidly on the NMR time scale with free ether at room temperature and show averaged resonances at 3.51 (CH₃) and 1.21 (CH₂) ppm. We assume this is a four-coordinate square planar complex, but the averaging of free and bound ether ligand resonances precludes establishing this through peak integration.

Exchange reaction with Free Mesitylene. Reaction of [(allyl)Pd(mes)][SbF₆], **5-H**, with excess mesitylene results in exchange of the free and bound mesitylene. This exchange is rapid at room temperature on the NMR timescale, but at low temperatures the resonances for free and bound mesitylene decoalesce (Figure 2.3). Due to poor solubility of **5-H** in CD₂Cl₂ at low temperatures, the slow exchange limit could not quite be reached. However, when **5-H** is exposed to 2, 4, or 6 equiv of free mesitylene at -67 °C, the peak width at half-height (26 Hz) for the aromatic signal of the bound mesitylene did not change, indicating that the exchange is independent of the concentration of free mesitylene. The linewidth at slow exchange is estimated to be ca. 5 Hz, from which the

rate constant for exchange, k_{ex} , where $k_{\text{ex}} = \pi(\Delta\omega)$, can be estimated as ca. 60 s^{-1} , corresponding to $\Delta G^\ddagger = 10.2 \text{ kcal/mol}$ (-67°C). This data eliminates an associative exchange mechanism involving external mesitylene in the transition state for exchange. Possible mechanisms would include a dissociative process in which loss of mesitylene (assisted by solvent coordination to Pd) is rate-determining, or a process in which the rate-limiting step is formation of an η^4 - or η^2 -mesitylene complex (potentially solvent stabilized) followed by rapid associative displacement.

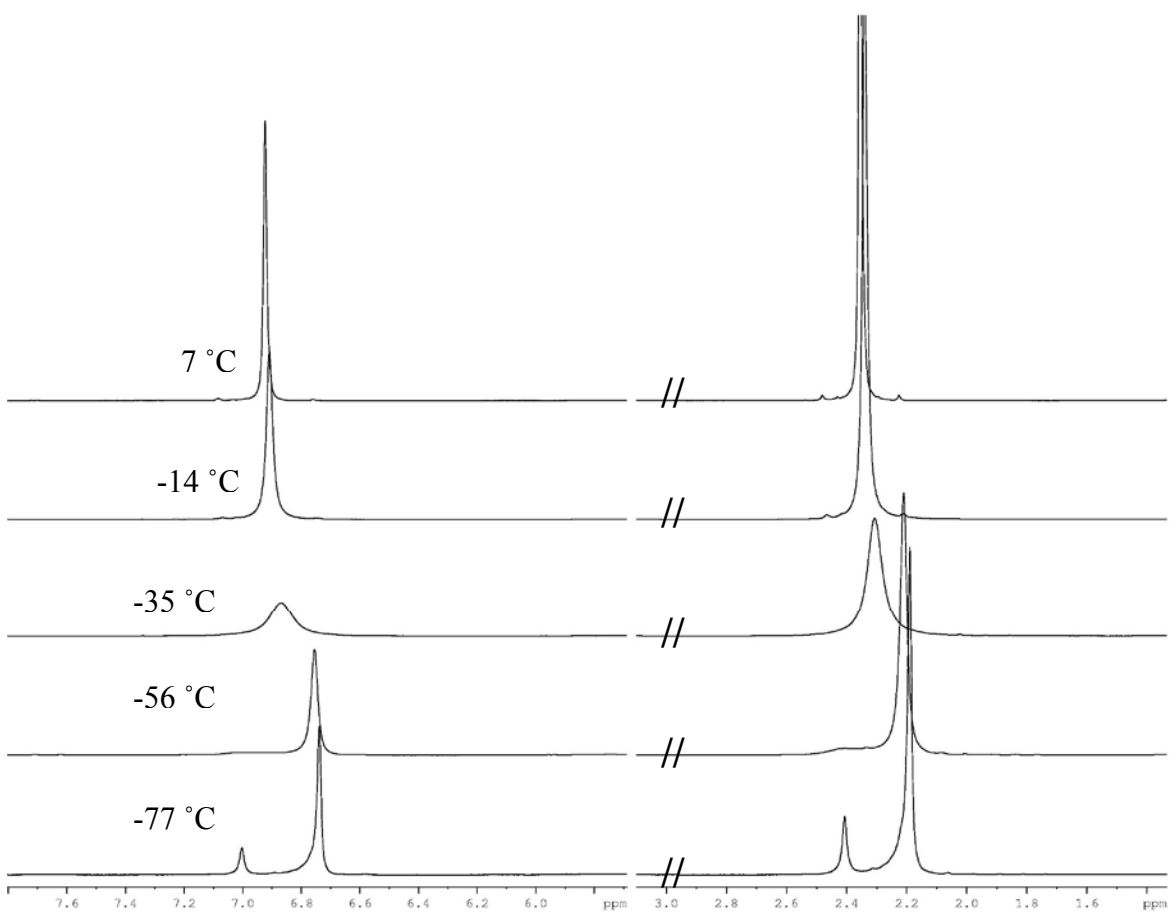


Figure 2.3. Variable temperature ^1H NMR overlay of the addition of 4 equiv mesitylene to **5-H**. Mesitylene aryl (δ 6.0 – 7.5) and methyl regions (δ 1.8 – 3.0) are shown.

In Situ Reactions with Olefins and Alkynes. Treatment of [(2-Cl-allyl)Pd(mes)][SbF₆], **5-Cl**, with excess olefin at temperatures as low as -120°C in

CDCl₂F results in rapid displacement of mesitylene and formation of bis-olefin adducts. Scheme 2.3 shows the reaction of **5-Cl** with ethylene to form **10-Cl**, the η^2 -coordinated bis-ethylene allyl palladium species. Exposure of **5-Cl** to 3 equiv of ethylene in CDCl₂F at -110 °C generates free mesitylene and the bis-ethylene complex whose ¹H NMR spectrum is shown in Figure 4. At -110 °C, resonances for the *syn* and *anti* protons appear as singlets at 5.14 and 3.91 ppm, respectively, which are shifted downfield from the analogous resonances in the mesitylene complex (δ 4.72 and 3.57). Two sets of bound ethylene resonances are seen at 5.24 (4H) and 5.00 (4H) ppm suggesting that rotation of ethylene is rapid on the NMR timescale and that both H₁/H_{1'} and H₂/H_{2'} sets of signals are averaged. A sharp free ethylene signal is seen at 5.48 ppm. Upon warming to -60 °C, the bound ethylene signals begin to broaden. At -20 °C, the signals for bound ethylene have nearly coalesced with the signal for free ethylene, implying rapid exchange between bound and free ethylene at this temperature. ¹H NMR variable temperature line broadening experiments at -77 °C to -56 °C showed the barrier for intermolecular exchange of free and bound ethylene, assuming a dissociative mechanism as with the case of mesitylene (*vide supra*) and cyclopentene (*vide infra*), to be $\Delta G^\ddagger = 10.4$ kcal/mol at -56 °C with a rate of exchange of $k_{\text{ex}} = 40 \text{ s}^{-1}$, where $k_{\text{ex}} = \pi(\Delta\omega)$. The signal for H_{*syn*} in CD₂Cl₂ (0 to -70 °C) is obscured by the ethylene resonance. The H_{*anti*} signal begins to broaden above 0 °C, indicating rapid *syn-anti* isomerization. When the sample is warmed to 25 °C, the ethylene and allyl resonances vanish. High field signals in the aliphatic region, as well as mass spectral detection of low molecular weight hydrocarbons, suggest formation of ethylene oligomers. ¹H NMR resonances for **10-H** are similar to those of **10-Cl** and also indicate the coordination of 2 equivalents of

ethylene to the cationic (allyl)Pd(II) center (see Experimental Section and Appendix I for complete list of chemical shifts and assignments).

Scheme 2.3. Formation of Pd(II) bis-ethylene adducts **10-H** and **10-Cl**.

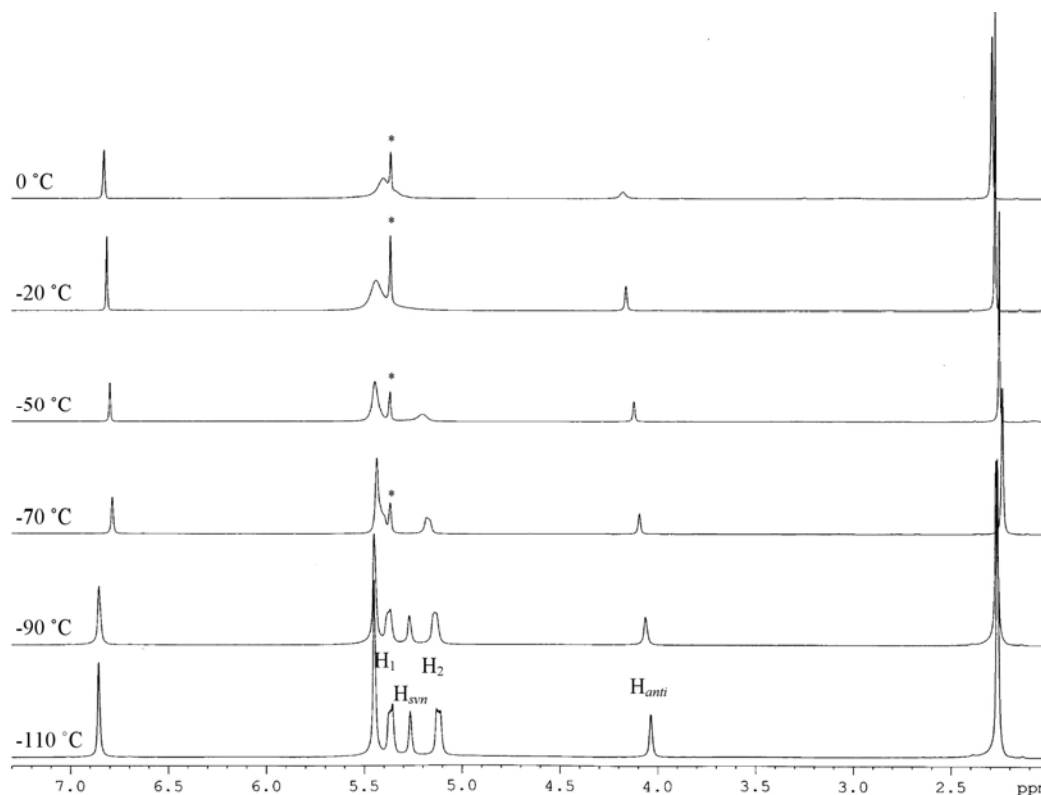
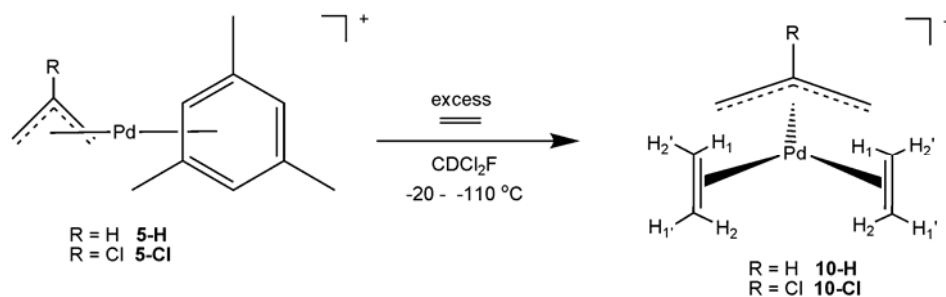
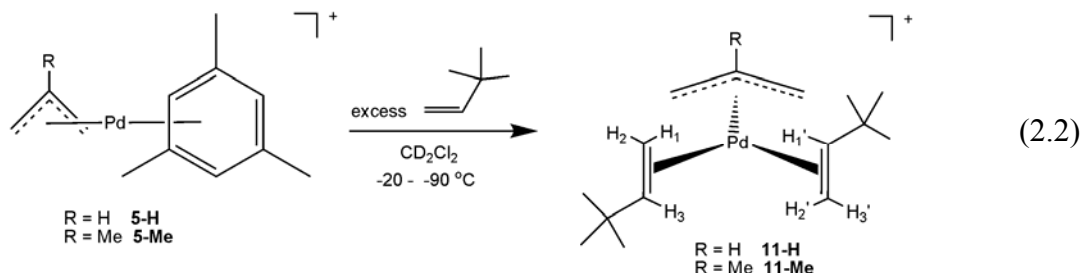


Figure 2.4. ^1H NMR variable temperature overlay showing the formation of (2-Cl-allyl)Pd(ethylene) $_2^+$, **10-Cl**, and exchange with free ethylene at higher temperatures. At -110 °C, the resonances for H_1 and $\text{H}_{1'}$ (shown above as H_1) appear at 5.24 ppm and at 5.00 ppm for H_2 and $\text{H}_{2'}$ (shown above as H_2). The *syn* and *anti* protons are at 5.14 and 3.91 ppm, respectively. Free ethylene is observed at 5.48 ppm and (*) indicates CHDCl_2 in the top four spectra, while the bottom two spectra are in CDCl_2F .

Similar to the formation of the bis-ethylene adduct **10-H**, reaction of [(allyl)Pd(mes)][SbF₆], **5-H**, or [(2-methallyl)Pd(mes)][SbF₆], **5-Me**, with excess *tert*-butylethylene (TBE) in CDCl₂F at temperatures as low as -120 °C results in displacement of mesitylene and subsequent formation of bis-(TBE) species **11-H** and **11-Me**, respectively (eq 2.2). In each case, only one isomer is formed which shows inequivalent TBE groups. These isomers are assigned as shown based on steric considerations, although other unsymmetrical species are consistent with the NMR data. Resonances for free mesitylene appears at 6.79 (Ar) and 2.20 (CH₃) ppm upon formation of either complex **11-H** or **11-Me**. The two *syn* and two *anti* allyl ¹H resonances are inequivalent and appear for species **11-H** at δ 5.10 (bs, H_{syn}), 5.02 (bs, H_{syn}), 3.89 (d, ³J_{H-H} = 13.0 Hz, H_{anti}), and 3.25 (d, ³J_{H-H} = 12.5 Hz, H_{anti}) at -60 °C. The central allyl resonance appears at δ 5.78 (m). The coordinated TBE ligands of **11-H** are also inequivalent as shown by six separate vinyl signals at δ 6.24 (1H, m, H₁), 6.13 (1H, m, H_{1'}), 5.40 (2H d, ³J_{H-H} = 16.5 Hz, H₃ and H_{3'} are coincident), 4.77 (1H, d, ³J_{H-H} = 8.5 Hz, H₂) and 4.41 (1H, d, ³J_{H-H} = 9.0 Hz, H_{2'}). ¹H NMR resonances for **11-Me** are similar to those of **11-H** and also indicate the coordination of 2 equiv of TBE to the cationic (2-methallyl)Pd(II) center (see Appendix I for complete chemical shifts and assignments).



Treatment of **5-Cl** with excess cyclopentene in CD₂Cl₂ at -70 °C results in formation of bis-cyclopentene complex **12-Cl** and free mesitylene (Scheme 2.4). Two

new resonances at 6.16 (2H) and 5.86 (2H) ppm correspond to the vinylic protons (H_1 and H_2) of bound cyclopentene and are shifted downfield from free cyclopentene (δ 5.76), as seen in the 1H NMR spectrum shown in Figure 2.5. The *syn* and *anti* protons appear as two singlets at δ 5.28 (2H) and 3.96 (2H), respectively. The allylic protons of bound cyclopentene appear as a broad 8H band at 2.51 ppm, while the two 2H resonances at 1.92 and 1.05 ppm are assigned to H_5 and H_5' for the *exo* and *endo* hydrogens. The definitive assignment of the *exo* versus *endo* protons could not be determined. At temperatures above -56 °C, the resonances for the bound and free cyclopentene broaden as the exchange rate increases. 1H NMR resonances for **12-H** are similar to those of **12-Cl** and also indicate the coordination of 2 equivalents of cyclopentene to the cationic (allyl)Pd(II) center (see Experimental Section for complete chemical shifts and assignments).

As with the mesitylene case, this exchange process was analyzed quantitatively. Screw-cap NMR tubes were charged with **5-Cl** and 6, 9, and 12 equivalents, respectively, of cyclopentene. Methylene chloride- d_4 was then added to reach the same total volume in each tube. Broadening of the bound vinyl 1H resonance (6.16 ppm) of cyclopentene was monitored between -56 °C and -45 °C. The peak width at half-height at -56 °C was 12 Hz for both 6 and 9 equiv and 13 Hz for 12 equiv of cyclopentene. At -45 °C the peak widths at half-height were 22 Hz (6 equiv), 23 Hz (9 equiv), and 24 Hz (12 equiv). These line widths are within experimental error and clearly show there is no dependence of the exchange rate on added cyclopentene, suggesting either a dissociative or solvent-assisted exchange mechanism. The rate constant for cyclopentene dissociation can be estimated

using the slow exchange approximation as ca. $k_{\text{ex}} = 53 \text{ s}^{-1}$ at -45°C , corresponding to $\Delta G^\ddagger = 11.4 \text{ kcal/mol}$.

Scheme 2.4. Synthesis of $(2\text{-R-allyl})\text{Pd}(\text{cyclopentene})_2^+$ adducts, **12-H** and **12-Cl**, at low temperature.

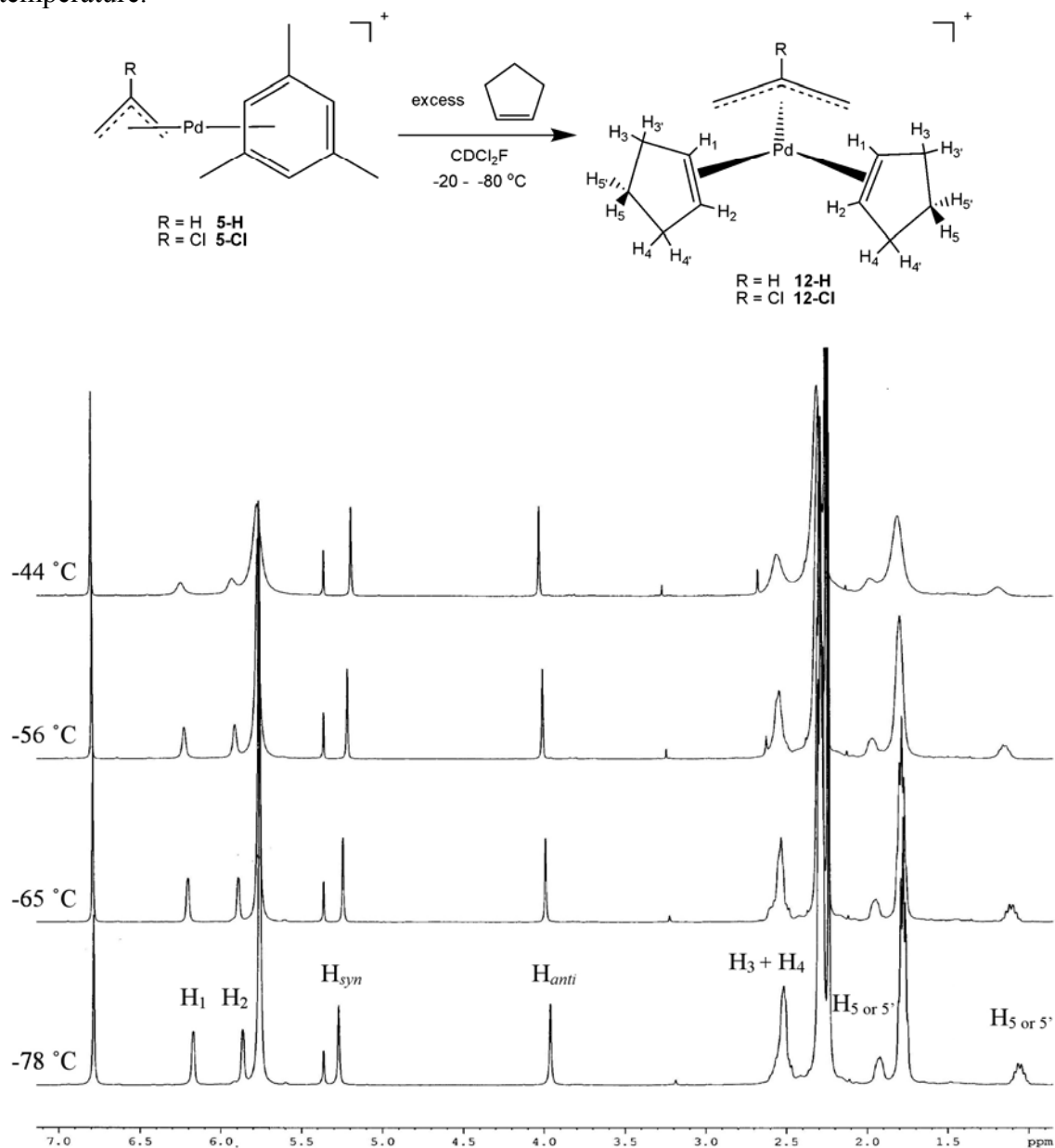
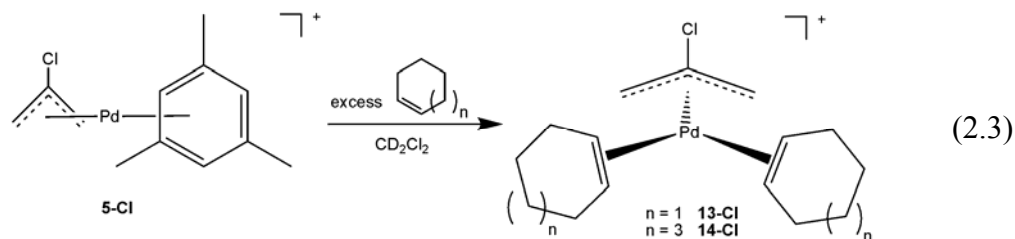


Figure 2.5. ^1H NMR overlay showing the formation of $(2\text{-Cl-allyl})\text{Pd}(\text{cyclopentene})_2^+$, **12-Cl**, and exchange with free cyclopentene at higher temperatures in CD_2Cl_2 . The protons labeled H_5 and $\text{H}_{5'}$ are for the *exo* and *endo* protons of the bound cyclopentene.

Similar to cyclopentene, cyclohexene and cyclooctene react with **5-Cl** to form bis-olefin adducts **13-Cl** and **14-Cl**, respectively (eq 2.3). ^1H NMR spectra for these species are similar to that of the bis-cyclopentene adduct and are reported in Appendix I.

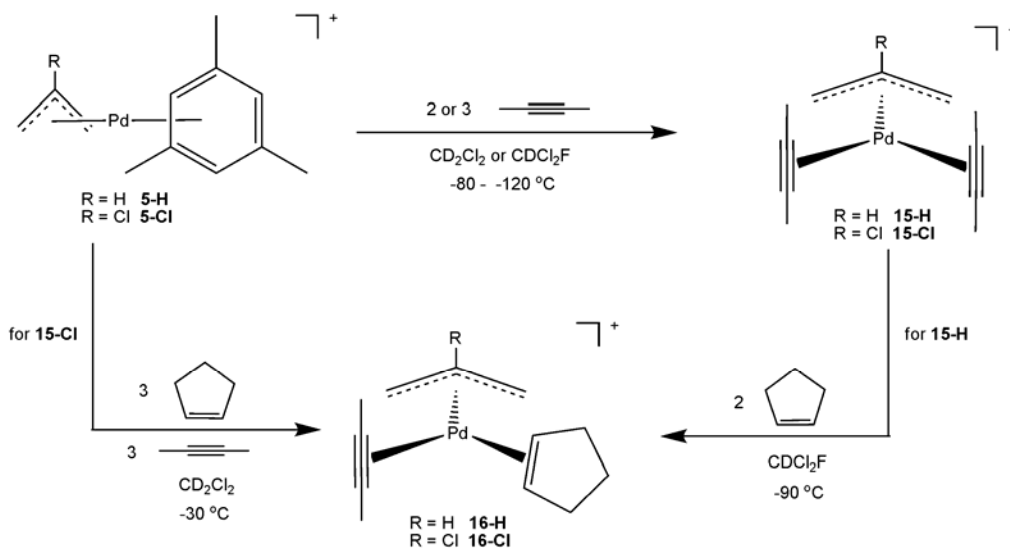


Exposure of **5-Cl** to α -olefins propene or 1-hexene results in the formation of a complex mixture of bis-olefin isomer adducts, and no attempt was made to structurally assign these species.

Exposure of **5-Cl** to 3 equiv of 2-butyne in CD_2Cl_2 at $-90\text{ }^\circ\text{C}$ results in displacement of mesitylene and formation of the bis-alkyne adduct **15-Cl** (Scheme 2.5). NMR studies were performed in the presence of 3 equiv of 2-butyne in CD_2Cl_2 from $-90\text{ }^\circ\text{C}$ to $23\text{ }^\circ\text{C}$. At $-90\text{ }^\circ\text{C}$, mesitylene is displaced as evidenced by free mesitylene in the ^1H NMR spectrum. The *syn* and *anti* protons of **15-Cl** appear as singlets at 4.83 and 3.94 ppm, while the methyl groups give rise to a singlet at 2.18 (12H) ppm. The equivalence of the methyl resonances suggests rapid rotation of the alkyne ligands on the NMR timescale at $-90\text{ }^\circ\text{C}$ and is supported by observation of single ^{13}C resonances for the methyl and methine carbons at 3.3 and 74.6 ppm, respectively. Line broadening of the methyl resonances for free and bound 2-butyne begins at $-40\text{ }^\circ\text{C}$ due to intermolecular ligand exchange; at $23\text{ }^\circ\text{C}$ free and bound methyl signals are present as one broad resonance. ^1H variable temperature NMR studies conducted at $-66\text{ }^\circ\text{C}$ to $-24\text{ }^\circ\text{C}$ showed the rate of exchange between free and bound 2-butyne, again assuming a dissociative mechanism as with the cases of mesitylene and cyclopentene (*vide supra*), to be $k_{\text{ex}} = 36$

s⁻¹ with the barrier to intermolecular exchange calculated as $\Delta G^\ddagger = 12.7$ kcal/mol at -24 °C (Complete experimental details can be found in Appendix I). After a period of 2 days at room temperature, the color of the solution has changed from colorless to dark purple. A small amount of free 2-butyne remains along with a small amount of white substance that has been shown by MS-ESI to be 2-butyne oligomers. The identity of the remaining Pd species has not been determined.

Scheme 2.5. Synthesis of Pd(II) bis-alkyne complexes **15-H** and **15-Cl** and Pd(II) mixed ligand complexes **16-H** and **16-Cl**.



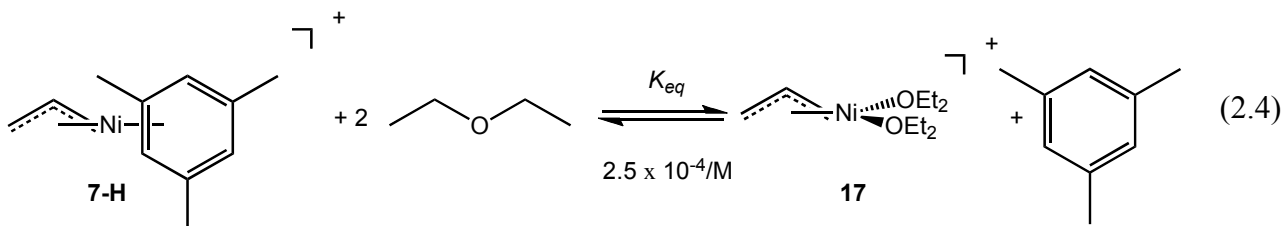
The addition of 3 equiv of both cyclopentene and 2-butyne, to **5-Cl** in CD₂Cl₂ at -70 °C, gives rise to a single complex, the mixed ligand species (2-Cl-allyl)Pd(2-butyne)(cyclopentene)⁺ (**16-Cl**), with no observable formation of either the bis-cyclopentene (**12-Cl**) or bis-2-butyne (**15-Cl**) adducts (Scheme 5). At -70 °C all four *syn* and *anti* allyl protons are inequivalent and appear as singlets at 5.05, 5.01, 4.19, and 4.11 ppm in a 1:1:1:1 ratio. Resonances for the vinylic protons of bound cyclopentene occur at 6.22 (1H) and 5.63 (1H) ppm and the two methyl resonances for 2-butyne appear as a

6H singlet at 2.10 ppm. At 0 °C, all allylic, vinylic, and methyl resonances of **16-Cl** begin to exhibit dynamic behavior due to exchange with free substrates.

A second set of experiments was conducted in which parent complex **5-H** was treated with 2 equiv of 2-butyne at -78 °C. The bis-2-butyne complex **15-H** was cleanly generated first and exhibited shifts similar to **16-Cl** (Scheme 2.5). Addition of 2 equiv of cyclopentene to **15-H** at -78 °C generates only the mixed ligand complex **16-H**, again with shifts similar to **16-Cl**. Addition of 2 equiv 2-butyne to the bis-cyclopentene complex, **12-H**, also generates only the mixed ligand complex **16-H**, indicating that either order of addition of olefin or alkyne, results in formation of the mixed ligand complex **16-H** as the thermodynamically most stable isomer (NMR assignments appear in the Experimental Section).

Reactions of (Allyl)Ni(II)(Arene)⁺ Complexes.

In Situ Reactions with Diethyl Ether. In contrast to the Pd systems, exposure of allyl nickel complex **7-H** at 25 °C to 14, 20, and 25 equiv of diethyl ether results in an equilibrium mixture of **7-H** and an ether adduct, (allyl)Ni(OEt₂)₂⁺, **17**. Monitoring these reactions over time shows that equilibration between **7-H** and **17** is achieved within 3 h with a calculated K_{eq} of $2.5 \times 10^{-4} \text{ M}^{-1}$. ¹H NMR resonances at 3.10 (2H, d, ³J_{H-H} = 7.2 Hz), 2.01 (2H, d, ³J_{H-H} = 13.2 Hz), 5.94 (1H, m) ppm correspond to new *syn*, *anti*, and central allylic hydrogens, respectively. Broadened resonances for diethyl ether indicate rapid exchange between bound and free ether on the NMR time scale.



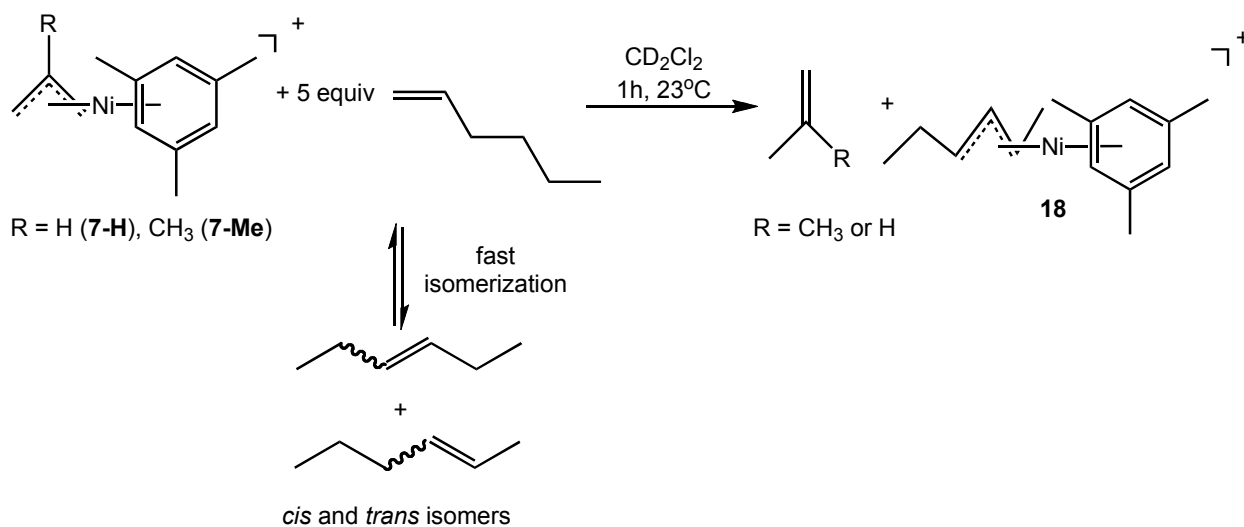
In Situ Arene Exchange Reactions. No line broadening of free or bound arene signals is observed upon treatment of (allyl)Ni(mes)⁺, **7-H**, with excess mesitylene in CD₂Cl₂ up to temperatures of 23 °C, indicating degenerate exchange is far slower than in the case of the Pd analogs described above. However, arene exchange on a preparative time scale could be observed. Treatment of **7-H** with 2.6 equiv of hexamethylbenzene at 23 °C in CD₂Cl₂ results in rapid (< 10 min), quantitative displacement of mesitylene (δ 6.79) to form (allyl)Ni(C₆Me₆)⁺ as supported by an 18H singlet at 2.31 ppm in the ¹H NMR spectrum for coordinated hexamethylbenzene and new allyl resonances at 3.24 ppm (2H, d, ³J_{H-H} = 6.6 Hz, H_{syn}) and 5.73 ppm (H₂, m). The H_{anti} resonance is masked by excess hexamethylbenzene.

In Situ Reactions with Olefins. Relative to the previously described Pd analogs, a quite different reactivity pattern is observed when the Ni complexes **7-H** or **7-Me** are treated with α -olefins (Scheme 2.6).²⁷ The reaction of **7-Me** with 4 equiv of 1-hexene was monitored at low temperature by ¹H NMR spectroscopy. At -80 °C, there is no evidence for ligand substitution and formation of a bis-olefin adduct. Only 1-hexene and starting complex **7-Me** are observed. Upon warming to -30 °C, no reaction of the (2-methallyl)Ni(II) complex is observed, but 1-hexene is partially isomerized to internal 2- and 3-hexenes. After 1.5 h at -30 °C, complete equilibration of 1-hexene with 2- and 3-hexenes is observed. At -10 °C, a new (allyl)Ni(mes)⁺ complex (see below) begins to appear together with free isobutylene (4.65 and 1.72 ppm).

In a second experiment, monitoring the reaction of **7-H** and 5 equiv of 1-hexene at room temperature showed that complete isomerization to the internal isomers of hexene (both *cis* and *trans*) was achieved in 30 min together with consumption of 80% of

7-H and formation of the new (allyl)Ni(mes)⁺ complex and propene. After ca. 1 h, quantitative conversion to the new allyl complex identified as (2-hexenyl)Ni(mes)⁺, **18**, had occurred (Scheme 2.6). Complex **18** exhibits two allyl resonances, one a triplet at 5.46 ppm (1H, ³J_{H-H} = 11.2 Hz), assigned to the central allyl H and the other two overlapping 1.0H multiplets centered at 3.14 ppm corresponding to the *anti* H's. A 2H pentet at 1.32 ppm (³J_{H-H} = 6.4 Hz) is assigned to the methylene of the ethyl group, while two methyl resonances appear at 1.05 (t, ³J_{H-H} = 7.2 Hz) and 1.02 (d, ³J_{H-H} = 6.8 Hz) ppm. Additionally, a new mesitylene aryl resonance at 6.44 ppm (shifted upfield from 6.66 ppm for complex **7-H**) is observed. ¹³C{¹H} NMR spectroscopy also validates the identity of complex **18** and displays three new allylic carbon resonances (105.4, 83.0, and 76.3 ppm) and three aliphatic carbon resonances (26.4, 19.5, and 18.8 ppm).

Scheme 2.6. Reaction of complexes **7-H** and **7-Me** with 1-hexene at room temperature.

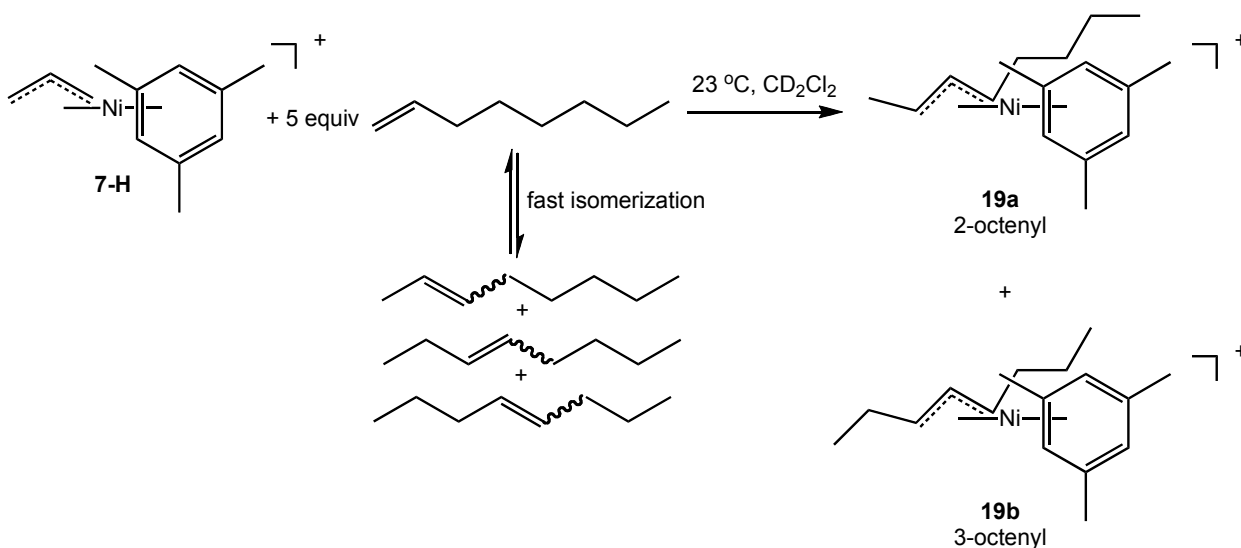


The production of propylene in the case of **7-H** and isobutene in the case of **7-Me**, as detected in the ¹H NMR spectrum, is evidence that an intramolecular hydrogen atom

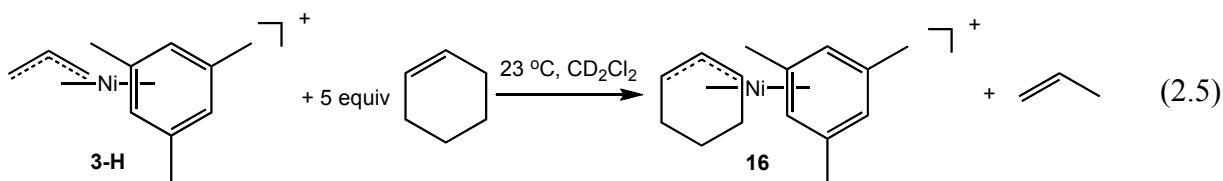
transfer reaction has occurred. This reaction is never observed for the analogous Pd complexes. Internal isomers of hexene exhibit similar reactivity with complexes **7-H** and **7-Me**. When (allyl)Ni(mes)⁺ (**7-H**) was treated with 5 equiv of either *cis* or *trans* 2-hexene at 23 °C, the new allyl species, **18**, is generated, which exhibits the same ¹H and ¹³C NMR spectral data as observed when **7-H** is treated with 1-hexene to generate **18**. Hexene isomers (*cis* and *trans* 2- and 3- isomers) are also seen in the ¹H NMR spectrum.

The reaction of 1-octene with complex **7-H** behaves similarly to the reaction of 1-hexene with **7-H**. Treatment of **7-H** with 5 equiv of 1-octene in CD₂Cl₂ at 23 °C results in formation of internal 2-, 3-, and 4-octenes within 30 minutes, together with the formation of (octenyl)Ni(mes)⁺ positional isomers **19a** and **19b** over the course of an hour (Scheme 2.7). ¹H NMR analysis shows that there are two isomers in solution in approximately a 50/50 ratio. The two isomers are assigned to the 2- and 3-octenyl positional isomers of the allyl moiety. The allyl resonances centered at 5.45 (1H, two overlapping triplets) and 3.13 (2H, appears as overlapping multiplets) ppm are assigned to the central hydrogen and *anti* H's of both isomers, respectively. The aliphatic methylene and methyl protons for both isomers appear as multiplets centered at 1.32 and 0.95 ppm. The mesitylene arene resonance shifts upfield to 6.44 ppm.

Scheme 2.7. Intramolecular hydrogen atom transfer with complex **7-H** and 1-octene.



Cyclohexene also reacts with **7-H** liberating an equivalent of propene and forming (cyclohexenyl) $\text{Ni}(\text{mes})^+$, **20**, (eq 2.5) as established by ^1H NMR spectroscopy. Complex **20** was synthesized independently.²⁸ All of these reactions are fast and complete within 1 h at 23 °C.

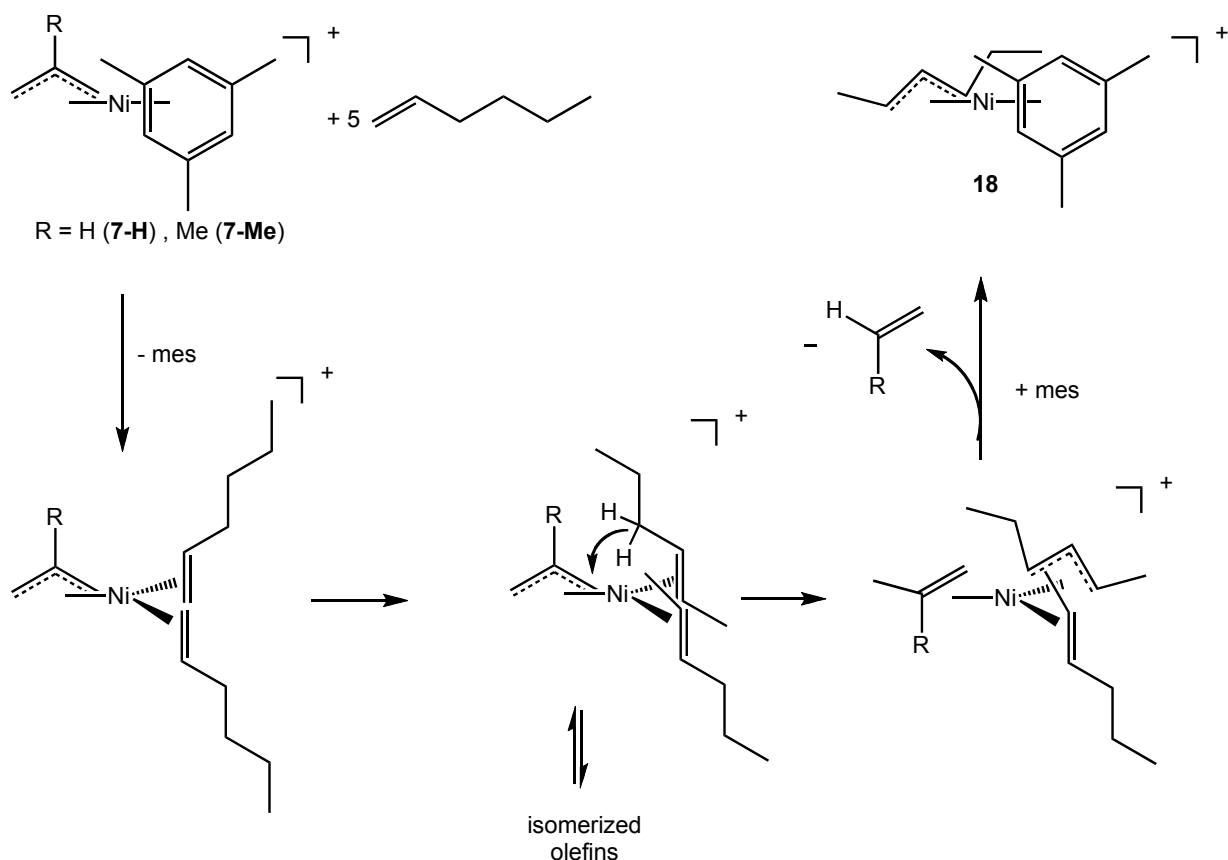


Mechanism of Hydrogen Transfer

The proposed mechanism for intramolecular hydrogen atom transfer with 1-hexene is shown in Scheme 2.8. We have no spectral evidence, even at low temperatures, that bis-olefin complexes form in the case of Ni. We propose these species as viable intermediates since they have been observed spectroscopically for the analogous

Pd complexes. The first step likely involves the displacement of mesitylene by 2 equiv of 1-hexene to generate a very reactive bis-olefin species. We believe isomerization to internal olefins then occurs. However, the mechanism for isomerization is not yet clear. Following isomerization, intramolecular hydrogen atom transfer (either concerted or via a Ni-H species) from the internal hexene isomers to the allyl group would generate propene or isobutylene coordinated to a (2-hexenyl)Ni⁺ fragment. Displacement of propene or isobutylene by mesitylene would generate the (2-hexenyl)Ni(mes)⁺ complex, **18**.

Scheme 2.8. Proposed mechanism of hydrogen atom transfer in the reaction of 1-hexene with (allyl)Ni(mes)⁺ complexes.



Conclusions

Syntheses and characterizations of highly labile (allyl)Pd(arene)⁺ and (allyl)Ni(arene)⁺ complexes have been described. Single crystal X-ray structural determinations of (allyl)Ni(mesitylene)⁺ (**7-H**) and (2-methallyl)Ni(hexamethylbenzene)⁺ (**8-Me**) reveal eighteen-electron complexes in which the arenes are bound in an η^6 -fashion. The arene ligands in these stable, readily prepared complexes are highly labile and thus are excellent precursors for the synthesis of a variety of (allyl)M-based complexes. The arene ligands in the Pd complexes are especially labile. Exchange of bound mesitylene with free mesitylene in (allyl)Pd(mesitylene)⁺ (**5-H**) occurs on an NMR timescale at -67 °C with a barrier of 10.2 kcal/mol. Mesitylene is displaced from various (2-R-allyl)Pd(mes)⁺ complexes (R = H, Me, Cl) by olefins and 2-butyne at temperatures as low as -120 °C to yield sixteen-electron bis-olefin complexes. These complexes exhibit dissociative exchange with barriers of 10-11 kcal/mol (ethylene, cyclopentene, and 2-butyne). These olefin complexes are unstable above ca. 10 °C and produce olefin oligomers in the presence of excess olefin.

The arene ligands in the (allyl)Ni(arene)⁺ complexes are less labile than in the Pd analogs. Arene exchange is observed on a preparative timescale at 25 °C ($t_{1/2} < 10$ mins). Excess diethyl ether results in displacement of mesitylene from (allyl)Ni(mes)⁺ at 23 °C over the course of 3 h. In contrast to the Pd analogs, treatment of (allyl)Ni(mes)⁺ complexes with 1- or 2-alkenes or cyclohexene results in hydrogen transfer from the alkenes to the allyl unit to yield new allylNi(mes)⁺ complexes and either propene from the allyl complex **7-H** or isobutylene from the 2-methallyl complex **7-Me**. This reaction is presumably initiated by olefin displacement of the arene ligand. We are currently

studying this reaction to better understand the mechanism of hydrogen atom transfer and how these results may help elucidate the mechanism of chain transfer in the polymerization of 1,3-dienes.

Acknowledgement

We thank the National Science Foundation (CHE-0615794) for financial support. We also thank Dr. Marc Walter for useful discussions and for synthesizing the (crotyl)Ni(mes)⁺ complex (**7-crotyl**).

Experimental

General Considerations.

All reactions, unless otherwise stated, were conducted under a dry, oxygen free argon atmosphere using standard high vacuum, Schlenk, or drybox techniques. Argon was purified by passage through BASF R3-11 catalyst (Chemalog) and 4Å molecular sieves. All nickel and palladium catalysts were stored under argon in an M.Braun glovebox at -35 °C. ¹H, ¹³C, and ¹⁹F NMR spectra were recorded on a Bruker DRX 500 MHz, a Bruker DRX 400 MHz, or a Bruker 300 MHz spectrometer. Chemical shifts are referenced relative to residual CH(D)Cl₂ (δ 5.32 for ¹H) and ¹³CD₂Cl₂ (δ 53.8 for ¹³C) in CD₂Cl₂ and CHCl₂F (δ 7.16 for ¹H) in CDCl₂F. Chemical shift assignments were supported through 2D HMQC and ¹H-¹H-COSY experiments. Elemental analyses were performed by Robertson Microlit Laboratories of Madison, NJ. The activation barriers were determined using the slow exchange limit. The linewidths were measured at three different temperatures to calculate the reported average ΔG[‡]. The linewidths were also simulated using Spin Works to validate.

Materials.

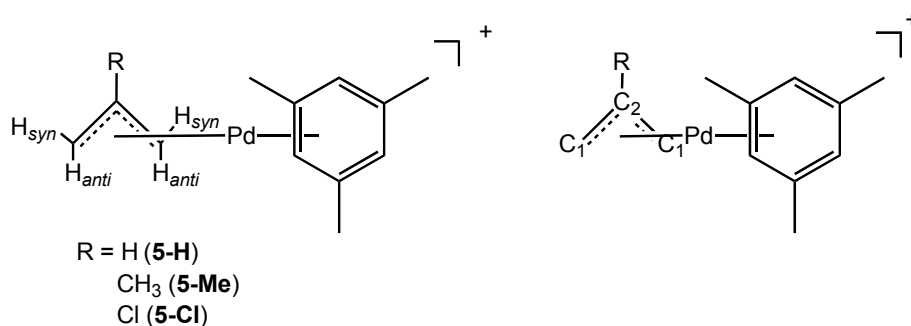
All solvents were deoxygenated and dried by passage over columns of activated alumina.^{29, 30} CD₂Cl₂, purchased from Cambridge Laboratories, Inc., was dried over CaH₂, vacuum transferred to a Teflon sealable Schlenk flask containing 4Å molecular sieves, and degassed via three freeze-pump-thaw cycles. CDCl₂F was synthesized according to literature methods.³¹ 1-Hexene, *cis*-2-hexene, *trans*-2-hexene, 1-octene, cyclooctene, and cyclohexene were purchased from Aldrich and dried over CaH₂ and vacuum transferred to a Teflon sealable Schlenk flask. 1-Butene was purchased from Aldrich and CO and 99.99% ethylene were purchased from National Welders and used as received. Ni[COD]₂, [(2-methallyl)NiCl]₂, and B(C₆F₅)₃ were purchased from Strem. PdCl₂ was purchased from J&J Materials and used as received. NaB(Ar_F)₄ (Ar_F = 3,5-(CF₃)₂C₆H₃) was synthesized using literature methods.³² Mesitylene, 2-butyne, 2,3-dichloropropene, 3-bromo-2-methyl-propene, allyl chloride, and allyl bromide were purchased from Aldrich and used without further purification. *tert*-Butyl ethylene purchased from Aldrich was distilled prior to use and hexamethyl benzene was purchased from Aldrich and sublimed prior to use. [(allyl)NiBr]₂, [(2-methallyl)NiBr]₂, [(allyl)NiCl]₂, [(allyl)PdBr]₂, [(allyl)PdCl]₂, [(2-Cl-allyl)PdCl]₂, [(2-methallyl)PdBr]₂, and [(2-methallyl)PdCl]₂ were synthesized according to literature methods.²³⁻²⁶

Spectral data for [B(Ar_F)₄]. The ¹H and ¹³C spectral data for the [B(Ar_F)₄]⁻ counteranion were unchanged for all Ni(II) cationic complexes and are not included in the characterization unless otherwise stated. ¹H NMR (400 MHz, CD₂Cl₂, 20 °C): δ 7.72 (s, 4H, Ar_F H_p), 7.57 (s, 8H, Ar_F H_o). ¹³C {¹H} NMR (101 MHz, CD₂Cl₂, 20 °C): δ 162.1

(q, $^1J_{C-B} = 49.8$ Hz, Ar_F C_{ipso}), 135.2 (s, Ar_F C_o), 129.2 (qq, $^3J_{C-B} = 3.0$ Hz, $^3J_{C-F} = 34.4$ Hz, Ar_F C_{CF₃}), 122.3 (q, $^1J_{C-F} = 273.2$ Hz, CF₃), 117.8 (bt, Ar_F C_p).

General Procedure for the Synthesis of [(Allyl)Pd(Arene)][SbF₆] Complexes.

Under an argon atmosphere, the corresponding palladium halide dimer was dissolved in dry methylene chloride (20 mL) and the resulting yellow solution was stirred at room temperature for five minutes to dissolve the solid. Four equivalents of the corresponding arene were then added via syringe, and the resulting solution cooled to -78 °C. A solution of two equivalents silver hexafluoroantimonate in 5 mL methylene chloride was then added dropwise at -78 °C and the mixture was stirred for ca. 30 min at low temperature before the solution was allowed to warm slowly to room temperature. The resulting solution was cannula filtered and the solvent evaporated in vacuo. The product was washed with 3 x 10 mL of pentane and dried under vacuum to yield product as a yellow powder, which was immediately stored in the glove box at -35 °C to prevent thermal degradation.



[(Allyl)Pd(mes)][SbF₆] (5-H). [(Allyl)PdBr]₂ (0.160 g, 0.440 mmol), mesitylene (240 μL , 1.76 mmol), and AgSbF₆ (0.300 g, 0.880 mmol). Yield: 0.419 g (94%). ^1H NMR (400 MHz, CD₂Cl₂, 25 °C): δ 7.03 (s, 3H, mes_{Ar}), 5.65 (m, 1H, R = H_c), 4.54 (d, 2H, $^3J_{H-H} = 4.8$ Hz, H_{syn}), 3.30 (d, 2H, $^3J_{H-H} = 11.4$ Hz, H_{anti}), 2.44 (s, 9H, mes_{CH₃}). $^{13}\text{C}\{^1\text{H}\}$ NMR

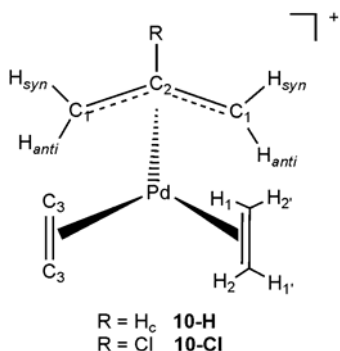
(100 MHz, CD₂Cl₂, 0 °C): δ 133.4 (s, mesC_{ipso}), 116.8 (s, mesC_{Ar}), 109.1 (s, C₂), 65.7 (s, C₁), 20.9 (s, mesC_{CH₃}). Anal. Calcd for C₁₂H₁₇F₆SbPd: C, 28.63; H, 3.41. Found: C, 28.60; H, 3.34.

[(2-Methallyl)Pd(mes)][SbF₆] (5-Me). [(2-Methallyl)PdBr]₂ (0.350 g, 0.720 mmol), mesitylene (500 μ L, 2.88 mmol), and AgSF₆ (0.600 g, 1.44 mmol). Yield: 0.677 g (82%). ¹H NMR (400 MHz, CD₂Cl₂, 25 °C): δ 7.03 (s, 3H, mes_{Ar}), 4.32 (s, 2H, H_{syn}), 3.10 (s, 2H, H_{anti}), 2.44 (s, 9H, mesCH₃), 2.08 (s, 3H, R = CH₃). ¹³C{¹H} NMR (100 MHz, CD₂Cl₂, 0 °C): δ 133.7 (s, mesC_{ipso}), 126.9 (s, C₂), 117.4 (s, mesC_{Ar}), 64.6 (s, C₁), 21.7 (s, R = CH₃), 20.9 (s, mesC_{CH₃}). Anal. Calcd for C₁₃H₁₉F₆SbPd: C, 30.17; H, 3.71. Found: C, 29.99; H, 3.59.

[(2-Cl-allyl)Pd(mes)][SbF₆] (5-Cl). [(2-Cl-allyl)PdCl]₂ (0.192 g, 0.440 mmol), mesitylene (240 μ L, 1.76 mmol), and AgSbF₆ (0.302 g, 0.880 mmol). Yield: 0.393 g (83%). ¹H NMR (400 MHz, CD₂Cl₂, 25 °C): δ 7.12 (s, 3H, mes_{Ar}), 4.72 (s, 2H, H_{syn}), 3.57 (s, 2H, H_{anti}), 2.44 (s, 9H, mesCH₃). ¹³C{¹H} NMR (100 MHz, CD₂Cl₂, 25 °C): δ 134.0 (s, mesC_{ipso}), 124.9 (s, C₂), 117.1 (s, mesC_{Ar}), 65.6 (s, C₁), 20.9 (s, mesC_{CH₃}). Anal. Calcd for C₁₂H₁₆F₆SbPd: C, 26.79; H, 3.00. Found: C, 27.70; H, 3.23.

[(Allyl)Pd(C₆Me₆)][SbF₆] (6-H). [(Allyl)PdCl]₂ (0.160 g, 0.440 mmol), hexamethylbenzene (0.286 g, 1.76 mmol), and AgSbF₆ (0.302 g, 0.880 mmol). Yield: 0.370 g (76%). ¹H NMR (400 MHz, CD₂Cl₂, 25 °C): δ 5.55 (m, 1H, R = H_c), 4.10 (d, ³J_{H-H} = 6.5, 2H, H_{syn}), 3.01 (d, ³J_{H-H} = 11.5 Hz, 2H, H_{anti}), 2.50 (s, 18H, hmbCH₃). ¹³C{¹H} NMR (100 MHz, CD₂Cl₂, 25 °C): δ 126.5 (s, hmbC_{ipso}), 109.1 (s, C₂), 64.0 (s, C₁), 17.2 (s, hmbCH₃). Anal. Calcd for C₁₅H₂₃F₆SbPd: C, 33.02; H, 4.26. Found: C, 33.33; H, 4.31.

Synthesis of (Allyl)Pd(II) Bis-Olefin Complexes.

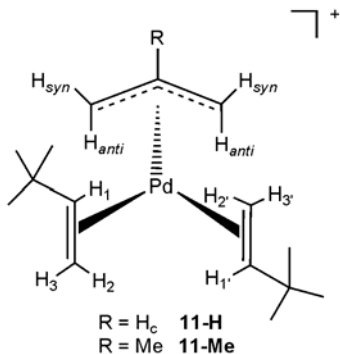


In situ generation of [(allyl)Pd(ethylene)₂][SbF₆] (10-H). A J-Young NMR tube was charged with [(allyl)Pd(mes)][SbF₆] (**5-H**) (0.011 g, 0.020 mmol) dissolved in ca. 400 μ L CDCl₂F. The yellow solution was frozen in liquid nitrogen, and approximately 2 equiv (67.5 mmHg, 0.040 mmol) of ethylene was admitted via a 10.94 mL calibrated gas bulb on a high vacuum line. The tube was then moved to a -78 °C dry ice/isopropyl alcohol bath. The tube was inverted to allow mixing and the solution turned from yellow to colorless.

¹H NMR (500 MHz, CDCl₂F, -110 °C): δ 5.73 (m, 1H, H_c), 5.32 (d, ³J_{H-H} = 7.0 Hz, 2H, H_{syn}), 5.28 (m, 4H, H₁ or H₂), 5.03 (m, 4H, H₂ or H₁), 3.80 (d, ³J_{H-H} = 13 Hz, 2H, H_{anti}). Free mesitylene was observed: (500 MHz, CDCl₂F, -110 °C): δ 6.79 (s, 3H, mes_{Ar}), 2.20 (s, 9H, mes_{CH₃}).

In situ generation of [(2-Cl-allyl)Pd(ethylene)₂][SbF₆] (10-Cl). A J-Young NMR tube was charged with [(2-Cl-allyl)Pd(mes)][SbF₆] (**5-Cl**) (0.010 g, 0.019 mmol) dissolved in ca. 500 μ L CDCl₂F. The yellow solution was frozen at -196 °C, and approximately 3 equivalents (93 torr, 0.056 mmol) of ethylene was admitted via a 10.94 mL calibrated gas bulb on a high vacuum line. The tube was then moved to a -78 °C dry ice-acetone bath. The tube was inverted to allow mixing and the solution turned from yellow to colorless. Variable temperature spectra are shown in Figure 4. ¹H NMR (500 MHz CDCl₂F, -110

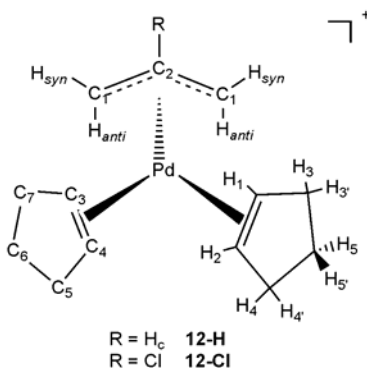
°C): δ 5.24 (m, 4H, $H_{1,1'}$ or $H_{2,2'}$), 5.00 (m, 4H, $H_{2,2'}$ or $H_{1,1'}$), 5.14 (s, 2H, H_{syn}), 3.91 (s, 2H, H_{anti}). $^{13}\text{C}\{^1\text{H}\}$ NMR (100 MHz, CDCl_2F , -110 °C) δ 128.3 (s, C_2), 96.4 (s C_3), 80.7 (s, C_1). Free mesitylene was observed: ^1H NMR (500 MHz CDCl_2F , -110 °C): δ 6.73 (s, 3H, mes_{Ar}), 2.14 (s, 9H, mes_{CH_3}). $^{13}\text{C}\{^1\text{H}\}$ NMR (100 MHz, CDCl_2F , -110 °C): δ 137.9 (s, $\text{mes}_{\text{C}_{\text{CH}_3}}$), 126.9 (s, $\text{mes}_{\text{C}_{\text{Ar}}}$), 21.4 (s, CH_3). Free ethylene was observed: ^1H NMR (500 MHz CDCl_2F , -110 °C): δ 5.33 (s, 2H, vinyl). $^{13}\text{C}\{^1\text{H}\}$ NMR (100 MHz, CDCl_2F , -110 °C): 122.7 (s, C_3).



In situ generation of $[(\text{allyl})\text{Pd}(\text{TBE})_2][\text{SbF}_6]$ (11-H). A screw-cap NMR tube was charged with $[(\text{allyl})\text{Pd}(\text{mes})][\text{SbF}_6]$, **5-H**, (0.011 g, 0.020 mmol) and dissolved in 500 μL CD_2Cl_2 . The tube was placed in a -78 °C bath and 2 equivalents *tert*-butyl ethylene (TBE) were added via syringe. The tube was shaken to allow for mixing and a color change from yellow to colorless was observed. Line broadening begins to occur due to exchange of bound and free TBE at -60 °C. ^1H NMR (400 MHz, CD_2Cl_2 , -90 °C): δ 6.24 (br. m, 1H, H_1), 6.13 (br. m, 1H, H_1), 5.78 (m, 1H, $\text{R} = \text{H}_c$), 5.40 (d, $^3J_{\text{H-H}} = 16.5$ Hz, 2H, H_3 , other H_3 overlapping), 5.10 (br. d, 1H, H_{syn}), 5.02 (br. d, 1H, H_{syn}), 4.77 (d, $^3J_{\text{H-H}} = 8.5$ Hz, 1H, H_2), 4.41 (d, $^3J_{\text{H-H}} = 9.0$ Hz, 1H, H_2), 3.89 (d, $^3J_{\text{H-H}} = 13.0$ Hz, 1H, H_{anti}), 3.25 (d, $^3J_{\text{H-H}} = 12.5$ Hz, 1H, H_{anti}), 1.06-0.98 (br. s, 18H, TBE-CH_3). Free mesitylene

was observed: ^1H (400 MHz, CD_2Cl_2 , $-90\text{ }^\circ\text{C}$): δ 6.79 (s, 3H, mes_{Ar}), 2.20 (s, 9H, mesCH_3).

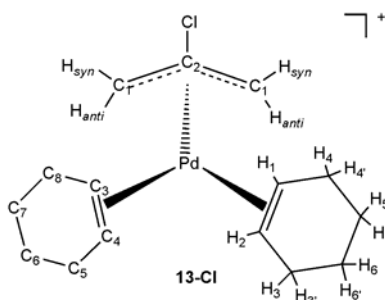
In situ generation of [(2-methallyl)Pd(TBE) $_2$][SbF $_6$] (11-Me). A screw-cap NMR tube was charged with [(2-methallyl)Pd(mes)][SbF $_6$], **5-Me**, (0.012 g, 0.020 mmol) dissolved in 500 μL CD_2Cl_2 . The tube was placed in a $-78\text{ }^\circ\text{C}$ bath and 2 equivalents TBE were added via syringe. The tube was quickly shaken to allow for mixing and a color change from yellow to colorless was observed. Exchange of bound and free TBE occurs at $-50\text{ }^\circ\text{C}$ on the NMR time scale. ^1H NMR (500 MHz, CD_2Cl_2 , $-60\text{ }^\circ\text{C}$): δ 6.32 (m, 1H, H_1), 6.25 (m, 1H, H_1), 5.36 (m, 1H, H_3), 5.30 (m, 1H, H_3), 4.84 (s, 2H, H_{syn}), 4.81 (d, 1H, H_2 , masked by H_{syn}), 4.45 (d, $^3J_{\text{H-H}} = 8.5\text{ Hz}$, 1H, H_2), 3.81 (s, 1H, H_{anti}), 3.16 (s, 1H, H_{anti}), 1.99 (s, 3H, CH_3), 1.06-0.98 (br. s, 18H, TBE- CH_3). Free mesitylene was observed: ^1H NMR (500 MHz, CD_2Cl_2 , $-60\text{ }^\circ\text{C}$): δ 6.79 (s, 3H, mes_{Ar}), 2.20 (s, 9H, mesCH_3).



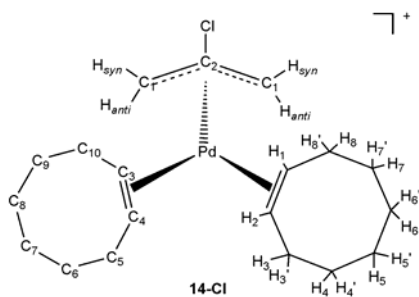
In situ generation of [(allyl)Pd(cyclopentene) $_2$][SbF $_6$] (12-H). A screw-cap NMR tube was charged with [(allyl)Pd(mes)][SbF $_6$] (**5-H**) (0.011 g, 0.020 mmol) dissolved in 400 μL CD_2Cl_2 . The tube was then placed in a $-78\text{ }^\circ\text{C}$ bath and 4 equivalents of cyclopentene (10 μL , 0.080 mmol) were added via syringe. The tube was inverted quickly to allow mixing and the solution turned from yellow to colorless. ^1H NMR (500 MHz, CD_2Cl_2 , $-60\text{ }^\circ\text{C}$): δ 6.03 (s, 2H, H_1 or H_2), 5.80 (s, 2H, H_2 or H_1), 5.58 (m, 1H, H_c), 5.17 (d, $^3J_{\text{H-H}} =$

7.0 Hz, 2H, H_{syn}), 3.65 (d, $^3J_{H-H} = 13.0$ Hz, 2H, H_{anti}), 2.51 (bs, 8H, $H_{4,4'}$ and $H_{3,3'}$), 1.92 (bs, 2H, H_5 or $H_{5'}$), 1.11 (m, 2H, $H_{5'}$ or H_5). Free mesitylene was observed: 1H NMR (500 MHz CD_2Cl_2 , -60 °C): δ 6.83 (s, 3H, mes_{Ar}), 2.26 (s, 9H, mes_{CH_3}). Free cyclopentene was observed: 1H NMR (500 MHz CD_2Cl_2 , -60 °C): δ 5.74 (s, 4H, $H_{1,2}$), 2.30 (bs, 8H, $H_{3,4}$), 1.81 (m, 4H, H_5).

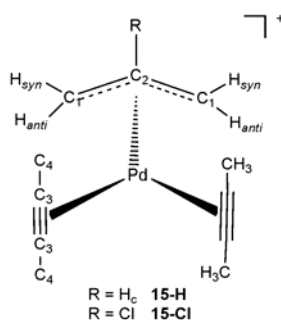
In situ generation of [(2-Cl-allyl)Pd(cyclopentene)₂][SbF₆] (12-Cl). A screw-cap NMR tube was charged with [(2-Cl-allyl)Pd(mes)][SbF₆], **5-Cl**, (0.010 g, 0.019 mmol) dissolved in 500 μ L CD_2Cl_2 . The tube was then placed in a -78 °C bath and 5 equivalents of cyclopentene (10 μ L, 0.093 mmol) were added via syringe. The tube was inverted quickly to allow mixing and the solution turned from yellow to colorless. Variable temperature spectra are shown in Figure 5. 1H NMR (500 MHz, CD_2Cl_2 , -76 °C): δ 6.16 (s, 2H, H_1 or H_2), 5.86 (s, 2H, H_2 or H_1), 5.28 (s, 2H, H_{syn}), 3.96 (s, 2H, H_{anti}), 2.51 (br. m, 8H, $H_{4,4'}$ and $H_{3,3'}$), 1.92 (br. m, 2H, H_5 or $H_{5'}$), 1.05 (m, 2H, $H_{5'}$ or H_5). $^{13}C\{^1H\}$ NMR (100 MHz, CD_2Cl_2 , -87 °C): δ 126.8 (C_2), 113.7 (C_3 or C_4), 113.3 (C_3 or C_4), 83.6 (C_1), 35.0 (C_5 or C_7), 34.8 (C_7 or C_5), 22.6 (C_6). Free mesitylene was observed: 1H NMR (500 MHz CD_2Cl_2 , -76 °C): δ 6.79 (s, 3H, mes_{Ar}), 2.24 (s, 9H, mes_{CH_3}). $^{13}C\{^1H\}$ NMR (100 MHz, CD_2Cl_2 , -87 °C): δ 137.7 (s, $mes_{C_{CH_3}}$), 126.8 (s, $mes_{C_{Ar}}$), 21.4 (s, CH_3). Free cyclopentene was observed: 1H NMR (500 MHz CD_2Cl_2 , -76 °C): δ 5.76 (s, 2H, $H_{1,2}$), 2.27 (t, $^3J_{H-H} = 7.5$ Hz, 4H, $H_{3,4}$), 1.78 (m, 2H, H_5). $^{13}C\{^1H\}$ NMR (100 MHz, CD_2Cl_2 , -87 °C): δ 130.8 (s, $C_{3,4}$), 32.6 (s, $C_{5,7}$), 23.0 (s, C_6).



In situ generation of [(2-Cl-allyl)Pd(cyclohexene)₂][SbF₆] (13-Cl). This compound was generated according to the above procedure, using **5-Cl** (0.010 g, 0.019 mmol) dissolved in 500 μ L of CD₂Cl₂ and 5 equivalents of cyclohexene (10 μ L, 0.0980 mmol). ¹H NMR (500 MHz, CD₂Cl₂, -77 °C): δ 6.47 (s, 2H, H₁ or H₂), 5.95 (s, 2H, H₂ or H₁), 4.82 (s, 2H, H_{syn}), 4.03 (s, 2H, H_{anti}), 2.40 (bm, 8H, H_{4,4'} and H_{3,3'}), 1.05 (m, 8H, H_{5,5'} and H_{6,6'}). ¹³C{¹H}NMR (100 MHz, CD₂Cl₂, -87 °C): δ 130.0 (s, C₂), 116.4 (s, C₃ or C₄), 114.3 (s, C₃ or C₄), 80.6 (s, C₁), 26.7 (s, C₅ or C₈), 26.4 (s, C₅ or C₈), 21.2 (s, C₆ or C₇), 20.9 (s, C₆ or C₇). Free mesitylene was observed: ¹H NMR (500 MHz CD₂Cl₂, -77 °C): δ 6.79 (s, 3H, mes_{Ar}), 2.24 (s, 9H, mes_{CH₃}). ¹³C{¹H} NMR (100 MHz, CD₂Cl₂, -87 °C): δ 137.9 (s, mesC_{CH₃}), 126.9 (s, mesC_{Ar}), 21.4 (s, CH₃). Free cyclohexene was observed: ¹H NMR (500 MHz, CD₂Cl₂, -77 °C): δ 5.73 (s, 2H, H_{1,2}), 2.24 (bs, 4H, H_{3,4}), 1.15 (bs, 4H, H_{5,6}). ¹³C{¹H} NMR (100 MHz, CD₂Cl₂, -87 °C): δ 127.3 (s, C_{3,4}), 25.3 (s, C_{5,8}), 22.8 (s, C_{6,7}).



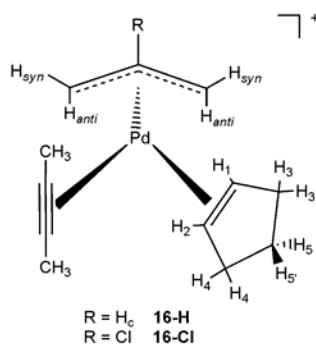
In situ generation of [(2-Cl-allyl)Pd(cyclooctene)₂][SbF₆] (14-Cl). This compound was generated according to the above procedure; in this instance **5-Cl** (0.010 g, 0.019 mmol) dissolved in 500 μ L CD₂Cl₂ and 2.2 equivalents of cyclooctene (5.2 μ L, 0.040 mmol) were employed. ¹H NMR (500 MHz, CD₂Cl₂, -50 °C): δ 6.08 (s, 2H, H₁ or H₂), 5.78 (s, 2H, H₂ or H₁), 4.72 (s, 2H, H_{syn}), 3.94 (s, 2H, H_{anti}), 2.48 (bm, 8H, H_{8,8'} and H_{3,3'} or H_{4,4'} and H_{7,7'}), 2.35 (bm, 8H, H_{8,8'} and H_{3,3'} or H_{4,4'} and H_{7,7'}), 1.88 (bm, 8H, H_{5,5'} and H_{6,6'}). ¹³C{¹H} NMR (100 MHz, CD₂Cl₂, -51 °C): δ 132.4 (s, C₂), 117.7 (s, C₃ or C₄), 116.0 (s, C₄ or C₃), 80.7 (s, C₁), 30.3 (s, C₅ or C₁₀), 30.2 (s, C₁₀ or C₅), 28.7 (s, C₆ or C₉), 28.5 (s, C₉ or C₆), 25.8 (s, C₇ or C₈), 25.6 (s, C₈ or C₇). Free mesitylene was observed: ¹H NMR (500 MHz CD₂Cl₂, -50 °C): δ 6.79 (s, 3H, mes_{Ar}), 2.24 (s, 9H, mes_{CH₃}). ¹³C{¹H} NMR (100 MHz, CD₂Cl₂, -51 °C): δ 137.8 (s, mesC_{CH₃}), 126.8 (s, mesC_{Ar}), 21.3 (s, CH₃). Free cyclooctene was observed: ¹H NMR (500 MHz, CD₂Cl₂, -50 °C): δ 5.70 (s, 2H, H_{1,2}), 2.24 (bs, 4H, H_{3,8}), 2.17 (bs, 4H, H_{4,7}), 1.51 (bs, 4H, H_{5,6}). ¹³C{¹H} NMR (100 MHz, CD₂Cl₂, -51 °C): δ 130.2 (s, C_{3,4}), 29.3 (s, C_{5,10}), 26.3 (s, C_{6,9}), 25.6 (s, C_{7,8}).



In situ generation of [(allyl)Pd(2-butyne)₂][SbF₆] (15-H). A screw-cap NMR tube was charged with [(allyl)Pd(mes)][SbF₆] (**5-H**) (0.011 g, 0.020 mmol) dissolved in ca. 400 μ L CDCl₂F. The tube was placed in a -78 °C bath and 2 equivalents 2-butyne (3.1 μ L, 0.040

mmol) were added via syringe. The number of equivalents of ligand added was NMR via NMR integration. The tube was shaken to allow for mixing and a color change from yellow to colorless was observed. ^1H NMR (500 MHz, CDCl_2F , $-120\text{ }^\circ\text{C}$): δ 6.05 (m, 1H, H_c), 4.72 (d, $^3J_{\text{H-H}} = 6.5\text{ Hz}$, 2H, H_{syn}), 3.72 (d, $^3J_{\text{H-H}} = 13.0\text{ Hz}$, 2H, H_{anti}), 2.11 (s, 12H, 2-butyne- CH_3). Free mesitylene was observed: (500 MHz, CDCl_2F , $-120\text{ }^\circ\text{C}$): δ 6.77 (s, 3H, mes_{Ar}), 2.22 (s, 9H, mes_{CH_3}).

In situ generation of [(2-Cl-allyl)Pd(2-butyne) $_2$][SbF $_6$] (15-Cl). This compound was generated according to the above procedure. [(2-Cl-allyl)Pd(mes)][SbF $_6$] (**5-Cl**) (0.020 g, 0.037 mmol) was dissolved in 500 μL CD_2Cl_2 and treated with 2-butyne (14 μL , 0.098 mmol). ^1H NMR (500 MHz, CD_2Cl_2 , $-90\text{ }^\circ\text{C}$): δ 4.83 (s, 2H, H_{syn}), 3.94 (s, 2H, H_{anti}), 2.18 (s, 12H, butyne- CH_3). $^{13}\text{C}\{^1\text{H}\}$ NMR (100 MHz, CD_2Cl_2 , $-90\text{ }^\circ\text{C}$): δ 132.1 (s, C_2), 75.8 (s, C_1), 68.6 (s, C_3), 7.32 (s, C_4). Free mesitylene was observed: ^1H NMR (500 MHz, CD_2Cl_2 , $-90\text{ }^\circ\text{C}$): δ 6.79 (s, 3H, mes_{Ar}), 2.24 (s, 9H, mes_{CH_3}). $^{13}\text{C}\{^1\text{H}\}$ NMR (100 MHz, CD_2Cl_2 , $-90\text{ }^\circ\text{C}$): δ 137.8 (s, $\text{mes}_{\text{C}_{\text{CH}_3}}$), 126.8 (s, $\text{mes}_{\text{C}_{\text{Ar}}}$), 21.3 (s, CH_3). Free 2-butyne was observed: ^1H NMR (500 MHz, CD_2Cl_2 , $-90\text{ }^\circ\text{C}$): δ 1.70 (s, 6H, CH_3). $^{13}\text{C}\{^1\text{H}\}$ NMR (100 MHz, CD_2Cl_2 , $-90\text{ }^\circ\text{C}$): δ 74.6 (s, C_3), 3.3 (s, C_4).



In situ generation of [(allyl)Pd(2-butyne)(cyclopentene)][SbF $_6$] (16-H). To the in situ complex [(allyl)Pd(2-butyne) $_2$][SbF $_6$] (**15-H**) described above, 2 equivalents of

cyclopentene (6 μ L, 0.040 mmol) were added via syringe while the tube was in a -78 $^{\circ}$ C dry ice/isopropyl alcohol bath. The tube was shaken to allow for mixing. ^1H NMR (500 MHz, CDCl_2F , -110 $^{\circ}$ C): δ 5.95, (bs, 1H, H_1 or H_2), 5.88 (m, 1H, H_c), 5.71, (bs, 1H, H_1 or H_2), 5.00 (d, $^3J_{\text{H-H}} = 6.5$ Hz, 1H, H_{syn_1} or H_{syn_2}), 4.86 (d, $^3J_{\text{H-H}} = 7.0$ Hz, 1H, H_{syn_1} or H_{syn_2}), 3.96 (d, $^3J_{\text{H-H}} = 13.0$ Hz, 2H, H_{anti_1} or H_{anti_2}), 3.76 (d, $^3J_{\text{H-H}} = 13.0$ Hz, 1H, H_{anti_1} or H_{anti_2}), 2.52 (bs, 4H, $\text{H}_{4,4'}$ and $\text{H}_{3,3'}$), 2.06 (s, 6H, 2-butyne- CH_3), 1.79 (m, 1H, $\text{H}_{5'}$ or H_5), 1.46 (m, 1H, $\text{H}_{5'}$ or H_5). Free mesitylene was observed: (500 MHz, CDCl_2F , -110 $^{\circ}$ C): δ 6.84 (s, 3H, mes_{Ar}), 2.24 (s, 9H, mes_{CH_3}).

In situ generation of [(2-Cl-allyl)Pd(2-butyne)(cyclopentene)][SbF₆] (16-Cl). [(2-Cl-allyl)Pd(mes)][SbF₆] (**5-Cl**) (0.020 g, 0.037 mmol) was dissolved in 500 μ L CD_2Cl_2 and treated with three equivalents 2-butyne (8.7 μ L, 0.11 mmol) and three equivalents of cyclopentene (9.7 μ L, 0.11 mmol), both added via syringe while the tube was in a -78 $^{\circ}$ C dry ice/isopropyl alcohol bath. The tube was shaken to allow for mixing. ^1H NMR (500 MHz, CDCl_2F , -30 $^{\circ}$ C): δ 6.22, (bs, 1H, H_1 or H_2), 5.63, (bs, 1H, H_1 or H_2), 5.05 (s, 1H, H_{syn_1} or H_{syn_2}), 5.01 (s, 1H, H_{syn_1} or H_{syn_2}), 4.19 (s, 2H, H_{anti_1} or H_{anti_2}), 4.11 (s, 1H, H_{anti_1} or H_{anti_2}), 2.38 (bm, 4H, $\text{H}_{4,4'}$ and $\text{H}_{3,3'}$), 2.11 (s, 6H, 2-butyne- CH_3), 1.93 (m, 1H, $\text{H}_{5'}$ or H_5), 1.15 (m, 1H, $\text{H}_{5'}$ or H_5). Free mesitylene was observed: (500 MHz, CDCl_2F , -30 $^{\circ}$ C): δ 6.78 (s, 3H, mes_{Ar}), 2.24 (s, 9H, mes_{CH_3}). Free 2-butyne was observed: (500 MHz, CDCl_2F , -30 $^{\circ}$ C): δ 1.74 (s, 6H, CH_3). Free cyclopentene was observed: (500 MHz, CDCl_2F , -30 $^{\circ}$ C): δ 5.63 (s, 4H, $\text{H}_{1,2}$), 2.37 (t, $^3J_{\text{H-H}} = 7.2$ Hz, 8H, $\text{H}_{3,4}$), 1.76 (m, 4H, H_5).

Dynamic Measurements using ^1H NMR Line Broadening.

^1H NMR line broadening experiment to determine the mechanism of exchange of bound and free mesitylene in 5-H. Three screw-cap NMR tubes were each charged

with [(allyl)Pd(mes)][SbF₆], **5-H**, (0.011 g, 0.020 mmol) and dissolved in CD₂Cl₂. 2 (4.0 μ L, 0.040 mmol), 4 (8.0 μ L, 0.080 mmol), and 6 (12 μ L, 0.120 mmol) equivalents of mesitylene were added respectively for a total volume of 500 μ L. The tubes were quickly shaken to allow for mixing and ¹H NMR spectra were recorded for each sample at low temperature after 5 minutes of equilibration. Due to poor solubility, NMR spectra could not be recorded below ca. -80 °C; however the changes in line-width at half-height of the coordinated mesitylene resonance (δ 7.90 ppm) were monitored for each of the three samples at -77 °C and -67 °C. The rate constant was calculated using the slow exchange approximation to yield $k_{\text{ex}} = 22$, 16, and 16 s⁻¹ for 6, 4, and 2 equivalents of added mesitylene, respectively, at -67 °C: $k_{\text{ex}} = \pi(\Delta\omega)$ where $\Delta\omega$ (6 equiv) = 6.9 Hz ($\Delta G^\ddagger = 10.7$ kcal/mol); $\Delta\omega$ (4 equiv) = 5.0 Hz ($\Delta G^\ddagger = 10.8$ kcal/mol); $\Delta\omega$ (2 equiv) = 5.1 Hz ($\Delta G^\ddagger = 10.8$ kcal/mol). See Figure 3 for variable temperature spectra of the exchange process.

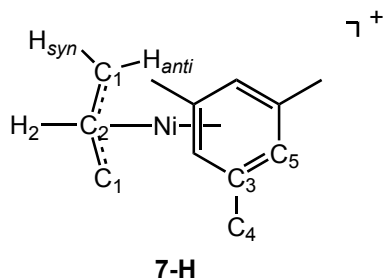
¹H NMR line broadening experiments to determine the mechanism of exchange of bound and free cyclopentene. Three separate screw-cap NMR tubes were charged with [(2-Cl-allyl)Pd(mes)][SbF₆] (**5-Cl**) (0.010 g, 0.019 mmol). In a -78 °C dry ice-acetone bath, 6 equiv (10.1 μ L, 0.11 mmol), 9 equiv (15.1 μ L, 0.17 mmol), and 12 equiv (20.1 μ L, 0.23 mmol) respectively, of cyclopentene were added to the three NMR tubes, followed by the addition of CD₂Cl₂ to reach a total volume of 500 μ L. Broadening of the bound vinyl ¹H resonance (6.16 ppm) was monitored between -56 °C and -45 °C. The initial half height line width at -56 °C was 12 Hz for 6 and 9 equiv, and 13 Hz for 12 equiv; and at -45 °C 22 Hz for 6 equiv, 23 Hz for 9 equiv and 24 Hz for 12 equiv. The rate constant was calculated using the slow exchange approximation to give $k_{\text{ex}} = 31$ s⁻¹ at 6 equiv, 35 s⁻¹ at 9 equiv 33 s⁻¹ at 12 equiv: $k_{\text{ex}} = \pi(\Delta\omega)$ where $\Delta\omega = 10$ Hz ($\Delta G^\ddagger = 11.7$

kcal/mol) for 6 equiv, 11 Hz ($\Delta G^\ddagger = 11.7$ kcal/mol) for 9 equiv, and 11 Hz ($\Delta G^\ddagger = 11.7$ kcal/mol) for 12 equiv. See Figure 5 for variable temperature spectra of exchange process.

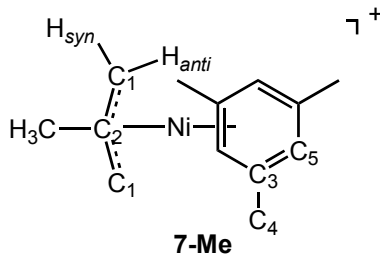
¹H line broadening experiments for the exchange of bound and free ethylene. Using line-broadening techniques, the rate of exchange of bound and free ethylene was determined upon the addition of ca. 3 equivalents of ethylene to **5-Cl**. Broadening of the coordinated ethylene groups (¹H NMR resonance 5.19 ppm) was monitored between -77 °C to -56 °C. The initial half height width at -77 °C was 16 Hz. The line width was 18 Hz at -66 °C and 24 Hz at -56 °C. The rate constants calculated using the slow exchange approximation are $k_{\text{ex}} = 7.4 \text{ s}^{-1}$ at -66 °C and $k_{\text{ex}} = 21 \text{ s}^{-1}$: where $\Delta\omega = 2.4$ Hz at -66 °C and $\Delta\omega = 7.7$ Hz at -56 °C. At -66 °C, $\Delta G^\ddagger = 11.4$ kcal/mol, assuming a dissociative mechanism as previously observed for cyclopentene exchange. See Figure 4 for variable temperature spectra for the exchange process.

¹H line broadening experiments for the exchange of bound and free 2-butyne. Using line-broadening techniques, the rate of exchange of bound and free 2-butyne was determined for the addition of ca. 3 equivalents of 2-butyne to **5-Cl**. Broadening of the methyl resonance (2.13 ppm) of 2-butyne was monitored between -66 °C and -24 °C. The initial half-height line width at -66 °C was 3.7 Hz. The line widths were measured as 5.2 and 15 Hz at -45 °C and -24 °C, respectively. The rate constants, calculated using the slow exchange approximation, are $k_{\text{ex}} = 4.6 \text{ s}^{-1}$ at -45 °C and $k_{\text{ex}} = 36 \text{ s}^{-1}$ at -24 °C: where $\Delta\omega = 1.5$ Hz at -45 °C and $\Delta\omega = 11.6$ Hz at -24 °C. At -45 °C, $\Delta G^\ddagger = 12.6$ kcal/mol, assuming a dissociative exchange mechanism as previously observed for cyclopentene exchange.

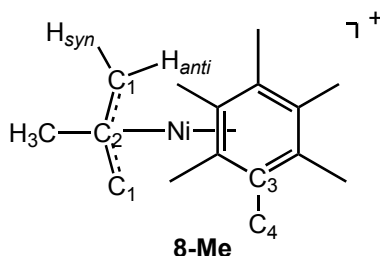
Synthesis of (Allyl)Ni(Arene)⁺ Complexes.



[(Allyl)Ni(mes)][B(Ar_F)₄] (7-H). A flame dried Schlenk flask was charged with [(allyl)NiBr]₂ (0.270 g, 0.751 mmol) and NaB(Ar_F)₄ (1.33 g, 1.50 mmol). The flask was cooled to -80 °C and Et₂O (12.0 mL) was added. To the stirring deep orange-red solution was added mesitylene (550 μL, 3.95 mmol) and the reaction was warmed to 0 °C and allowed to stir for 1h. The volatiles were then removed in vacuo and the red residue was dissolved CH₂Cl₂ and filtered through Celite. The solvent was removed in vacuo and the solid product was washed with pentane (3 x 10 mL). The pentane was decanted and the product was dried in vacuo to give **7-H** (0.920 g, 0.849 mmol) in 57 % yield. Red X-ray quality crystals were obtained by dissolving **7-H** in CH₂Cl₂ (2.0 mL) and layering with pentane (6.0 mL) and placing in a -30 °C freezer for 2 days. ¹H NMR (300 MHz, CD₂Cl₂, 25 °C): δ 6.66 (s, 3H, mes_{Ar}), 5.85 (m, 1H, H₂), 3.69 (d, ³J_{H-H} = 6.6 Hz, 2H, H_{syn}), 2.45 (d, ³J_{H-H} = 12.6 Hz, 2H, H_{anti}), 2.35 (s, 9H, mes_{CH₃}). ¹³C{¹H} NMR (126 MHz, CD₂Cl₂, 25 °C): δ 124.8 (s, C₃), 109.5 (s, C₅), 107.5 (s, C₂), 59.7 (s, C₁), 20.6 (s, C₄). ¹⁹F NMR (376 MHz, CD₂Cl₂, 25 °C): δ -63.4 (s, 24F). Anal. Calcd for C₄₄H₂₉F₂₄BNi: C, 48.79; H, 2.70. Found: C, 48.40; H, 2.68.



[(2-Methallyl)Ni(mes)][B(Ar_F)₄] (7-Me). This complex was synthesized following the above procedure for **7-H** starting from [(2-methallyl)NiBr]₂ (0.101 g, 0.260 mmol), NaB(Ar_F)₄ (0.460 g, 0.519 mmol), and mesitylene (215 μ L, 1.55 mmol). Yield of **7-Me**: 83 % (0.474 g, 0.432 mmol). ¹H NMR (400.1 MHz, CD₂Cl₂, 25 °C): δ 6.62 (s, 3H, Mes_{Ar}), 3.54 (s, 2H, H_{syn}), 2.34 (s, 2H, H_{anti}), 2.35 (s, 9H, MesCH₃) 2.13 (s, 3H, CH₃). ¹³C{¹H} NMR (126 MHz, CD₂Cl₂, 25 °C): δ 124.5 (s, C₃), 109.2 (s, C₅ overlapping C₂), 60.1 (s, C₁), 22.2 (s, CH₃ overlapping C₄). ¹⁹F NMR (376 MHz, CD₂Cl₂, 25 °C): δ -63.4 (s, 24F). Anal. Calcd for: C₄₅H₃₁F₂₄BNi: C, 49.26; H, 2.85. Found: C, 48.89; H, 2.63.



[(2-Methallyl)Ni(hexamethylbenzene)][B(Ar_F)₄] (8-Me). A Schlenk flask was charged with (0.100 g, 0.340 mmol) of [(2-methallyl)NiCl]₂ and NaB(Ar_F)₄ (0.604 g, 0.683 mmol) and dissolved in 8.0 mL of diethyl ether in a -78 °C dry ice-acetone bath. To this, hexamethylbenzene (0.224 g, 12.2 mmol) dissolved in 2.0 mL of CH₂Cl₂ was added via cannula. The mixture was removed from the cooling bath until a color change was observed, then the reaction mixture was held at 0 °C for an additional 2 hours. The reaction mixture was then cannula filtered into a second Schlenk flask, and taken to

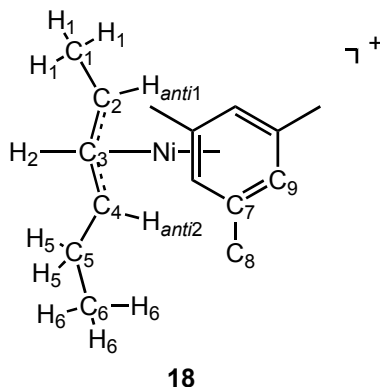
dryness in dynamic vacuum. The resulting red solid was washed with pentane (3 x 10.0 mL) and dried in vacuo. Red X-ray quality crystals were obtained by dissolving **8-Me** in CH₂Cl₂ (2.0 mL) layering with pentane (6.0 mL) and placing in a -30 °C freezer until solvent evaporation occurred. ¹H NMR (500 MHz, CD₂Cl₂, 25 °C): δ 3.04 (s, 2H, H_{syn}), 2.31 (s, 18H, hmb_{CH₃}), 2.09 (s, 2H, H_{anti}), 2.03 (s, 3H, CH₃). ¹³C{¹H} NMR (CD₂Cl₂, 100 MHz, 25 °C): δ 123.8 (s, C₂), 119.5 (s, C₃), 59.1 (s, C₁), 21.8 (s, CH₃), 17.2 (s, C₄). Anal. Calcd for: C₄₈H₃₇F₂₄BNi: C, 50.60; H, 3.27. Found: C, 50.32; H, 3.08.

In situ generation of (allyl)Ni(hmb)⁺. A screw top NMR tube was charged with **7-H** (0.010 g, 0.009 mmol), and dissolved in 600 μL of CD₂Cl₂. Hexamethylbenzene (0.004 g, 0.025 mmol) was added and the NMR tube was inverted to allow for mixing. (Allyl)Ni(hmb)⁺ was generated quantitatively as determined by ¹H NMR. This reaction was complete within 10 minutes. ¹H NMR (300 MHz, CD₂Cl₂, 25 °C): δ 6.80 (s, 3H, free mes, mes_{Ar}), 5.73 (m, 1H, H_c), 3.24 (d, ³J_{H-H} = 6.6 Hz, 2H, H_{syn}), 2.31 (s, 18H, hmb_{CH₃}), 2H *anti* doublet under mesitylene and hexamethylbenzene.

Addition of diethyl ether to (allyl)Ni(mes)⁺. Three screw-top NMR tubes were each charged with [(allyl)Ni(mes)][B(Ar_F)₄] (**7-H**) (0.010 g, 0.010 mmol) and dissolved in CD₂Cl₂. 14 (14.5 μL, 0.138 mmol), 20 (19.4 μL, 0.185 mmol), and 25 (24.2 μL, 0.231 mmol) equivalents of diethyl ether were added respectively to yield a total volume of 500 μL in each tube. The reaction was monitored by ¹H NMR spectroscopy. An equilibrium concentration of [(allyl)Ni(OEt₂)₂][B(Ar_F)₄] (**17**) was observed within 3 h as evidenced by the presence of new central, *syn*, and *anti* signals, as well as free mesitylene (δ 6.79). Exchange of bound and free diethyl ether is observed at room temperature. The *K_{eq}* was calculated at 14, 20, and 25 equivalents of diethyl ether to be 2.5 x 10⁻⁴ M⁻¹. ¹H NMR

(400 MHz, CD₂Cl₂, 25 °C) δ : 5.94 (m, 1H, H₂), 3.10 (d, $^3J_{\text{H-H}} = 7.2$ Hz, 2H, H_{syn}), 2.01 (d, $^3J_{\text{H-H}} = 13.2$ Hz, 2H, H_{anti}).

Reaction of Olefins with Complexes 7-H or 7-Me.



In situ generation of [(2-hexenyl)Ni(mes)][B(Ar_F)₄] (18**).** A J-Young tube was charged with **7-H** (0.010 g, 0.009 mmol) and dissolved in CD₂Cl₂ (500 μ L). 1-Hexene (4.50 μ L, 0.037 mmol) was added via microliter syringe and the solution was mixed. The reaction was monitored by ¹H NMR spectroscopy at room temperature. Complete formation of (2-hexenyl)Ni(Mes)[B(Ar_F)₄], **18**, was observed within an hour.

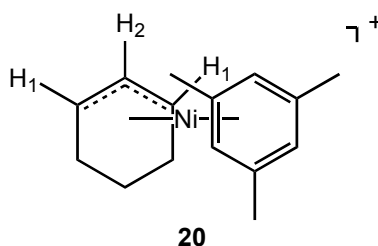
The same procedure, as described above was followed to generate **18** using *cis*-2-hexene. Complex **7-H** (0.099 g, 0.009 mmol) was treated with *cis*-2-hexene (5.70 μ L, 0.045 mmol) in CD₂Cl₂ (600 μ L). The reaction was complete within 1 h.

The same procedure, as described above, was followed to generate **18** using *trans*-2-hexene. Complex **7-H** (0.010 g, 0.009 mmol) was treated with *trans*-2-hexene (5.70 μ L, 0.045 mmol) in CD₂Cl₂ (600 μ L). The reaction was complete within 1 h.

To obtain complete NMR characterization of **18**, the volatiles were removed in vacuo and the residue was redissolved in CD₂Cl₂ in the drybox. ¹H NMR (400 MHz, CD₂Cl₂, 25 °C): δ 6.44 (s, 3H, mes_{Ar}), 5.46 (t, $^3J_{\text{H-H}} = 11.2$ Hz, 1H, H₂), 3.14 (m, 2H, H_{anti1}

overlapping H_{anti_2}), 2.32 (s, 9H, mes_{CH_3}), 1.32 (pent., $^3J_{H-H} = 6.4$ Hz, 2H, H_5), 1.05 (t, $^3J_{H-H} = 7.2$, 3H, H_6), 1.01 (d, 3H, $^3J_{H-H} = 6.8$ Hz, H_1). $^{13}C\{^1H\}$ NMR (101 MHz, CD_2Cl_2 , 25 °C): δ 123.2 (s, C_7), 109.0 (s, C_9), 105.4 (s, C_3), 83.0 (s, C_4), 76.3 (s, C_2), 26.4 (s, C_4), 19.5 (s, C_8), 18.8 (s, C_1), 12.6 (s, C_6). 1H NMR shifts for free propene: 1H NMR (400 MHz, CD_2Cl_2 , 25 °C): δ 5.84 (m, 2H, H_{vinyl}), 5.03 (d, $^3J_{H-H} = 16.0$ Hz, 1H, H_{trans}), 4.93 (d, $^3J_{H-H} = 8.0$ Hz, 1H, H_{cis}), 1.71 (d, 3H, $^3J_{H-H} = 8.0$ Hz, CH_3).

Low temperature 1H NMR study of the reaction of 7-Me with 1-hexene. A screw top NMR tube was charged with complex **7-Me** (0.010 g, 0.009 mmol) and dissolved in CD_2Cl_2 (600 μ L). The tube was placed in a dry ice/acetone bath at -80 °C. At this point, 1-hexene (4.4 μ L, 0.035 mmol) was added via microliter syringe. The reaction was monitored by low temperature 1H NMR spectroscopy. No change in the spectrum occurred until -30 °C. At this temperature isomerization occurred. Monitoring the reaction at this temperature, showed isomerization was complete within 1.5 h. At -10 °C, complex **18** began to grow in while starting complex **7-Me** was slowly being consumed. Free isobutylene is observed: 1H NMR (400 MHz, CD_2Cl_2 , -10 °C): δ 4.65 (s, 2H, vinyl CH_2), 1.72 (s, 6H, CH_3).



In situ generation of $[(Cyclohexenyl)Ni(mes)][B(Ar_F)_4]$ (20**).** Complex **7-H** (0.010 g, 0.009 mmol) was added to a J-Young tube and dissolved in CD_2Cl_2 (600 μ L). The

solution was mixed and cyclohexene (4.7 μL , 0.046 mmol) was added via syringe. The reaction was monitored by ^1H NMR spectroscopy at 25 $^\circ\text{C}$. Formation of $[(\text{cyclohexenyl})\text{Ni}(\text{mes})][\text{B}(\text{Ar}_\text{F})_4]$, **20**, and propene were observed immediately in the ^1H NMR spectrum. Complete conversion was observed within 1 hour. ^1H NMR (400 MHz, CD_2Cl_2 , 25 $^\circ\text{C}$): δ 6.55 (s, 3H, mes_{Ar}), 5.86 (t, $^3J_{\text{H-H}} = 6.4$ Hz, 1H, H_2), 4.81 (br. t, 2H, H_1), 2.34 (s, 9H, mes_{CH_3}), 1.50-1.00 (m, 6H, CH_2).

Crystal Structure Determination of **7-H** and **8-Me**.

The crystallographic information for **7-H** and **8-Me** is reported in Appendix I. The data was obtained on a Bruker SMART APEX-2 X-ray diffractometer at -173 $^\circ\text{C}$ using Mo- $\text{K}\alpha$ radiation for **7-H** and Cu- $\text{K}\alpha$ radiation for **8-Me**.

References

1. Crabtree, R. H., In *The Organometallic Chemistry of the Transition Metals*. John Wiley & Sons, Inc.: New York, **2001**.
2. In *Comprehensive Organometallic Chemistry*. Mingos, D. M. P., Crabtree, R. H., Parkin, G. Ed.; Elsevier: New York, **2007**.
3. Gouriou, L.; Lloyd-Jones, G. C.; Vyskočil, Š.; Kočovský, P. *J. Organomet. Chem.* **2003**, *687*, 525-537.
4. Bray, K. L.; Charmant, J. P. H.; Fairlamb, I. J. S.; Lloyd-Jones, G. C. *Chem. Eur. J.* **2001**, *7*, 4205-4215.
5. O'Connor, A. R.; White, P. S.; Brookhart, M. *J. Am. Chem. Soc.* **2007**, *129*, 4142-4143.
6. Mabbott, D. J.; Mann, B. E.; Maitlis, P. M. *J. Chem. Soc. Dalton Trans.* **1977**, 294-299.
7. Goodall, B. L. Cycloaliphatic polymers via late transition metal catalysis. In *Late Transition Metal Polymerization Catalysis*, Rieger, B., Saunders Baugh, L., Kacker, S., Striegler, S. Eds.; Wiley-VCH: Weinheim, **2003**; 101-133.
8. Taube, R.; Wache, S. *J. Organomet. Chem.* **1992**, *428*, 431-442.
9. Taube, R.; Sylvester, G. Stereospecific Polymerization of Butadiene or Isoprene. In *Applied Homogeneous Catalysis with Organometallic Complexes*, Cornils, B., Herrmann, W. A. Eds.; VCH: Weinheim, Germany, **1996**; 280-318.
10. Taube, R.; Schmidt, U.; Gehrke, J. P.; Anacker, U. *J. Prakt. Chem.* **1984**, *326*, 1-11.
11. Taube, R.; Langlotz, J.; Sieler, J.; Gelbrich, T.; Tittes, K. *J. Organomet. Chem.* **2000**, *597*, 92-104.
12. Taube, R.; Gehrke, J. P.; Schmidt, U. *Makromol. Chem., Macromol. Symp.* **1986**, *3*, 389-404.
13. Taube, R.; Gehrke, J. P.; Schmidt, U. *J. Organomet. Chem.* **1985**, *292*, 287-296.
14. Taube, R.; Gehrke, J. P.; Böhme, P.; Scherzer, K. *J. Organomet. Chem.* **1991**, *410*, 403-416.
15. Taube, R.; Gehrke, J. P.; Böhme, P.; Kötnitz, J. *J. Organomet. Chem.* **1990**, *395*, 341-358.

16. Taube, R.; Gehrke, J. P.; Böhme, P. *Wiss. Z. Tech. Leuna-Merseburg* **1987**, *29*, 310-325.
17. Taube, R.; Gehrke, J. P. *J. Organomet. Chem.* **1985**, *291*, 101-115.
18. Taube, R.; Gehrke, J. P. *J. Organomet. Chem.* **1987**, *328*, 393-401.
19. Cámpora, P. J.; Carmona, G. E.; Conejo Argandoña, M. M. ES Patent 2200698, **2004**.
20. Cámpora, J.; Conejo, M. D. M.; Reyes, M. L.; Mereiter, K.; Passaglia, E. *Chem. Commun.* **2003**, 78-79.
21. Tobisch, S.; Taube, R. *Organometallics* **2008**, *27*, 2159-2162.
22. For Ni complexes, R₂ = substituent on the 1 position of the allyl moiety.
23. Aranyos, A.; Szabó, K. J.; Castaño, A. M.; Bäckvall, J.-E. *Organometallics* **1997**, *16*, 1058-1064.
24. Auburn, P. R.; Mackenzie, P. B.; Bosnich, B. *J. Am. Chem. Soc.* **1985**, *107*, 2033-2046.
25. Dent, W. T.; Long, R.; Wilkinson, A. J. *J. Chem. Soc.* **1964**, 1585-1588.
26. Wilke, G.; Bogdanovic, B.; Heimbach, P.; Keim, W.; Krüner, M.; Oberkirch, W.; Tanaka, K.; Steinrücke, E.; Walter, D.; Zimmerman, H. *Angew. Chem. Int. Ed.* **1966**, *5*, 151-164.
27. Similar reactivity is also observed with olefins and **3-Crotyl**.
28. O'Connor, A. R.; Brookhart, M. *Manuscript in Preparation*.
29. Alaimo, P. J.; Peters, D. W.; Arnold, J.; Bergman, R. G. *J. Chem. Educ.* **2001**, *78*, (1), 64.
30. Pangborn, A. B.; Giardello, M. A.; Grubbs, R. H.; Rosen, R. K.; Timmers, F. J. *Organometallics* **1996**, *15*, 1518-1520.
31. Siegel, J. S.; Anet, F. A. *J. Org. Chem.* **1988**, *53*, 2629-2630.
32. Yakelis, N. A.; Bergman, R. G. *Organometallics* **2005**, *24*, 3579-3581.

CHAPTER THREE

Reactivity of [(Allyl)Palladium(Arene)]⁺ Complexes with Dienes

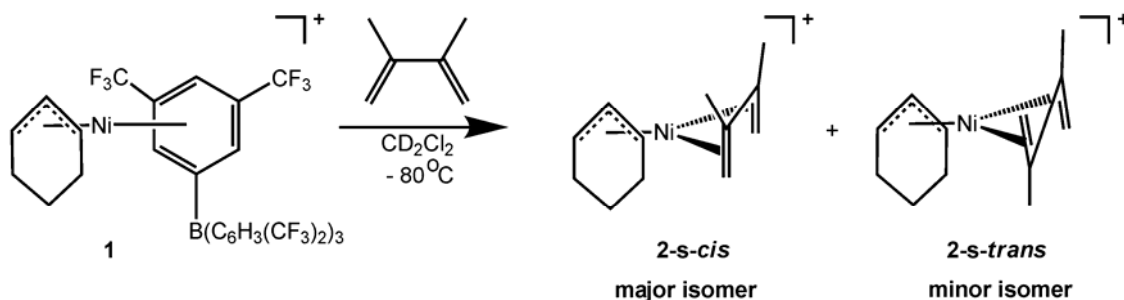
Introduction

Polymerizations of butadiene using cationic (allyl)Ni(II) complexes containing highly labile ligands have been reported by Taube,¹⁻⁹ Cámpora,^{10,11} and our laboratory¹² (also see chapter 2). O'Connor and Brookhart have used the [(allyl)Ni][B(Ar_F)₄] species as an initiator and shown that it reacts rapidly with butadiene at -80 °C to yield the highly reactive and observable [(allyl)Ni(η⁴-1,3-butadiene)]⁺ complex, a key and previously unobserved intermediate.¹² Further reaction of this species with butadiene formed a wrap-around complex following three insertions of butadiene into the original allyl moiety. The chain growth was monitored by NMR spectroscopy and provided additional mechanistic details of the chain growth process including the nature of the catalyst resting state.¹²

The [(allyl)Ni(η⁴-1,3-butadiene)]⁺ complex represents the first example of an η⁴-bound 1,3-diene to a d⁸ metal center. O'Connor has also treated [(cyclohexenyl)Ni][B(Ar_F)₄]⁺ with butadiene, isoprene, and dimethylbutadiene to produce the corresponding [(cyclohexenyl)Ni(η⁴-diene)]⁺ species.¹³ In the case of butadiene and isoprene, only the *s-cis* η⁴-diene isomer was observed. However, in the case of dimethylbutadiene, a mixture of two isomers was observed *in situ*; the *s-cis* and *s-trans*

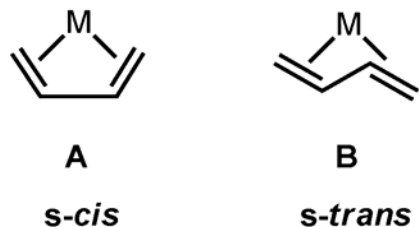
isomers are bound in an η^4 -fashion to the cationic nickel center. The major isomer is $[(\text{cyclohexenyl})\text{Ni}(\eta^4\text{-s-cis-dimethylbutadiene})]^+$ whereas the minor isomer is $[(\text{cyclohexenyl})\text{Ni}(\eta^4\text{-s-trans-dimethylbutadiene})]^+$. This is the first example a Ni(II) complex bearing an η^4 -*trans* coordinated diene (Scheme 3.1).¹³ While clearly observed when these “naked” cationic Ni allyl complexes are used as precursors, no η^4 -diene coordinated species are observed when the $[(\text{allyl})\text{Ni}(\text{mes})]^+$ complex is treated with 1,3-dienes.¹³

Scheme 3.1. *In situ* generation of $(\text{cyclohexenyl})\text{Ni}(\eta^4\text{-dimethylbutadiene})^+$.



The two diene coordination modes for mononuclear complexes are depicted in Scheme 3.2. Some of these η^4 -diene complexes, particularly ones with unsubstituted 1,3-dienes, are so reactive that they rapidly insert additional diene to yield oligomers and polymers, depending on the conditions.¹⁴ The η^4 -*s-cis* coordination of a 1,3-diene to a metal center (mode **A**) is predicted by DFT calculations to be the most stable isomer.¹⁵ While η^4 -*s-trans* coordination (mode **B**) of dienes to transition metals are rare, several examples exist for early transition metals such as Zr,^{16,17} Nb,^{18,19} Ta,^{20,21} Mo,²²⁻²⁶ W,^{27,28} and Re,²⁹ but only a few examples have been reported for late transition metals and include Ru³⁰⁻³³ and the Ni(II) example reported in our lab by O'Connor.¹³

Scheme 3.2. Typical coordination modes observed for mononuclear η^4 -1,3-diene complexes.



The previous chapter detailed the synthesis of [(allyl)Pd(mes)][SbF₆] complexes (mes = mesitylene) as useful precursors to [(allyl)Pd(olefin)₂]⁺ complexes due to the labile nature of the arene ligand. It is reasonable to assume that these complexes would exhibit similar behavior with dienes, and perhaps the elusive η^4 -bound dienes may be observed and studied. Herein, the reactivity of [(2-R-allyl)Pd(mes)]⁺ and [(cyclohexenyl)Pd(mes)]⁺ complexes with various dienes is described.

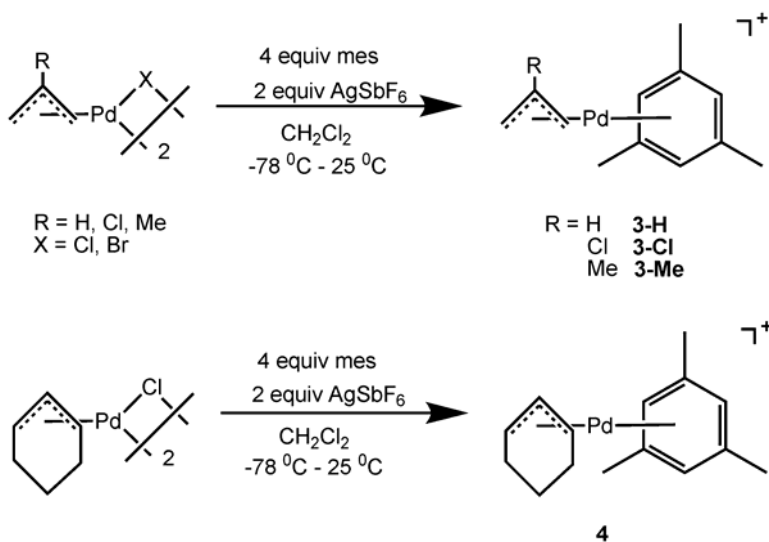
Results and Discussion

Synthesis of [(cyclohexenyl)Pd(arene)][SbF₆], 4. Syntheses of complexes **3-H**, **3-Cl**, and **3-Me** (see Scheme 3.3) are described in chapter 2. The cyclohexenyl derivative, **4**, was synthesized via the same method (Scheme 3.3).³⁴ To a methylene chloride solution of the corresponding [(cyclohexenyl)PdCl]₂ dimer, four equivalents of mesitylene were added, and then a methylene chloride solution of AgSbF₆ was added dropwise at -78 °C. The reaction mixture was stirred at low temperature and then allowed to warm slowly. The resulting solution was cannula filtered and solvent removed under vacuum to yield a bright orange powder.

As representative for these systems, allyl ¹H resonances of [(allyl)Pd(mes)]⁺ **3-H** in CD₂Cl₂ appear at δ 5.65 (m), 4.54 (d, ³J_{H-H} = 4.8 Hz), 3.30 (d, ³J_{H-H} = 11.4 Hz) for the central, *syn*, and *anti* protons, respectively, while for the cyclohexenyl derivative **4**, ¹H

resonances appear at δ 5.50 (bs) and 5.47 (m) for the *syn* and central protons, respectively. The bound mesitylene signals for the aromatic hydrogens for **3-H** are shifted downfield to δ 7.03 relative to free mesitylene, whereas they appear at δ 6.95 for **4**. Reactions of 2,3-dimethyl-1,3-butadiene with these cationic palladium complexes can now be explored, with the goal of observing the elusive η^4 -bound diene as was the case with the “naked” cationic nickel species.

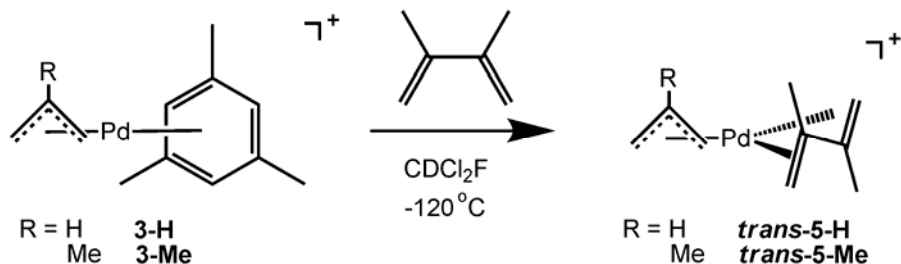
Scheme 3.3. Cationic Pd(arene) complexes.



***In Situ* Generation of [(allyl)Pd(*s-trans*- η^4 -2,3-dimethyl-1,3-butadiene)][SbF₆], *s-trans*-5-H, and [(2-methallyl)Pd(*s-trans*- η^4 -2,3-dimethyl-1,3-butadiene)][SbF₆], *s-trans*-5-Me.** Treatment of [(allyl)Pd(mes)][SbF₆] **3-H** with excess 2,3-dimethyl-1,3-butadiene (DMBD) *in situ* at temperatures as low as -120 °C in CDCl₂F results in rapid mesitylene displacement and sole formation of *s-trans* η^4 -diene palladium adduct (Scheme 3.4), in contrast to the *cis/trans* mix of isomers observed with the Ni system.¹³ The ¹H NMR spectra recorded at variable temperature for this species are shown in Figure 3.1. For *s-trans*-5-H at -120 °C, the *syn* and *anti* protons on the allyl

fragment split into four distinct doublet resonances at δ 5.31 ($^3J_{\text{HH}} = 6.0$ Hz), 5.24 ($^3J_{\text{HH}} = 6.0$ Hz) and 3.95 ($^3J_{\text{HH}} = 13.0$ Hz), 3.57 ($^3J_{\text{HH}} = 13.0$ Hz), respectively, and are consistent with an unsymmetrical species. The olefinic protons of bound DMBD resonate as singlets at δ 5.27, 5.18, 4.49, and 4.49. Free DMBD olefinic protons resonate at δ 5.02 and 4.96 and no geminal coupling can be observed, consistent with expectations for a terminal vinyl unit. Similarly, the two methyl groups of DMBD in ***s-trans*-5-H** are inequivalent and resonate at δ 1.96 and 1.80, upfield and downfield from the free DMBD methyl resonance at 1.85 ppm, respectively. The *s-trans* conformation of the bound DMBD in ***s-trans*-5-H** is suggested by the inequivalent resonances for the two *syn* and two *anti* allyl hydrogens as well as the two sets of signals for the methyl groups and *cis* and *trans* vinylic hydrogens of the bound DMBD. A possible alternative to the *s-trans* assignment for the bound DMBD would be a 50:50 mixture of prone and supine *s-cis* isomers (Scheme 3.5). This alternative possibility was ruled out by 2D TOSCY and 2D NOESY experiments. The 2D TOSCY experiment show that the two H_{anti} resonances are part of the same spin system, and therefore belong to the same species. If the product had been a mixture of prone and supine *s-cis* isomers, the cross peaks would not exist, and therefore we can definitively assign this species as the *s-trans* isomer. This represents a rare example of a *s-trans* η^4 -bound 1,3-diene to a d^8 metal center.¹³

Scheme 3.4. *In situ* generation of ***s-trans*-5-H**.



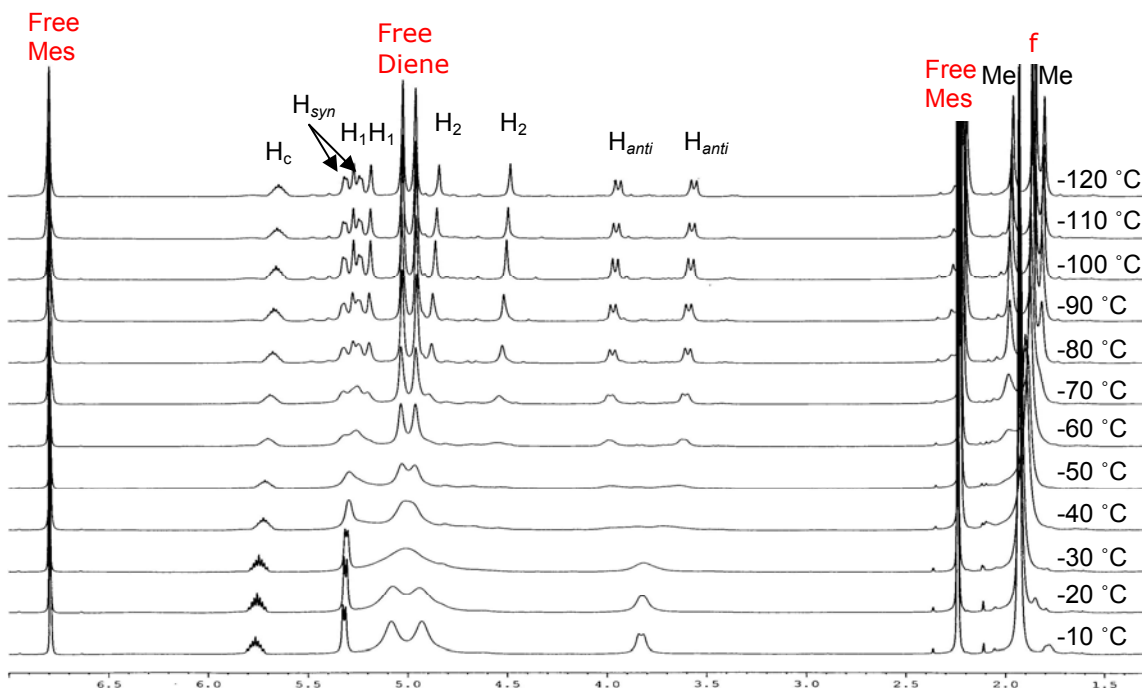
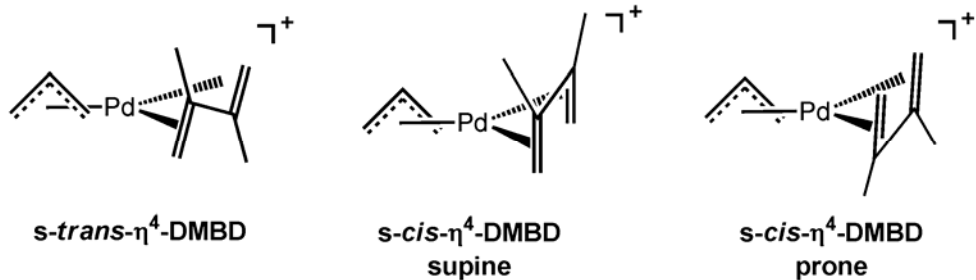


Figure 3.1. Variable temperature ^1H NMR spectra of the *in situ* reaction of DMBD with $[(\text{allyl})\text{Pd}(\text{mes})][\text{SbF}_6]$, **3-H**, to form the *s-trans* $[(\text{allyl})\text{Pd}(\eta^4\text{-DMBD})][\text{SbF}_6]$ species ***s-trans*-5-H**.

Scheme 3.5. Possible isomers for the η^4 -coordination of DMBD to palladium(II).



Upon warming to $-70\text{ }^\circ\text{C}$, the allyl and DMBD resonances begin to broaden (see Figure 3.1). At temperatures above $-40\text{ }^\circ\text{C}$, the bound DMBD olefinic signals coalesce with the free DMBD olefinic signals, indicating fast exchange between bound and free DMBD at temperatures above $-40\text{ }^\circ\text{C}$. This exchange between bound and free ligand has been previously observed and is presumed to be dissociative or solvent assisted, similar to that described for olefin binding in chapter 2. Additionally, the H_{syn} and H_{anti}

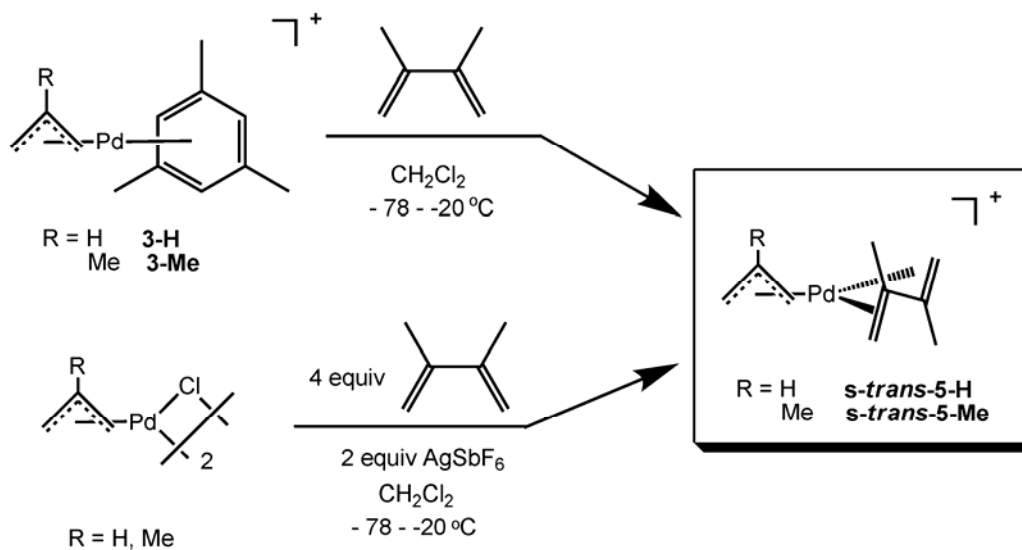
resonances of the allyl unit broaden and coalesce into two resonances at 5.33 (H_{syn}) and 3.32 (H_{anti}) ppm at temperatures above -40 °C; the averaging of these resonances is the result of rapid DMBD exchange. At temperatures above -10 °C the complex decomposes.

The [(2-methallyl)Pd(mes)][SbF₆] **3-Me** reacts *in situ* similarly with DMBD. Formation of the [(2-methallyl)Pd(η^4 -DMBD)][SbF₆] complex, **s-trans-5-Me**, occurs at temperatures as low as -120 °C. For **s-trans-5-Me** at -120 °C, the *syn* and *anti* protons resonate as singlets at δ 5.10, 5.06 and 3.77, 3.40, respectively, and are consistent with the same *s-trans* assignment as for **s-trans-5-H**. The olefinic protons of bound DMBD resonate as singlets at δ 5.35, 5.29, 4.86, and 4.56, whereas the free DMBD olefinic protons resonate at δ 5.02 and 4.96. The two methyl groups of DMBD in **s-trans-5-Me** are inequivalent and resonate at δ 2.08 and 1.97, upfield from the free DMBD methyl resonance at 1.85 ppm, respectively.

Isolation and Independent Synthesis of s-trans [(allyl)Pd(η^4 -DMBD)][SbF₆], s-trans-5-H, and s-trans [(2-methallyl)Pd(η^4 -DMBD)][SbF₆], s-trans-5-Me. *S-trans* [(allyl)Pd(η^4 -DMBD)][SbF₆] can be synthesized independently via two methods (Scheme 3.6), and represents the first example of an [(allyl)Pd(η^4 -1,3-diene)]⁺ that has been isolated and characterized. Similar to the *in situ* experiment described above, [(allyl)Pd(mes)]⁺ complex **3-H** was dissolved in CH₂Cl₂ and cooled to -78 °C in a dry ice/isopropanol bath. Exposure of this solution to DMBD results in an apparent color change from yellow to pale yellow. Removal of the solvent, free mesitylene, and excess DMBD under dynamic vacuum at temperatures below -30 °C yields a pale yellow solid of *s-trans* [(allyl)Pd(η^4 -DMBD)][SbF₆] complex **s-trans-5-H**.

Alternatively, *s-trans* [(allyl)Pd(η^4 -DMBD)][SbF₆] can be synthesized from [(allyl)PdCl]₂ at low temperatures. A CH₂Cl₂ solution of [(allyl)PdCl]₂ was cooled to -78 °C in a dry ice/isopropanol bath, and 4 equivalents of DMBD were added. A solution of 2 equivalents of AgSbF₆ in CH₂Cl₂ was then added drop-wise under stirring at -78 °C for about 30 minutes. The resulting solution was cannula filtered and the solvent evaporated *in vacuo* at -20 °C, resulting in a pale yellow powder of the *s-trans* [(allyl)Pd(η^4 -DMBD)][SbF₆] complex ***s-trans*-5-H**. ***s-trans*-5-Me** was also synthesized via this method. The ¹H NMR spectra of independently prepared [(allyl)Pd(η^4 -DMBD)][SbF₆] and [(2-methallyl)Pd(η^4 -DMBD)][SbF₆] match those of the *in situ* generated complexes, and elemental analyses confirmed the elemental compositions. Attempts to recrystallize either ***s-trans*-5-H** or ***s-trans*-5-Me** by a variety of methods were unsuccessful.

Scheme 3.6. Synthetic routes to obtain ***s-trans*-5-H** and ***s-trans*-5-Me**.

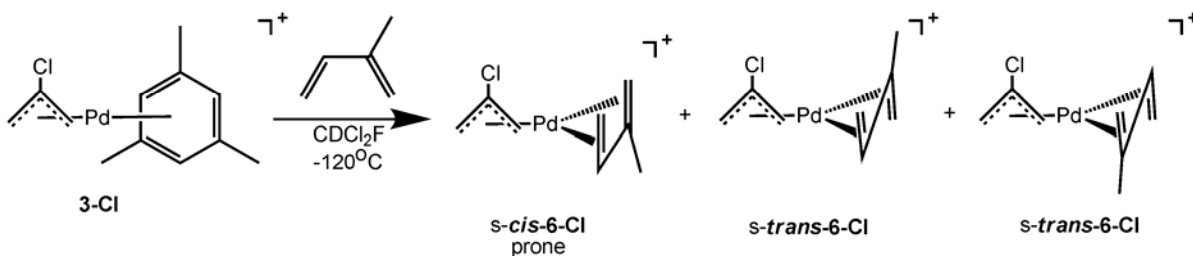


While the 2,3-disubstituted-1,3-butadiene yielded 100% *s-trans* isomer, it was of interest to explore the reactivity of mono- and unsubstituted 1,3-dienes with the

$[(\text{allyl})\text{Pd}(\text{arene})]^+$ complexes. Perhaps the same reactivity will be observed, or perhaps with less substituted 1,3-dienes other possible isomers will be favored.

***In Situ* Generation of *s-cis/s-trans*-6-Cl with Isoprene.** Since the $[(\text{allyl})\text{Pd}(\eta^4\text{-DMBD})]^+$ complexes yielded solely *s-trans*-coordinated DMBD, reaction of less substituted 1,3-dienes, such as isoprene, with the labile $[(2\text{-R-allyl})\text{Pd}(\text{mes})]^+$ complexes may also yield similar adducts. In fact, *in situ* treatment of $[(2\text{-Cl-allyl})\text{Pd}(\text{mes})][\text{SbF}_6]$ **3-Cl** with excess isoprene (IP) at temperatures as low as -120°C in CDCl_2F also results in rapid displacement of mesitylene and formation of an η^4 -bound diene complex (Scheme 3.7).

Scheme 3.7. Generation of several η^4 -diene isomer adducts.



With mono-substituted isoprene, three isomers are observed and exist in a 1:1:0.30 ratio. The two major isomers, present in equal amounts, are assigned to the two possible diastereomers of *s-trans*-6-Cl. These two *s-trans* isomers, one with the methyl group on the isoprene unit directed away from the chloro substituent on the allyl unit and one directed toward the chloro substituent on the allyl unit, should be nearly equal in energy and therefore the two isomers are present in equal amounts. The minor isomer is assigned to the *s-cis* product *s-cis*-6-Cl and is proposed to exist in the prone form. Tobisch calculated a significant energy difference of 7.0 kcal/mol between the prone and supine *s-cis* isomers for the $[(\text{allyl})\text{Ni}(\eta^4\text{-1,3-butadiene})]^+$ complex.¹⁵ Based on this

significant energy difference between the prone and supine *s-cis* isomers, the third, minor isomer in solution is therefore assigned as the prone ***s-cis*-6-Cl** isomer. In this case, the supine *s-cis* isomer is not observed.

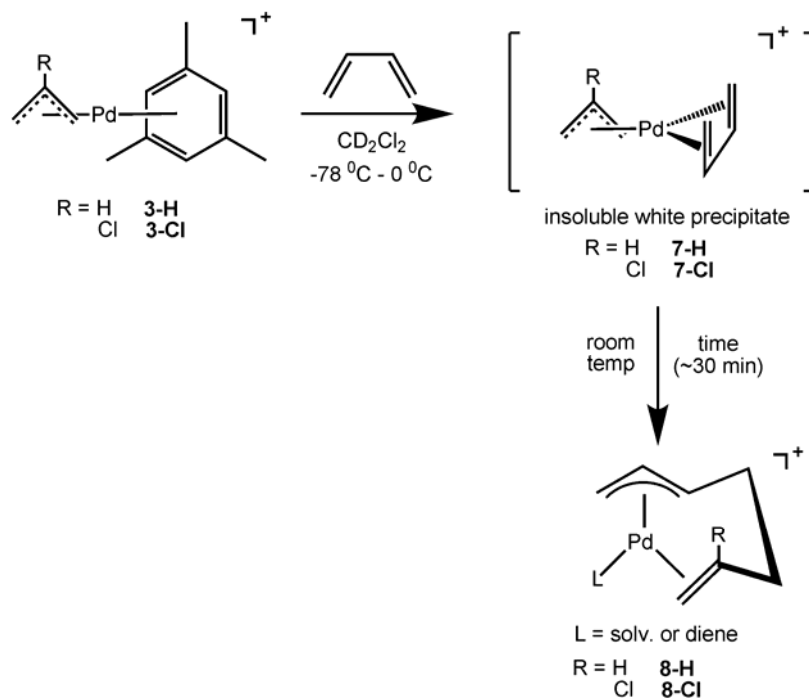
For the minor, prone *s-cis* isoprene adduct, distinct signals exist in the ^1H NMR spectrum for isoprene and resonate at δ 6.26 for the allylic H_1 proton, 5.76 ($^3J_{\text{HH}} = 9.0$ Hz) for H_2 , and 4.22 ($^3J_{\text{HH}} = 19.5$ Hz) for H_3 . Two vinyl protons for bound isoprene resonate as singlets at 5.49 and 3.98 ppm, while the methyl group resonates as a singlet at 2.31 ppm. For the 2-chloroallyl moiety, four separate singlets resonate at 5.64 and 5.59 ppm for the H_{syn} protons and 3.98 and 3.89 ppm for the H_{anti} protons, respectively, and confirm the unsymmetrical nature of the prone ***s-cis*-6-Cl** minor isomer.

The two major *s-trans* isomers, ***s-trans*-6-Cl**, each have distinct resonances for all protons in these unsymmetrical species. It is difficult to conclusively assign each resonance to a specific isomer due to the 2-chloro substitution on the allyl moiety and the methyl group on the isoprene unit, as these substituents eliminate coupling between protons. However, it is clear that eight singlets exist for the H_{syn} and H_{anti} protons of the allyl unit for the two isomers (see Experimental Section for details). Additionally, four separate signals exist as singlets for the terminal vinyl protons of the bound isoprene unit and resonate at 5.47, 5.44, 4.79, and 4.45 ppm, whereas the methyl groups resonate at 1.93 and 1.81 ppm for the two major *s-trans* isomers. The other protons for bound isoprene overlap and resonate at 5.86 ppm for H_1 , 5.70 ppm ($^3J_{\text{HH}} = 8.5$ Hz) for H_2 , and 4.90 ppm ($^3J_{\text{HH}} = 16.0$ Hz) for H_3 . The coupling for H_3 is larger for the *s-cis* isomer ($^3J_{\text{HH}} = 19.5$ Hz) than for the *s-trans* isomers ($^3J_{\text{HH}} = 16.0$ Hz).

In these isoprene adducts, the *s-trans* isomers, **s-trans-6-Cl**, are the major products, but a minor isomer corresponding to prone *s-cis* product, **s-cis-6-Cl**, is also observed. Interestingly, this isomer distribution is in contrast to the previous, di-substituted DMBD adducts, which yielded solely *s-trans* product. Since the mono-substituted 1,3-diene, isoprene, yielded a mixture of *s-cis/s-trans* isomers, we next studied the reactivity of unsubstituted 1,3-butadiene with the labile Pd(II)arene complexes.

***In Situ* Generation of 7-H and 7-Cl with 1,3-Butadiene.** Treatment of [(2-Cl-allyl)Pd(mes)][SbF₆] **3-Cl** or [(allyl)Pd(mes)][SbF₆] **3-H** with excess 1,3-butadiene (BD) *in situ* at temperatures as low as -120 °C in CDCl₂F results in rapid displacement of mesitylene and formation of pale yellow, nearly colorless precipitates, presumably the [(allyl)Pd(η^4 -BD)] complexes **7-Cl** or **7-H** (Scheme 3.8). This colorless precipitate **7-H** can be synthesized on a large scale and isolated by removal of the solvent at temperatures below -20 °C. Elemental analysis of the precipitate is consistent with formation of [(allyl)Pd(η^4 -BD)][SbF₆] complex **7-H** (see Experimental Section for details). Attempts to dissolve **7-H** in a variety of solvents, such as CD₂Cl₂, CDCl₂F, methanol-d₄, and chlorobenzene-d₅, in order to characterize the complex by NMR were unsuccessful due to either the insolubility of the complex or solvent displacement of the η^4 -bound BD. For example, [(allyl)Pd(η^4 -BD)][SbF₆] complex **7-H** dissolves in methanol-d₄ but displacement of BD by methanol-d₄ occurs, as indicated by ¹H NMR resonances corresponding to free BD. Attempts to recrystallize complexes **7-H** and **7-Cl** were unsuccessful.

Scheme 3.8. Reactivity of **3-H** and **3-Cl** with 1,3-butadiene.



When the colorless precipitates **7-Cl** or **7-H** formed by the *in situ* reaction of [(2-Cl-allyl)Pd(mes)][SbF₆] **3-Cl** or [(allyl)Pd(mes)][SbF₆] **3-H** with two equivalents of 1,3-butadiene (BD), respectively, are warmed and shaken at room temperature, the insertion of BD into the allyl unit occurs to form the η^3, η^2 -wrap-around complex **8-Cl** or **8-H** (Scheme 3.8). Conversion of the insoluble precipitate **7-Cl** to the wrap-around **8-Cl** is complete in about 30 min for the 2-Cl-allyl derivative and in about 90-120 min for the unsubstituted allyl derivative, **8-H**. The ¹H NMR spectrum for the *in situ* wrap-around complex is shown in Figure 3.2. The H_{syn} and H_{anti} protons on the allyl moiety resonate at 4.75 and 3.84 ppm, respectively, and the bound olefinic protons H₆ and H₇ shift upfield and resonate at 5.42 and 4.95 ppm, respectively. The fourth coordination site is occupied by solvent or BD. Coordinated BD is shifted upfield and exhibits three peaks at 6.25, 5.34, and 5.05 ppm, and is most likely η^2 -bound to the metal center but undergoes rapid

exchange at room temperature. This is the first direct observation of a wrap-around first insertion product from the coupling of an allyl moiety to bound BD.

Scheme 3.9. Formation of the η^3, η^2 -wrap-around complex **8-Cl** *in situ*.

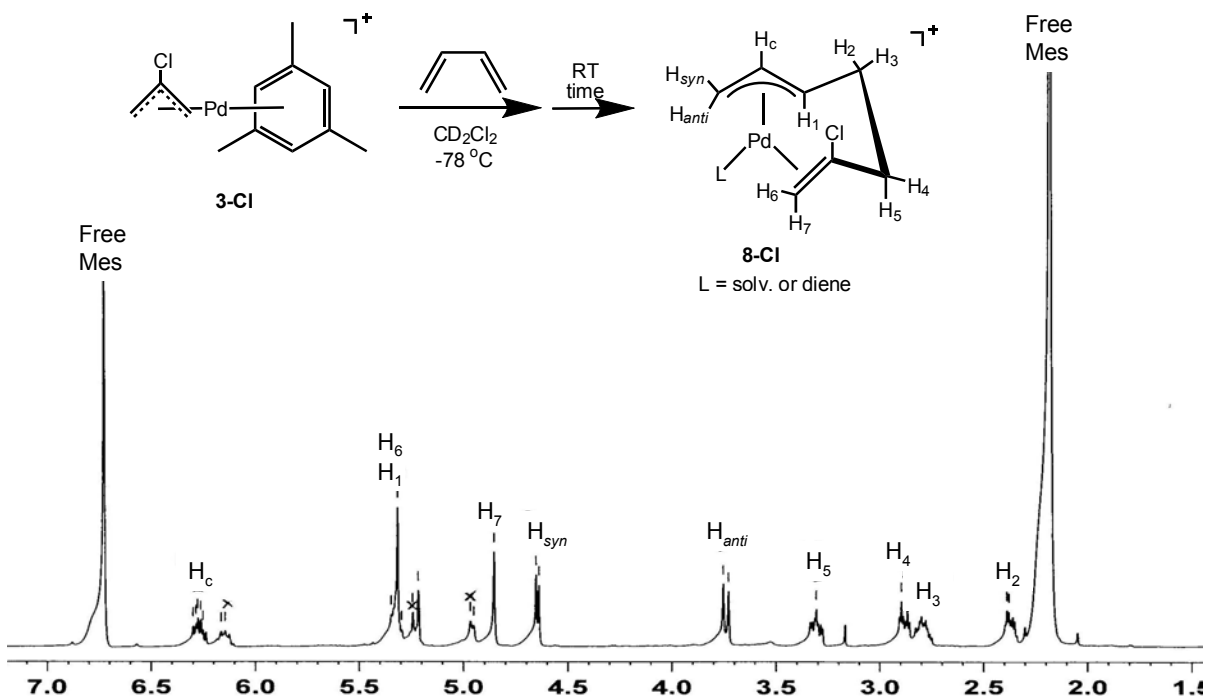
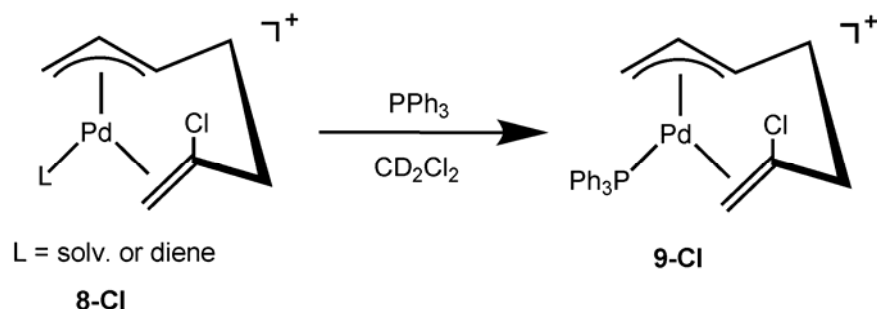


Figure 3.2. Room temperature ^1H NMR spectrum of wrap-around complex **8-Cl** generated *in situ* in CD_2Cl_2 . The “x” denotes bound 1,3-butadiene.

Due to the labile nature of the solvent or diene in the fourth coordination site, the wrap-around complex **8-Cl** could not be isolated. However, “trapping” of the wrap-around by addition of one equivalent of PPh_3 resulted in displacement of solvent or diene and PPh_3 coordination to form complex **9-Cl** (Scheme 3.10). This wrap-around complex is much more stable and exhibits NMR spectra consistent with wrap-around complexes that have been independently synthesized and characterized (see chapter 4 and Experimental Section for more details). Further reactivation of these first-insertion intermediates with BD results in oligomerization and eventual catalyst decomposition.

The reactivity with 1,3-dienes and the mechanism of chain transfer with wrap-around complexes is discussed in chapter 4 in greater detail.

Scheme 3.10. Trapping with PPh_3 to form **9-Cl**, a known complex.



Reaction of $[(\text{allyl})\text{Pd}(\text{mes})]^+$ with di-, mono-, and unsubstituted 1,3-butadiene results in facile mesitylene displacement and formation of η^4 -bound diene adducts. These 1,3-diene adducts are present as several different η^4 *s-trans* and *s-cis* isomers, depending on the amount of substitution on the diene (*vide supra*). Conversely, cyclic 1,3-dienes must exist solely in the *cis* conformation, and so reaction of $[(\text{allyl})\text{Pd}(\text{mes})]^+$ complexes may provide additional details for the *cis* isomers for the η^4 -diene adducts.

***In Situ* Reaction of 3-H with Cyclohexa-1,3-diene to Form a *s-cis* η^4 -bound Diene Complex.** Exposure of $[(\text{allyl})\text{Pd}(\text{mes})][\text{SbF}_6]$ **3-H** to an excess of cyclohexa-1,3-diene (CHD) *in situ* at temperatures as low as $-100\text{ }^\circ\text{C}$ in CDCl_2F results in rapid displacement of mesitylene and formation of the $[(\text{allyl})\text{Pd}(\eta^4\text{-CHD})][\text{SbF}_6]$ complex **10-H** (Scheme 3.11). At $-100\text{ }^\circ\text{C}$ the ^1H NMR spectrum of this *s-cis* η^4 -diene species exhibits one resonance corresponding to H_{syn} at 5.48 ppm ($^3J_{\text{HH}} = 7.0\text{ Hz}$) and one H_{anti} resonance at 3.67 ppm ($^3J_{\text{HH}} = 13.5\text{ Hz}$), indicative of a symmetrical species, as opposed to the *s-trans* $[(\text{allyl})\text{Pd}(\eta^4\text{-DMBD})]^+$ complex ***s-trans*-5-H** which had four distinct resonances for the *syn* and *anti* protons. The olefinic protons, H_2 and H_1 , of the bound

CHD resonate downfield at 6.62 and 6.13 ppm, respectively, whereas free CHD olefinic protons resonate at 6.19 and 6.03 ppm.

Scheme 3.11. Generation of **10-H**.

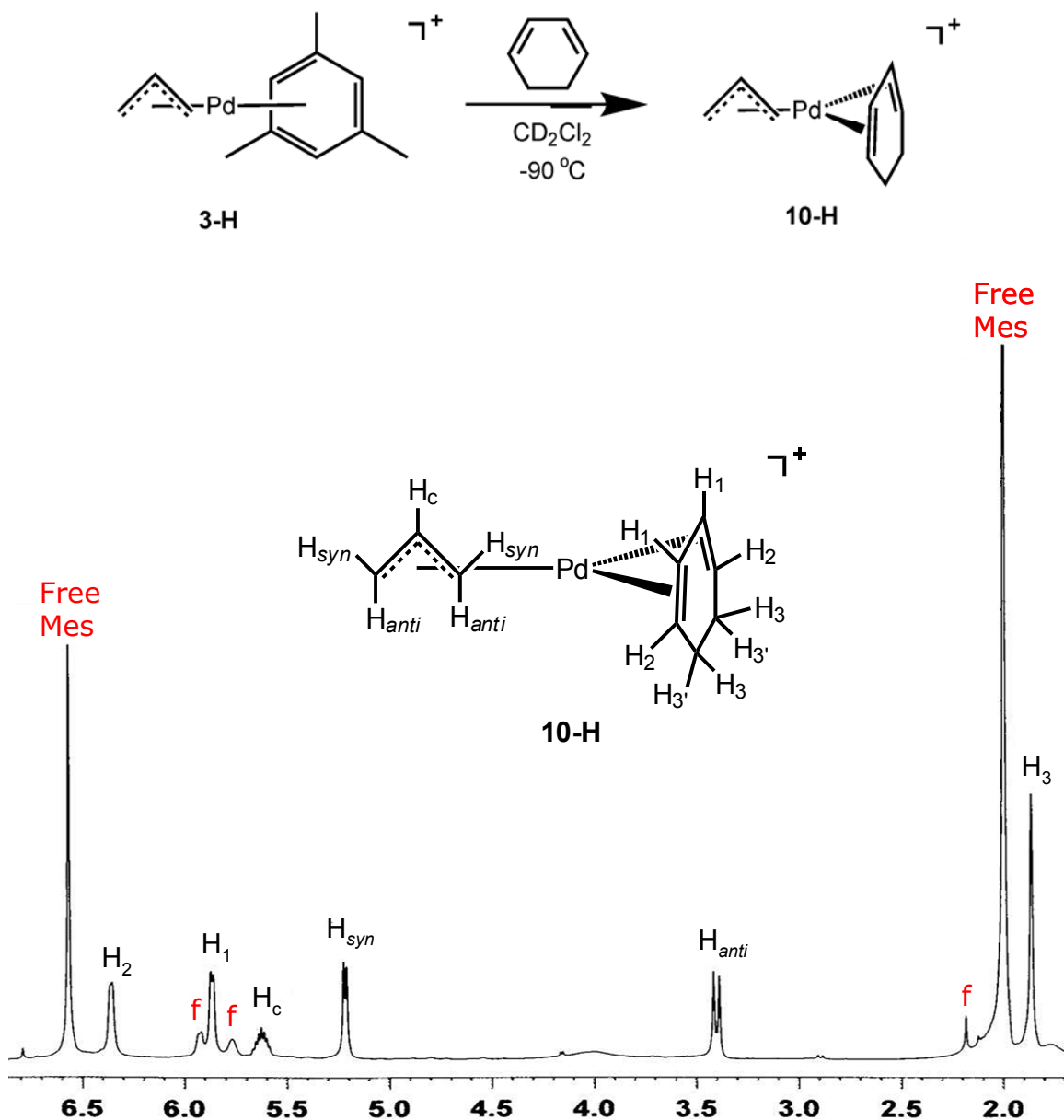
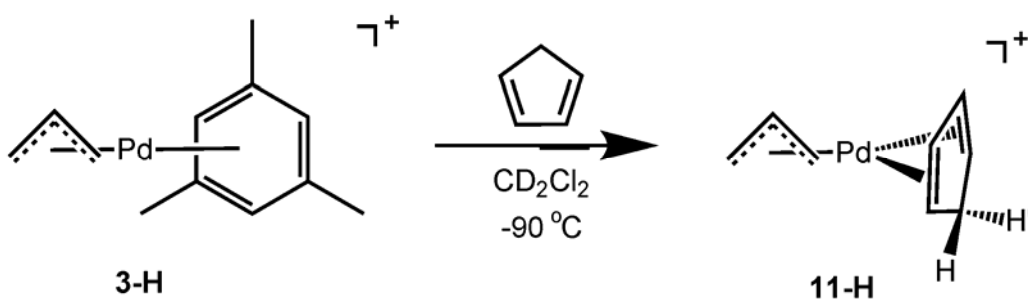


Figure 3.3. ^1H NMR spectrum of the *in situ* reaction of 1,3-cyclohexadiene with $[(\text{allyl})\text{Pd}(\text{mes})][\text{SbF}_6]$, **3-H**, to form the *s-cis* $[(\text{allyl})\text{Pd}(\eta^4\text{-CHD})][\text{SbF}_6]$ species **10-H** at -100°C in CDCl_2F . “f” denotes free 1,3-cyclohexadiene.

***In Situ* Reactivity of 3-H with Cyclopentadiene.** Similar to the formation of the *s-cis* η^4 -bound CHD complex **10-H**, reaction of [(allyl)Pd(mes)][SbF₆] **3-H** with two equivalents of cyclopentadiene at low temperatures in either CD₂Cl₂ or CDCl₂F generates free mesitylene and [(allyl)Pd(η^4 -cyclopentadiene)][SbF₆] complex **11-H** (Scheme 3.12). At -90 °C the ¹H NMR spectrum of this *s-cis* species exhibits one resonance corresponding to H_{syn} at 3.66 ppm and one H_{anti} resonance at 3.50 ppm (³J_{HH} = 14.0 Hz). The olefinic protons of the bound cyclopentadiene, similar to previously discussed η^4 complexes, shift downfield from that of free cyclopentadiene to 6.65 ppm. At the low temperature limit, there is still some line broadening due to rapid exchange between free and bound cyclopentadiene. However, in addition to the downfield shifts of the olefinic proton resonances, a clear indication that the cyclopentadiene is indeed bound is evident in the roofed doublets observed for H₃ and H_{3'} (H and H' in Scheme 3.12 for **11-H**). These protons resonate at 3.29 and 3.20 ppm and exhibit a large geminal coupling of 25.5 Hz (see Experimental Section for details).

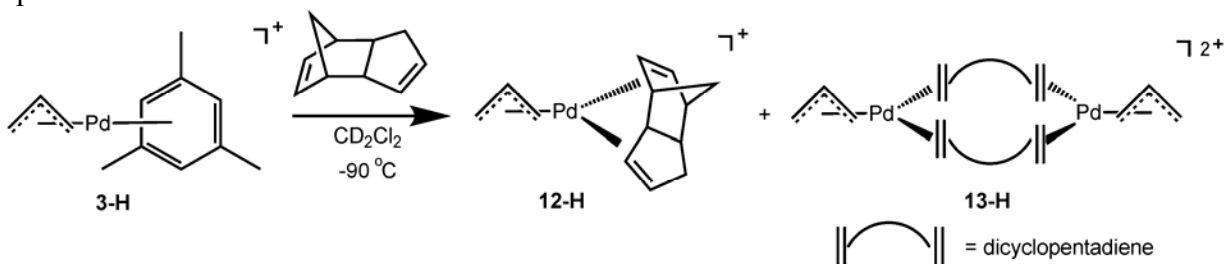
Scheme 3.12. Generation of [(allyl)Pd(η^4 -cyclopentadiene)]⁺, **11-H**.



Upon standing at -30 °C overnight, the signals for both the bound and free cyclopentadiene in the *in situ* sample disappear, while a multitude of new resonances corresponding to two new complexes appeared. One complex was assigned as the coordinated dicyclopentadiene Diels-Alder product [(allyl)Pd(η^4 -dicyclopentadiene)]⁺

complex, **12-H**. The assignment of this species was confirmed independently by the *in situ* reaction of [(allyl)Pd(mes)][SbF₆] **2-H** with one equivalent of dicyclopentadiene (Scheme 3.13). The ¹H NMR spectrum for this reaction is shown in Figure 3.4.

Scheme 3.13. Reaction with dicyclopentadiene to form a mononuclear and dinuclear species.



As the major isomer, complex **12-H** is unsymmetrical, the allyl moiety exhibits two H_{syn} resonances at 4.90 and 4.70 ppm (³J_{HH} = 7.0 Hz), and two H_{anti} resonances at 3.67 and 3.52 ppm (³J_{HH} = 13.0 Hz). The bound vinyl protons are shifted dramatically downfield from that of free dicyclopentadiene to 7.92, 7.28, 6.57, and 6.12 ppm. The minor isomer is likely a dinuclear species and could be one of four isomers (Scheme 3.14). For the dinuclear species, the allyl moiety exhibits two H_{syn} resonances at 4.73 and 4.68 ppm (³J_{HH} = 7.5 Hz), and two H_{anti} resonances at 3.75 and 3.68 ppm (³J_{HH} = 13.0 Hz), while the bound vinyl protons of dicyclopentadiene resonate at 7.69, 7.33, 6.65, and 5.98 ppm. At room temperature, the ratio of the major to minor isomer is 4 to 1, but when the temperature is lowered the population of the minor isomer increases and the ratio changes to 2 to 1. This is consistent with the minor species being a dinuclear complex, the formation of which is entropically favored at lower temperatures. Of the four possibilities for the dinuclear species, *exo* dinuclear isomers **exo-1** and **exo-2** were eliminated as dicyclopentadiene exists as 95.5% *endo* and 0.5% *exo*. This leaves two

endo dinuclear isomers **endo-1** and **endo-2** to consider. The two allyl moieties on **endo-1** are equivalent, whereas the two allyl moieties on **endo-2** are inequivalent which should distinguish one isomer from the other. In the 2D COSY NMR, a crosspeak exists between the two H_{anti} signals. This crosspeak would not exist for **endo-2**, and so the dinuclear species is likely **endo-1**.

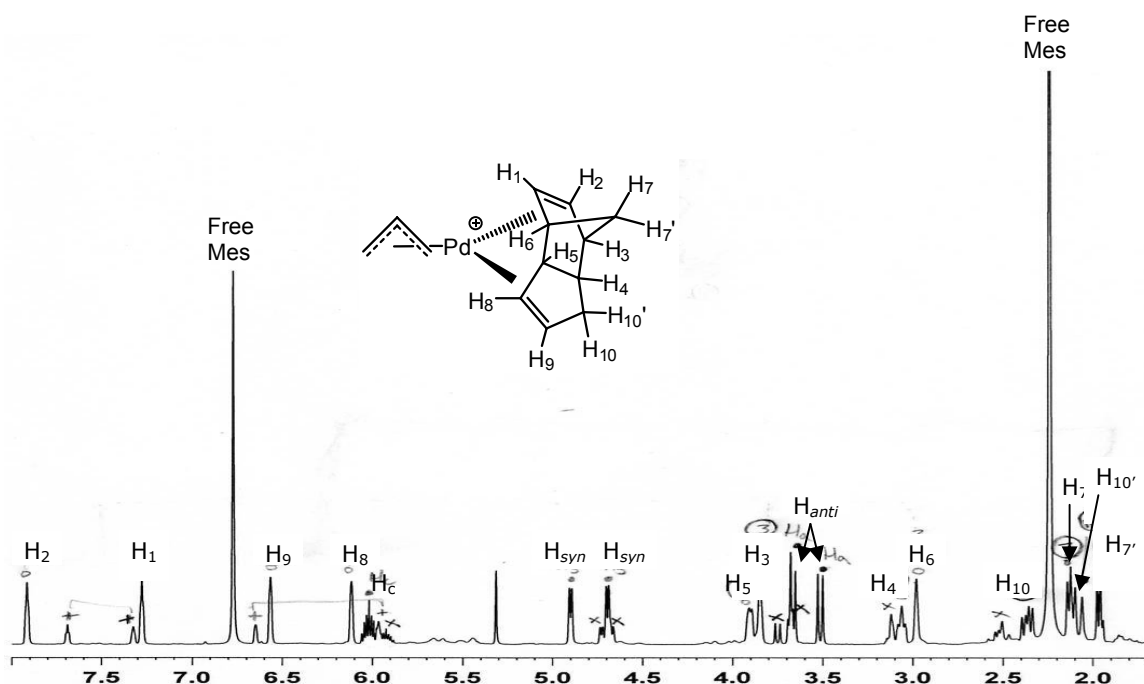
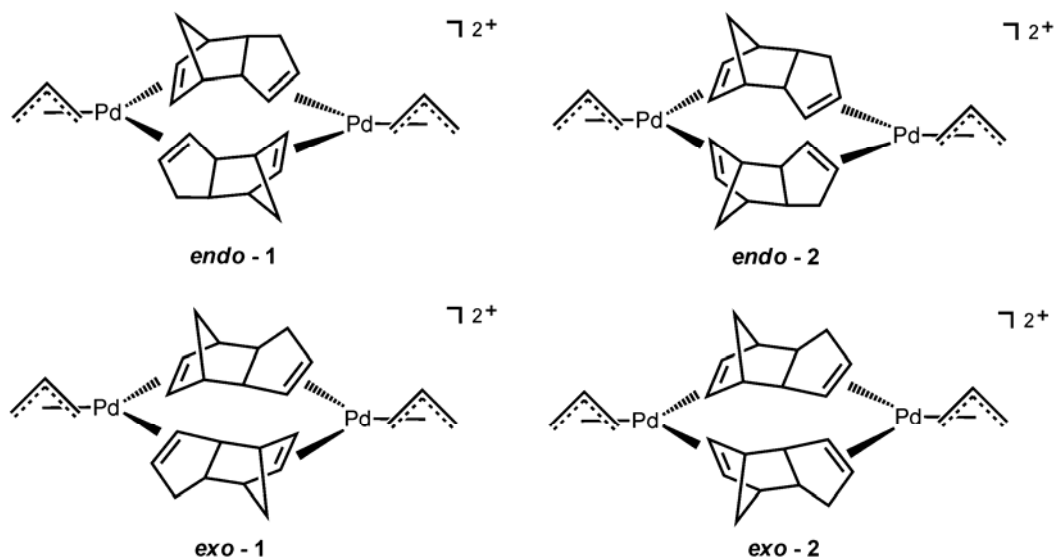


Figure 3.4. Room temperature ^1H NMR spectrum of the reaction of $[(\text{allyl})\text{Pd}(\text{mes})][\text{SbF}_6]$ **3-H** with one equivalent of dicyclopentadiene in CD_2Cl_2 . Two isomers exist; the major isomer corresponds to the mononuclear complex **12-H** and the minor isomer (denoted as “+” and “x” in the spectrum) corresponds to a dinuclear complex.

Scheme 3.14. Possible isomers for the dinuclear species **13-H**.



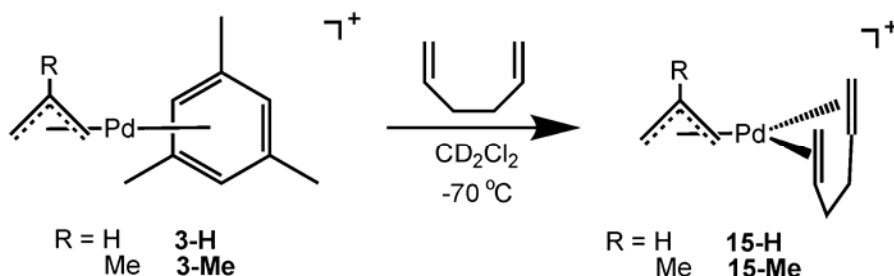
The *in situ* dimerization of cyclopentadiene in dilute conditions at low temperature to form the metal-coordinated dicyclopentadiene species **12-H** and *exo-1* is quite remarkable. When the reaction is warmed to temperatures above 0 °C in the presence of excess cyclopentadiene, cross-linked polycyclopentadiene is produced. The unique Diels-Alder reactivity prompted examination of reactivity of [(allyl)Pd(mes)][SbF₆] **3-H** with cyclopentadiene and either ethylene or 2-butyne to generate the Diels-Alder products norbornene or 2,3-dimethylnorbornadiene, respectively. However, neither reaction produced Diels-Alder adducts. Instead, with ethylene only a mixture of (allyl)palladium(II) bis-ethylene species,³⁴ [(allyl)Pd(η^4 -dicyclopentadiene)]⁺ complex **11-H**, and a mixed species [(allyl)Pd(η^2 -dicyclopentadiene)(η^2 -ethylene)]⁺ was observed at low temperatures. No attempt was made to fully characterize the mixed species [(allyl)Pd(η^2 -dicyclopentadiene)(η^2 -

ethylene)]⁺. Warming above 0 °C resulted in decomposition of the metal complex and an unidentified mixture of oligomers (likely ethylene oligomers).

This chapter has thus far described the reactivity of Pd(II) complexes with 1,3-dienes, which provided a route to the first examples of [(allyl)Pd(η⁴-1,3-diene)]⁺ species. Previously, Maitlis reported several [(allyl)Pd(η⁴-1,5-diene)]⁺ species, one of which was the hexa-1,5-diene complex.³⁵ In order to compare our systems to those that Maitlis observed, reactivity of the [(allyl)Pd(mes)]⁺ complexes with hexa-1,5-diene was explored.

***In Situ* Reactions of 3-H and 3-Me with Hexa-1,5-diene.** Treatment of either [(allyl)Pd(mes)][SbF₆] **3-H** or [(2-Me-allyl)Pd(mes)][SbF₆] **3-Me** with excess hexa-1,5-diene at low temperatures in either CD₂Cl₂ or CDCl₂F generates free mesitylene and forms either [(allyl)Pd(η⁴-hexa-1,5-diene)][SbF₆] complex **14-H** or [(2-Me-allyl)Pd(η⁴-hexa-1,5-diene)][SbF₆] complex **14-Me** (Scheme 3.15). The ¹H NMR spectrum of **14-Me** agrees with the peak assignment Maitlis reported (see Experimental Section for assignment details).³⁵

Scheme 3.15. Reactivity with hexa-1,5-diene.



Synthesis of [(allyl)Pd(η⁴-hexa-1,5-diene)][SbF₆], 15-H, and [(2-methallyl)Pd(η⁴-hexa-1,5-diene)][SbF₆], 15-Me. Similar to the methods Maitlis

employed, either the $[(\text{allyl})\text{PdCl}]_2$ or $[(2\text{-methallyl})\text{PdCl}]_2$ dimer was treated with AgSbF_6 in the presence of hexa-1,5-diene at $-78\text{ }^\circ\text{C}$, and after workup yielded either complex $[(\text{allyl})\text{Pd}(\eta^4\text{-hexa-1,5-diene})][\text{SbF}_6]$, **15-H**, or $[(2\text{-methallyl})\text{Pd}(\eta^4\text{-hexa-1,5-diene})][\text{SbF}_6]$, **15-Me**, respectively. The ^1H NMR spectra of independently prepared $[(\text{allyl})\text{Pd}(\eta^4\text{-hexa-1,5-diene})][\text{SbF}_6]$ and $[(2\text{-methallyl})\text{Pd}(\eta^4\text{-hexa-1,5-diene})][\text{SbF}_6]$ agree with those of the *in situ* generated complexes and with what Maitlis and coworkers observed.³⁵ Attempts to recrystallize either **15-H** or **15-Me** by a variety of methods were unsuccessful.

Summary

$[(\text{Allyl})\text{Pd}(\text{mes})]^+$ complexes readily react with dienes to form $[(\text{allyl})\text{Pd}(\eta^4\text{-diene})]^+$ species. In the case of 2,3-dimethyl-1,3-butadiene, sole formation of the $[(\text{allyl})\text{Pd}(\eta^4\text{-s-trans-DMBD})]^+$ species is observed *in situ*. Additionally, these previously elusive species can be isolated and synthesized independently for the first time. Isoprene reacts *in situ* with $[(\text{allyl})\text{Pd}(\text{mes})]^+$ to yield a mixture of *s-cis*, *s-trans*, prone and supine isomers of the cationic η^4 -bound diene palladium complex. Reaction with butadiene forms an insoluble colorless precipitate that is presumably $[(\text{allyl})\text{Pd}(\eta^4\text{-BD})]^+$, which can undergo insertion of BD into the allyl moiety to form the soluble $\eta^3\text{-}\eta^2$ -bound wrap-around complex. This is the first direct observation of an $\eta^3\text{-}\eta^2$ -bound wrap-around intermediate for the polymerization of 1,3-dienes. Further reaction with BD results in oligomers and decomposition of the catalyst, which will be discussed in greater detail in chapter 4.

Cyclic 1,3-dienes, such as cyclohexa-1,3-diene (CHD) and cyclopentadiene (CPD) also readily displace mesitylene in $[(\text{allyl})\text{Pd}(\text{mes})]^+$ complexes to form the *s-cis* $[(\text{allyl})\text{Pd}(\eta^4\text{-cyclic diene})]^+$ complexes, respectively, *in situ*. When $[(\text{allyl})\text{Pd}(\eta^4\text{-CPD})]^+$ is warmed to temperatures above 0 °C in the presence of excess CPD, formation of an insoluble, presumably cross-linked, cyclopentadiene polymer is formed. Interestingly, when $[(\text{allyl})\text{Pd}(\eta^4\text{-CPD})]^+$ is kept at -30 °C overnight in the presence of one equivalent of CPD, the dicyclopentadiene (DCPD) Diels-Alder product $[(\text{allyl})\text{Pd}(\eta^4\text{-DCPD})]^+$ is formed. Independent *in situ* reaction of $[(\text{allyl})\text{Pd}(\text{mes})]^+$ with DCPD confirmed formation of two isomers of $[(\text{allyl})\text{Pd}(\eta^4\text{-DCPD})]^+$ in a ratio of 4 to 1. The major isomer is the mononuclear, *endo* $[(\text{allyl})\text{Pd}(\eta^4\text{-DCPD})]^+$ complex, whereas the minor isomer is a dinuclear species with two DCPD molecules as bridges. Efforts aimed at reaction of $[(\text{allyl})\text{Pd}(\eta^4\text{-CPD})]^+$ with ethylene or 2-butyne to form the Diels-Alder adducts were unsuccessful. A mixture of bis-olefin, $\eta^4\text{-CPD}$, and (olefin)($\eta^2\text{-CPD}$) was observed at low temperature; however, upon warming the solution only catalyst decomposition and oligomers (likely ethylene oligomers) were observed.

Reaction of $[(2\text{-R-allyl})\text{Pd}(\text{mes})]^+$ (R = H, Me) with hexa-1,5-diene forms the $[(\text{allyl})\text{Pd}(\eta^4\text{-hexa,1-5,diene})]^+$ species *in situ*. These species were also independently synthesized from the palladium dimer to compare to similar results obtained by the Maitlis group.³⁵

Experimental Section

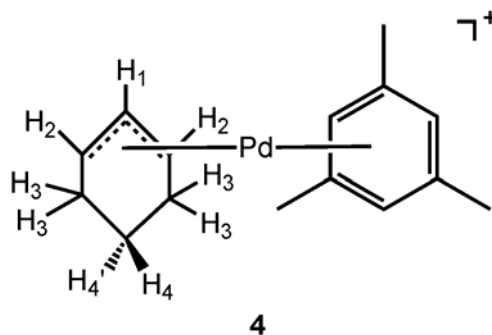
General Considerations.

All reactions, unless otherwise stated, were conducted under a dry, oxygen free argon atmosphere using standard high vacuum, Schlenk, or drybox techniques. Argon was purified by passage through BASF R3-11 catalyst (Chemalog) and 4Å molecular sieves. All palladium complexes were stored under argon in an M.Braun glovebox at -35 °C. ^1H and ^{13}C NMR spectra were recorded on a Bruker DRX 500 MHz or a Bruker DRX 400 MHz. Chemical shifts are referenced relative to residual CH(D)Cl_2 (δ 5.32 for ^1H) and $^{13}\text{CD}_2\text{Cl}_2$ (δ 53.8 for ^{13}C) in CD_2Cl_2 and CHCl_2F (δ 7.16 for ^1H) in CDCl_2F . Chemical shift assignments were supported through 2D HMQC and ^1H - ^1H -COSY experiments, and in some cases 2D NOESY and TOSCY experiments. Elemental analyses were performed by Robertson Microlit Laboratories of Madison, NJ.

Materials.

All solvents were deoxygenated and dried by passage over columns of activated alumina.^{36,37} CD_2Cl_2 , purchased from Cambridge Laboratories, Inc., was dried over CaH_2 , vacuum transferred to a Teflon sealable Schlenk flask containing 4Å molecular sieves, and degassed via three freeze-pump-thaw cycles. CDCl_2F was synthesized according to literature methods.³⁸ CO and 99.99% ethylene were purchased from National Welders and used as received. PdCl_2 was purchased from J&J Materials and used as received. 1,3-Cyclohexadiene was purified by drying over NaBH_4 overnight, vacuum transferred into a Teflon sealable flask and degassed via three freeze-pump-thaw cycles. 2,3-Dimethyl-1,3-butadiene was purified by degassing via three freeze-pump-thaw cycles. Mesitylene, 2,3-dichloropropene, 3-bromo-2-methyl-propene, allyl

chloride, and allyl bromide were purchased from Aldrich and used without further purification. $[(\text{allyl})\text{PdBr}]_2$, $[(\text{allyl})\text{PdCl}]_2$, $[(2\text{-Cl-allyl})\text{PdCl}]_2$, $[(\text{cyclohexenyl})\text{PdCl}]_2$, $[(2\text{-methallyl})\text{PdBr}]_2$, and $[(2\text{-methallyl})\text{PdCl}]_2$ were synthesized according to literature methods.³⁹⁻⁴²



Procedure for the Synthesis of $[(\text{Cyclohexenyl})\text{Pd}(\text{Arene})][\text{SbF}_6]$ Complex 4. The $[(2\text{-R-allyl})\text{Pd}(\text{mes})]^+$ derivatives have been previously synthesized and are described in chapter 2. Under an argon atmosphere, the palladium chloride dimer $[(\text{Cyclohexenyl})\text{PdCl}]_2$ (0.100 g, 0.22 mmol) was dissolved in dry methylene chloride (20 mL) and the resulting yellow solution was stirred at room temperature for five minutes to dissolve the solid. Four equivalents of mesitylene (120 μL , 0.90 mmol) were then added via syringe, and the resulting solution cooled to -78°C . A solution of two equivalents silver hexafluoroantimonate (0.154 g, 0.45 mmol) in 5 mL methylene chloride was then added dropwise at -78°C and the mixture was stirred for ca. 30 min at low temperature before the solution was allowed to warm slowly to room temperature. The resulting solution was cannula filtered and the solvent evaporated in vacuo. The product was washed with 3 x 10 mL of pentane and dried under vacuum to yield product as a yellow powder, which was immediately stored in the glove box at -35°C to prevent thermal degradation. Yield: 0.210 g (86%). ^1H NMR (500 MHz, CD_2Cl_2 , -80°C): δ 6.95 (s, 3H,

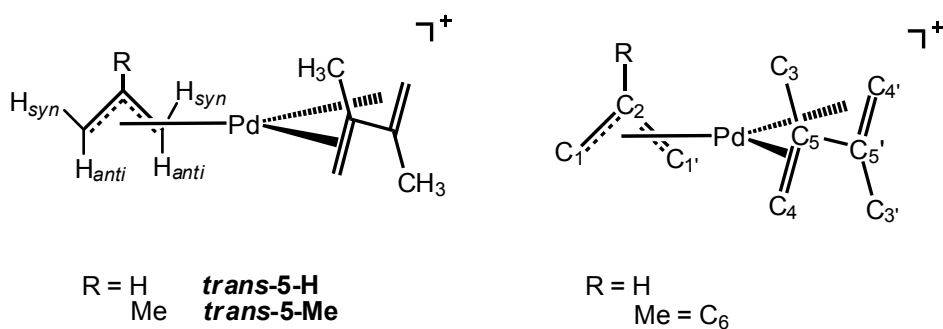
mes_{Ar}), 5.50 (bs, 2H, H₂), 4.47 (m, 1H, H₁), 2.38 (s, 9H, mes_{CH₃}), 1.58 (bs, 4H, H₃), 1.44 (m, 1H, H₄ or H_{4'}), 1.27 (m, 1H, H₄ or H_{4'}). ¹³C{¹H} NMR (50 MHz, CD₂Cl₂, -80 °C): δ 131.2 (s, MesC_{ipso}), 115.6 (s, MesC_{Ar}), 97.9 (s, C₁), 85.1 (s, C₂), 27.3 (s, C₃), 21.4 (s, C₄) 20.2 (s, Mes_{CH₃}).

***In Situ* Generation of [(allyl)Pd(DMBD)][SbF₆] *s-trans*-5-H.** A screw-cap NMR tube was charged with [(allyl)Pd(Mes)][SbF₆] (0.0106g, 2.0 x 10⁻⁵ mol) dissolved in ca. 400 μL CDCl₂F. The tube was placed in a -78 °C bath and two equivalents 2,3-dimethyl-1,3-butadiene(DMBD) (5.6 μL, 2.0 x 10⁻⁵ mol) were added via syringe. The tube was quickly shaken to allow mixing and a color change from yellow to colorless was observed. More than one equivalent of diene added resulted in an exchange between excess diene and the diene adduct in solution; this exchange process was temperature dependent. **NMR Characterization:** ¹H and ¹³C NMR spectra for *s-trans*-5-H were identical to the independently synthesized species (see below), but also contained free mesitylene and free DMBD: ¹H NMR (500 MHz in CDCl₂F, -120 °C): free mesitylene δ 6.79 (s, 6H, ArH), 2.20 (s, 18H, ArMe). free dimethylbutadiene δ 5.02 (s, 6H, H), 4.96 (s, 6H, Me), 1.85 (s, 18H, Me).

***In Situ* Generation of [(2-methallyl)Pd(DMBD)][SbF₆] *s-trans*-5-Me.** A screw-cap NMR tube was charged with [(2-methallyl)Pd(Mes)][SbF₆] (0.0102g, 2.0 x 10⁻⁵ mol) and dissolved in ca. 400 μL CDCl₂F. The tube was placed in a -78 °C bath and two equivalents 2,3-dimethyl-1,3-butadiene(DMBD) (5.6 μL, 2.0 x 10⁻⁵ mol) were added via syringe. The tube was quickly shaken to allow mixing and a color change from yellow to colorless was observed. More than one equivalent of diene added resulted in line broadening, indicating exchange of bound and free diene. This exchange process was

temperature dependent. **NMR Characterization:** ^1H and ^{13}C NMR spectra for ***s-trans*-5-H** were identical to the independently synthesized species (see below), but also contained free mesitylene and free DMBD: ^1H NMR (500 MHz in CDCl_2F , $-120\text{ }^\circ\text{C}$): free mesitylene δ 6.79 (s, 6H, ArH), 2.20 (s, 18H, ArMe). free dimethylbutadiene δ 5.02 (s, 6H, H), 4.96 (s, 6H, Me), 1.85 (s, 18H, Me).

Independent Synthesis of [(allyl)Pd(DMBD)][SbF₆], *s-trans*-5-H, from 3-H. Under an argon atmosphere, [(allyl)Pd(mes)][SbF₆] **3-H** (0.100 g, 0.20 mmol) was dissolved in dry methylene chloride (20 mL) and the resulting yellow/orange solution was stirred at room temperature for five minutes to dissolve the solid, and then the resulting solution was cooled to $-78\text{ }^\circ\text{C}$. Four equivalents of 2,3-dimethyl-1,3-butadiene (90 μL , 0.80 mmol) was stirred for ca. 30 min at low temperature before the solution was allowed to warm slowly to $-20\text{ }^\circ\text{C}$. Then the solvent evaporated *in vacuo* from $-20\text{ }^\circ\text{C}$ to $0\text{ }^\circ\text{C}$ to yield a yellow powder. The syntheses were completed in 2 hours and immediately stored in the glove box at $-35\text{ }^\circ\text{C}$. ^1H and ^{13}C NMR spectra for ***s-trans*-5-H** were identical to the *in situ* generated species and the independently synthesized species from the dimer (see below).



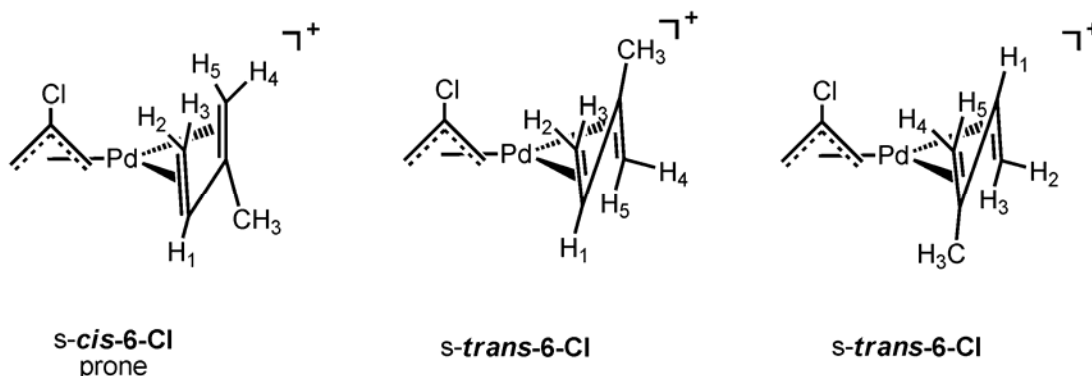
Synthesis of [(allyl)Pd(DMBD)][SbF₆], *s-trans*-5-H, from palladium dimer. Under an argon atmosphere, the palladium halide dimer [(allyl)PdCl]₂ (0.267 g, 0.73 mmol) was dissolved in dry methylene chloride (20 mL) and the resulting yellow solution was stirred at room temperature for five minutes to dissolve the solid. Four equivalents DMBD (330

uL, 2.9 mmol) were added and then a solution of two equivalents silver hexafluoroantimonate (0.60 g, 1.45 mmol) in 5 mL methylene chloride was added dropwise at -78 °C and the mixture was stirred for ca. 30 min at low temperature before the solution was allowed to warm slowly to -20 °C. The resulting solution was cannula filtered and the solvent evaporated *in vacuo* from -20 °C to 0 °C. The product was washed with 3x10 mL of dry pentane and dried under vacuum to yield a yellow powder. The syntheses were completed in 4-5 hours and immediately stored in the glove box at -35 °C. Yield: 0.563 g (82%) **NMR Characterization:** ^1H NMR (500 MHz in CDCl_2F , -120 °C): δ 5.65 (m, 1H, H_c), 5.31 (d, 1H, $^3J_{\text{HH}} = 6.0$ Hz, H_{syn}), 5.27 (s, 1H, H_1), 5.24 (d, 1H, $^3J_{\text{HH}} = 6.0$ Hz, H_{syn}), 5.18 (s, 1H, H_1), 4.85 (s, 1H, H_2), 4.49 (s, 1H, H_2), 3.95 (d, 1H, $^3J_{\text{HH}} = 13.0$ Hz, H_{anti}), 3.57 (d, 1H, $^3J_{\text{HH}} = 13.0$ Hz, H_{anti}), 1.96 (s, 3H, Me), 1.80 (s, 3H, Me). $^{13}\text{C}\{^1\text{H}\}$ NMR (126 MHz, CD_2Cl_2 , -120 °C): δ 139.2 (s, C_5 or $\text{C}_{5'}$), 137.4 (s, C_5 or $\text{C}_{5'}$), 120.4 (s, C_2), 85.7 (s, C_4 or $\text{C}_{4'}$), 85.4 (s, C_4 or $\text{C}_{4'}$), 76.4 (s, C_1 or $\text{C}_{1'}$), 75.6 (s, C_1 or $\text{C}_{1'}$), 20.9 (s, C_3 or $\text{C}_{3'}$), 20.6 (s, C_3 or $\text{C}_{3'}$). Anal. Calcd for $\text{C}_9\text{H}_{15}\text{F}_6\text{SbPd}$: C, 23.22; H, 3.26. Found: C, 25.36; H, 3.52.

Synthesis of [(2-methallyl)Pd(DMBD)][SbF₆], *s-trans*-5-Me. from palladium dimer.

Under an argon atmosphere, the palladium halide dimer [(2-methallyl)PdCl]₂ (0.284 g, 0.73 mmol) was dissolved in dry methylene chloride (20 mL) and the resulting yellow solution was stirred at room temperature for five minutes to dissolve the solid. The resulting solution was cooled to -78 °C and four equivalents DMBD (330 uL, 2.9 mmol) were added. A solution of two equivalents silver hexafluoroantimonate (0.60 g, 1.45 mmol) in 5 mL methylene chloride was then added dropwise at -78 °C and the mixture was stirred for ca. 30 min at low temperature before the solution was allowed to warm

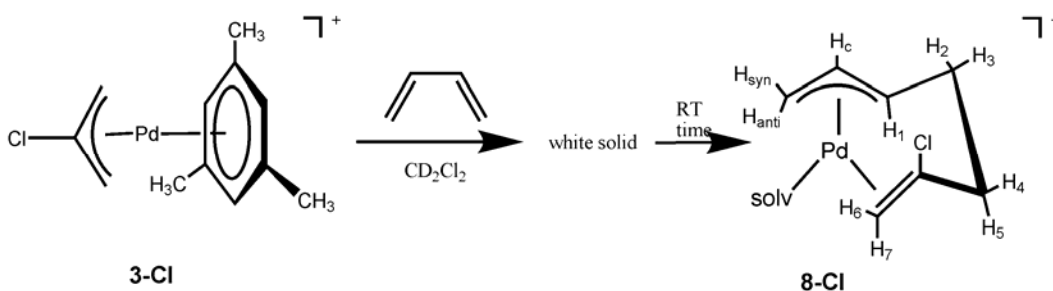
slowly to -20 °C. The resulting solution was cannula filtered and the solvent evaporated *in vacuo* from -20 °C to 0 °C. The product was washed with 3x10 mL of dry pentane and dried under vacuum to yield a yellow powder. The syntheses were completed in 4-5 hours and immediately stored in the glove box at -35 °C. Yield: 0.506 g (73%) ^1H NMR (500 MHz in CDCl_2F , -120 °C): δ 5.35 (s, 1H, H_1), 5.29 (s, 1H, H_1), 5.10 (s, 1H, H_{syn}), 5.06 (s, 1H, H_{syn}), 4.86 (s, 1H, H_2), 4.56 (s, 1H, H_2), 3.77 (s, 1H, H_{anti}), 3.40 (s, 1H, H_{anti}), 2.08 (s, 3H, Me_{DMBD}), 1.97 (s, 3H, $\text{R} = \text{Me}$), 1.84 (s, 3H, Me_{DMBD}). $^{13}\text{C}\{^1\text{H}\}$ NMR (126 MHz, CD_2Cl_2 , -120 °C): δ 138.8 (s, C_5 or C_5'), 137.0 (s, C_5 or C_5'), 120.4 (s, C_2), 85.9 (s, C_4 or C_4'), 84.7 (s, C_4 or C_4'), 75.0 (s, C_1 or C_1'), 73.6 (s, C_1 or C_1'), 22.8 (s, C_6), 20.8 (s, C_3 or C_3'), 20.5 (s, C_3 or C_3'). Anal. Calcd. for $\text{C}_{10}\text{H}_{17}\text{F}_6\text{SbPd}$: C, 25.05; H, 3.58. Found: C, 24.92; H, 3.51.



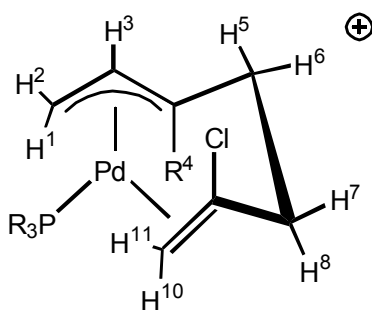
***In Situ* Generation of [(2Cl-allyl)Pd(isoprene)][SbF₆] 6-Cl.** A screw-cap NMR tube was charged with [(allyl)Pd(Mes)][SbF₆] (0.0106g, 2.0×10^{-5} mol) dissolved in ca. 400 μL CDCl_2F . The tube was placed in a -78 °C bath and one equivalent isoprene (20 μL of 1.0 M isoprene/ CD_2Cl_2 solution) was added via syringe. The tube was quickly shaken to allow mixing and a color change from yellow to colorless was observed. More than one equivalent of diene added results in line broadening, indicative of rapid exchange between free and bound diene, which is dependent upon temperature. **NMR**

Characterization: ^1H NMR (500 MHz in CD_2Cl_2 , $-90\text{ }^\circ\text{C}$): Prone *s-cis* minor isomer: δ 6.26 (dd, $^3J_{\text{HH}} = 9.0\text{ Hz}$, $^3J_{\text{HH}} = 19.5\text{ Hz}$, 1H, H_1), 5.76 (d, $^3J_{\text{HH}} = 9.0\text{ Hz}$, 1H, H_2), 5.64 (s, 1H, H_{syn}), 5.59 (s, 1H, H_{syn}), 5.49 (s, 1H, H_4), 3.98 (s, 1H, H_5), 3.98 (s, 1H, H_{anti}), 3.89 (s, 1H, H_{anti}), 2.31 (s, 3H, CH_3). ^1H NMR (500 MHz in CD_2Cl_2 , $-90\text{ }^\circ\text{C}$): two *s-trans* major isomers: δ 5.86 (dd, $^3J_{\text{HH}} = 8.5\text{ Hz}$, $^3J_{\text{HH}} = 16.0\text{ Hz}$, 2H, H_1), 5.70 (d, $^3J_{\text{HH}} = 8.5\text{ Hz}$, H_2), 5.66 (s, 1H, H_{syn}), 5.47 (s, 1H, H_4), 5.44 (s, 1H, H_4), 5.44 (s, 1H, H_{syn}), 5.42 (s, 1H, H_{syn}), 5.31 (s, 1H, H_{syn}), 4.90 (d, $^3J_{\text{HH}} = 16.0\text{ Hz}$, 2H, H_3), 4.79 (s, 1H, H_5), 4.45 (s, 1H, H_5), 4.30 (s, 1H, H_{anti}), 4.26 (s, 1H, H_{anti}), 3.89 (s, 1H, H_{anti}), 3.89 (s, 1H, H_{anti}), 1.93 (s, 3H, CH_3), 1.81 (s, 3H, CH_3). free mesitylene δ 6.80 (s, 3H, ArH), 2.29 (s, 9H, ArMe).

Synthesis of precipitate $[(\text{allyl})\text{Pd}(\eta^4\text{-BD})][\text{SbF}_6]$ 7-H. Under an argon atmosphere, $[(\text{allyl})\text{Pd}(\text{mes})][\text{SbF}_6]$ **3-H** (0.100 g, 0.20 mmol) was dissolved in dry methylene chloride (20 mL) and the resulting yellow/orange solution was stirred at room temperature for five minutes to dissolve the solid, and then the resulting solution was cooled to $-78\text{ }^\circ\text{C}$. Four equivalents of 1,3-butadiene (70 μL , 0.80 mmol) was stirred for ca. 30 min at low temperature before the mixture containing the colorless product as a precipitate was allowed to warm slowly to $-20\text{ }^\circ\text{C}$. Then the solvent evaporated *in vacuo* from $-20\text{ }^\circ\text{C}$ to $0\text{ }^\circ\text{C}$ to yield the colorless powder precipitate. The syntheses were completed in 2 hours and immediately stored in the glove box at $-35\text{ }^\circ\text{C}$.

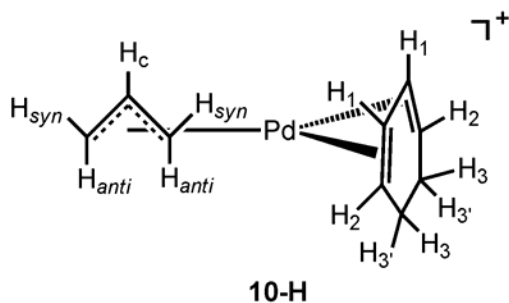


In Situ generation of wrap-around complex 8-Cl. A screw-cap NMR tube was charged with [(2Cl-allyl)Pd(Mes)][SbF₆] (0.011 g, 2.0 x 10⁻⁵ mol) dissolved in 500 μ L CD₂Cl₂. The tube was placed in a -78°C bath and two equivalents 1,3-butadiene (40 μ L of 1.0 M 1,3-butadiene/CD₂Cl₂ solution) were added via syringe. The tube was quickly and briefly shaken to allow mixing and a solution color change from yellow to colorless was observed in addition to observation of a white precipitate. The white precipitate was presumably the η^4 -diene adduct that could not be observed by NMR due to its insolubility. The mixture was warmed to room temperature and shaken, resulting in disappearance of the precipitate and a color change of the solution from clear to pale yellow and formation of the wrap-around **8-Cl**. **NMR Characterization:** ¹H NMR (500 MHz in CD₂Cl₂, 25 °C): δ 6.37 (m, 1H, H_c), 5.46 (s, 1H, H₆), 5.45 (m, 1H, H₁), 4.95 (s, 1H, H₇), 4.75 (d, 1H, ³J_{HH} = 7.0 Hz, H_{syn}), 3.84 (d, 1H, ³J_{HH} = 12.5 Hz, H_{anti}), 3.41 (m, 1H, H₅), 2.98 (dt, 1H, ³J_{HH} = 15.0 Hz, ²J_{HH} = 4.6 Hz, H₄), 2.89 (m, 1H, H₃), 2.47 (m, 1H, H₂). free mesitylene δ 6.82 (s, 6H, ArH), 2.34 (s, 18H, ArMe).

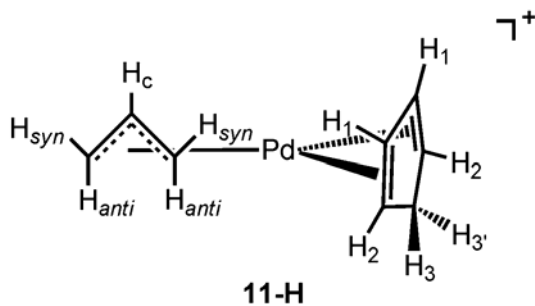


Trapping of wrap-around 9-Cl with PPh₃. To the solution generated in the previous experiment, 1 equivalent PPh₃ was added via syringe to form **9-Cl**, which has identical spectra to the same, independently prepared complex (see chapter 4). ¹H NMR (400 MHz, CD₂Cl₂, 25 °C): δ 7.4-7.6 (m, 15H, PPh₃), 6.39 (m, 1H, H₃), 6.07 (m, 1H, R₄ = H), 5.13 (s, 1H, H₁₀), 4.51 (s, 1H, H₁₁), 4.02 (td, ³J_{HH} = 13.5 Hz, ³J_{HH} = 4.0 Hz, 1H, H₈), 3.77

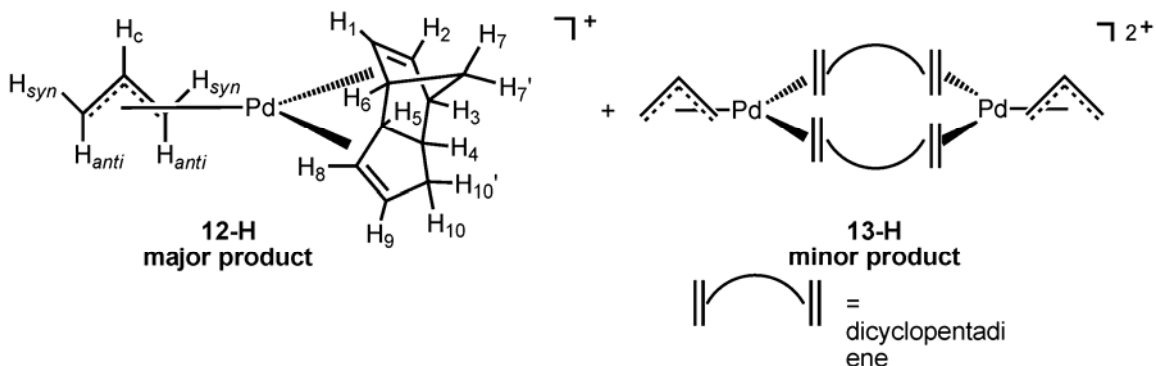
(d, $^3J_{\text{HH}} = 6.4$ Hz, 1H, H₂), 3.53 (m, 1H, H₇), 3.49 (d, $^3J_{\text{HH}} = 12.0$ Hz, 1H, H₁), 3.26 (m, 1H, H₆), 2.90 (m, 1H, H₅). $^{31}\text{P}\{^1\text{H}\}$ NMR (160 MHz, CD₂Cl₂, 25 °C): δ 27.7.



In Situ Generation of [(allyl)Pd(η^4 -cyclohexa-1,3-diene)][SbF₆] 10-H. A screw-cap NMR tube was charged with [(allyl)Pd(Mes)][SbF₆] (0.0106g, 2.0×10^{-5} mol) dissolved in ca. 400 μL CDCl₂F. The tube was placed in a -78 °C bath and two equivalents cyclohexa-1,3-diene(CHD) (3.8 μL , 2.0×10^{-5} mol) were added via syringe. The tube was quickly shaken to allow mixing and a color change from yellow to colorless was observed. More than one equivalent of diene added resulted in an exchange between excess diene and the diene adduct in solution; this exchange process was temperature dependent. **NMR Characterization:** ^1H NMR (500 MHz in CDCl₂F, -100 °C): δ 6.62 (bs, 2H, H₂), 6.13 (d, $^3J_{\text{HH}} = 6.5$ Hz, 2H, H₁), 5.89 (m, 1H, H_c), 5.48 (d, $^3J_{\text{HH}} = 7.0$ Hz, 2H, H_{syn}), 3.67 (d, $^3J_{\text{HH}} = 13.5$ Hz, 2H, H_{anti}), 2.13 (bs, 4H, H₃ and H_{3'}). Free mesitylene: δ 6.83 (s, 3H, ArH), 2.26 (s, 9H, ArMe). Free CHD: δ 6.19, 6.03, 2.44.



***In Situ* Generation of [(allyl)Pd(η^4 -cyclopentadiene)][SbF₆] 11-H.** A screw-cap NMR tube was charged with [(allyl)Pd(Mes)][SbF₆] (0.0106g, 2.0×10^{-5} mol) dissolved in ca. 400 μ L CDCl₂F. The tube was placed in a -78 °C bath and two equivalents cyclopentadiene (2.0 μ L, 4.0×10^{-5} mol) were added via syringe. The tube was quickly shaken to allow mixing and a color change from yellow to colorless was observed. More than one equivalent of diene added resulted in an exchange between excess diene and the diene adduct in solution; this exchange process was temperature dependent. **NMR Characterization:** ¹H NMR (500 MHz in CD₂Cl₂, -90 °C): δ 6.65 (bs, 2H, H₁ + H₂), 6.01 (m, 1H, H_c), 3.66 (bs, 2H, H_{syn}), 3.50 ppm (d, ³J_{HH} = 14.0 Hz, 2H, H_{anti}), 3.29 (d, ³J_{HH} = 25.5 Hz, 1H, H₃ or H_{3'}), 3.20 (d, ³J_{HH} = 25.5 Hz, 1H, H₃ or H_{3'}). Free mesitylene: δ 6.73 (s, 3H, ArH), 2.18 (s, 9H, ArMe). Free cyclopentadiene: δ 6.57, 6.52, 2.94.



***In Situ* Generation of [(allyl)Pd(η^4 -dicyclopentadiene)][SbF₆] 12-H and dinuclear species 13-H.** A screw-cap NMR tube was charged with [(allyl)Pd(Mes)][SbF₆] (0.0106g, 2.0×10^{-5} mol) dissolved in ca. 400 μ L CDCl₂F. The tube was placed in a -78 °C bath and one equivalent dicyclopentadiene (DCPD) (3.0 mg, 2.0×10^{-5} mol) was added via syringe. The tube was quickly shaken to allow mixing and a color change from yellow to colorless was observed. **NMR Characterization: Major Isomer** ¹H NMR (500 MHz in CD₂Cl₂, 25 °C): δ 7.92 (s, 1H, H₂), 7.28 (s, 1H, H₁), 6.57 (s, 1H, H₉), 6.12

(s, 1H, H₈), 6.02 (m, 1H, H_c), 4.90 (d, $^3J_{\text{HH}} = 7.0$ Hz, 1H, H_{syn}), 4.70 (d, $^3J_{\text{HH}} = 7.0$ Hz, 1H, H_{syn}), 3.91 (bs, overlap with minor isomer, 1H, H₅), 3.85 (bs, overlap with minor isomer, 1H, H₃), 3.67 (d, $^3J_{\text{HH}} = 13.0$ Hz, 1H, H_{anti}), 3.52 (d, $^3J_{\text{HH}} = 13.0$ Hz, 1H, H_{anti}), 3.06 (dd, $^3J_{\text{HH}} = 9.5$ Hz, $^3J_{\text{HH}} = 9.5$ Hz, 1H, H₄), 2.98 (bs, overlap with minor isomer, 1H, H₆), 2.37 (dd, $^3J_{\text{HH}} = 10.5$ Hz, $^3J_{\text{HH}} = 19.0$ Hz, 1H, H₁₀), 2.13 (overlap, 1H, H₇), 2.10 (overlap, 1H, H_{10'}), 1.97 (d, $^3J_{\text{HH}} = 9.0$ Hz, overlap with minor isomer, 1H, H_{7'}). **Minor Isomer** ¹H NMR (500 MHz in CD₂Cl₂, 25 °C): δ 7.69 (s, 1H, H₂), 7.33 (s, 1H, H₁), 6.65 (s, 1H, H₉), 5.98 (s, 1H, H₈), 5.97 (m, 1H, H_c), 4.73 (d, $^3J_{\text{HH}} = 7.5$ Hz, 1H, H_{syn}), 4.68 (d, $^3J_{\text{HH}} = 7.5$ Hz, 1H, H_{syn}), 3.91 (bs, overlap with minor isomer, 1H, H₅), 3.85 (bs, overlap with minor isomer, 1H, H₃), 3.75 (d, $^3J_{\text{HH}} = 13.0$ Hz, 1H, H_{anti}), 3.68 (d, $^3J_{\text{HH}} = 13.0$ Hz, 1H, H_{anti}), 3.12 (bs, 1H, H₄), 2.98 (bs, overlap with minor isomer, 1H, H₆), 2.52 (m, 1H, H₁₀), 2.13 (overlap, 1H, H₇), 2.10 (overlap, 1H, H_{10'}), 1.97 (d, $^3J_{\text{HH}} = 9.0$ Hz, overlap with minor isomer, 1H, H_{7'}).

***In Situ* Reaction of [(allyl)Pd(mes)][SbF₆] 3-H with ethylene and cyclopentadiene.** A J-Young NMR tube was charged with [(allyl)Pd(Mes)][SbF₆] (0.0106g, 2.0×10^{-5} mol) dissolved in ca. 400 μL CDCl₂F. The NMR tube was placed in a dry ice/isopropanol bath and then two equivalents cyclopentadiene (4.0 μL, 4.0×10^{-5} mol) were added via syringe. The tube was then placed in liquid nitrogen and one equivalent ethylene was added via a calibrated gas bulb. The tube was placed back in the dry ice/isopropanol bath and quickly shaken to allow mixing and a color change from yellow to colorless was observed. At -120 °C, the [(allyl)Pd(η⁴-cyclopentadiene)]⁺ species (see experimental data above), the [(allyl)Pd(ethylene)₂]⁺ species (see experimental section, chapter 2), and a

species presumed to be $[(\text{allyl})\text{Pd}(\eta^2\text{-cyclopentadiene})(\eta^2\text{-ethylene})]^+$ were observed. The $[(\text{allyl})\text{Pd}(\eta^2\text{-cyclopentadiene})(\eta^2\text{-ethylene})]^+$ was not fully characterized.

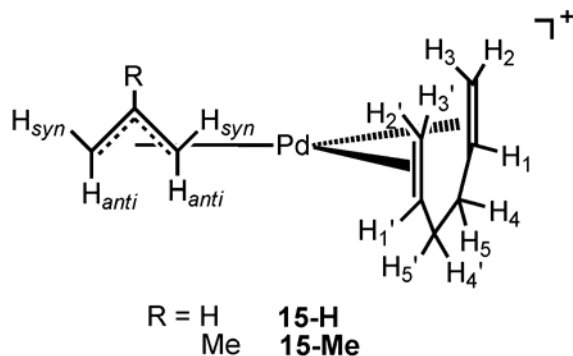
***In Situ* Reaction of $[(\text{allyl})\text{Pd}(\text{mes})][\text{SbF}_6]$ 3-H with 2-butyne and cyclopentadiene.**

Similar to the previous experiment, a screw-cap NMR tube was charged with $[(\text{allyl})\text{Pd}(\text{Mes})][\text{SbF}_6]$ (0.0106g, 2.0×10^{-5} mol) dissolved in ca. 400 μL CDCl_2F and cooled to -78°C . Two equivalents of both cyclopentadiene and 2-butyne were added via syringe, and formation of the $[(\text{allyl})\text{Pd}(\eta^4\text{-cyclopentadiene})]^+$ species (see NMR assignments above) was observed along with the $[(\text{allyl})\text{Pd}(\text{2-butyne})_2]^+$ species (see chapter 2 for NMR assignments) and a third species presumed to be $[(\text{allyl})\text{Pd}(\eta^2\text{-cyclopentadiene})(\eta^2\text{-2-butyne})]^+$, which was not characterized.

***In Situ* Generation of $[(2\text{-Me-allyl})\text{Pd}(1,5\text{-hexadiene})][\text{SbF}_6]$ Complex 15-Me.** A screw-cap NMR tube was charged with $[(2\text{-Me-allyl})\text{Pd}(\text{Mes})][\text{SbF}_6]$ (0.0106g, 2.0×10^{-5} mol) dissolved in 400 μL CD_2Cl_2 . The tube was placed in a -78°C bath and one equivalent 1,5-hexadiene was added via syringe. The tube was quickly and briefly shaken to allow mixing and a color change from yellow to colorless was observed. More than one equivalent of diene added results in line broadening, indicative of rapid exchange between bound and free diene in solution; the exchange is dependent upon temperature. **NMR Characterization:** ^1H and ^{13}C NMR spectra for **15-Me** were identical to the independently synthesized species (see below), but also contained free mesitylene and free hexa-1,5-diene: ^1H NMR (500 MHz in CD_2Cl_2 , -90°C): free mesitylene δ 6.79 (s, 3H, ArH), 2.20 (s, 9H, ArMe). free hexa-1,5-diene δ 5.76 (m, 2H, H_1), 4.97 (overlap, 2H, H_2), 4.91 (d, 2H, H_3), 2.06 (s, $\text{H}_4 + \text{H}_5$).

***In Situ* Generation of [(allyl)Pd(1,5-hexadiene)][SbF₆] Complex 15-H.** A screw-cap NMR tube was charged with [(allyl)Pd(Mes)][SbF₆] (0.0104g, 2.0 x 10⁻⁵ mol) dissolved in ca. 400 μ L CDCl₂F. The tube was placed in a -78°C bath and one equivalent 1,5-hexadiene was added via syringe. The tube was quickly and briefly shaken to allow mixing and a color change from yellow to colorless was observed. More than one equivalent of diene added results in line broadening, indicative of rapid exchange between bound and free diene in solution; the exchange is dependent upon temperature.

NMR Characterization: ¹H and ¹³C NMR spectra for **15-H** were identical to the independently synthesized species (see below), but also contained free mesitylene and free hexa-1,5-diene: ¹H NMR (500 MHz in CD₂Cl₂, -90 °C): free mesitylene δ 6.79 (s, 3H, ArH), 2.20 (s, 9H, ArMe). free hexa-1,5-diene δ 5.76 (m, 2H, H₁), 4.97 (overlap, 2H, H₂), 4.91 (d, 2H, H₃), 2.06 (s, H₄ + H₅).



Synthesis of [(2-methallyl)Pd(1,5-hexadiene)][SbF₆] Complex 15-Me. This complex was synthesized similar to Maitlis literature procedure.³⁵ Under an argon atmosphere, the palladium halide dimer [(2-methallyl)PdCl]₂ (0.35 g, 0.73 mmol) was dissolved in dry methylene chloride (20 mL) and the resulting yellow solution was stirred at room temperature for five minutes to dissolve the solid. Four equivalents hexa-1,5-diene (0.34 mL, 2.90 mmol) were added and then a solution of two equivalents silver

hexafluoroantimonate (0.60 g, 1.45 mmol) in 5 mL methylene chloride was added dropwise at -78 °C and the mixture was stirred for ca. 30 min at low temperature before the solution was allowed to warm slowly to room temperature. The resulting solution was cannula filtered and the solvent evaporated *in vacuo* and then washed with 3x10 mL of dry pentane and dried under vacuum to yield a yellow powder. The syntheses were completed in 4-5 hours and immediately stored in the glove box at -35 °C. **NMR Characterization:** ¹H NMR (500 MHz in CDCl₂F, 20 °C): δ 6.33 (m, 1H, H₁ or H_{1'}), 6.28 (m, 1H, H₁ or H_{1'}), 5.56 (d, ³J_{HH} = 12.0 Hz, 2H, H₂ or H_{2'}), 5.00 (d, ³J_{HH} = 12.0 Hz, 2H, H₂ or H_{2'}), 5.42 (d, ³J_{HH} = 21.5 Hz, 1H, H₃ or H_{3'}), 4.79 (s, 2H, H_{syn}), 4.45 (d, ³J_{HH} = 21.5 Hz, 1H, H₃ or H_{3'}), 3.62 (s, 2H, H_{anti}), 2.94 (m, 2H, H₅ and H_{5'}), 2.63 (m, 2H, H₄ and H_{4'}), 2.25 (s, 3H, CH₃).

Synthesis of [(allyl)Pd(1,5-hexadiene)][SbF₆] Complex 15-H. This complex was also synthesized similar to Maitlis literature procedure.³⁵ Under an argon atmosphere, the palladium halide dimer [(allyl)PdCl]₂ (0.38 g, 0.73 mmol) was dissolved in dry methylene chloride (20 mL) and the resulting yellow solution was stirred at room temperature for five minutes to dissolve the solid. Four equivalents hexa-1,5-diene (0.34 mL, 2.90 mmol) were added. Then a solution of two equivalents silver hexafluoroantimonate (0.60 g, 1.45 mmol) in 5 mL methylene chloride was added dropwise at -78 °C and the mixture was stirred for ca. 30 min at low temperature before the solution was allowed to warm slowly to room temperature. The resulting solution was cannula filtered and the solvent evaporated *in vacuo* and then washed with 3x10 mL of dry pentane and dried under vacuum to yield a yellow powder. The syntheses were completed in 4-5 hours and immediately stored in the glove box at -35 °C. **NMR**

Characterization: ^1H NMR (500 MHz in CD_2Cl_2 , $-90\text{ }^\circ\text{C}$): δ 6.18 (m, 1H, H_1 or $\text{H}_{1'}$), 6.11 (m, 1H, H_1 or $\text{H}_{1'}$), 5.96 (m, 1H, H_c), 5.54 (d, $^3J_{\text{HH}} = 8.0\text{ Hz}$, 2H, H_2 and $\text{H}_{2'}$), 4.97 (d, $^3J_{\text{HH}} = 7.5\text{ Hz}$, 2H, H_{syn}), 4.77 (d, $^3J_{\text{HH}} = 16.5\text{ Hz}$, 1H, H_3 or $\text{H}_{3'}$), 4.31 (d, $^3J_{\text{HH}} = 16.5\text{ Hz}$, 1H, H_3 or $\text{H}_{3'}$), 3.63 (d, $^3J_{\text{HH}} = 13.5\text{ Hz}$, 2H, H_{anti}), 2.86 (m, 2H, H_5 and $\text{H}_{5'}$), 2.59 (m, 2H, H_4 and $\text{H}_{4'}$).

References and Notes

- (1) Taube, R.; Wache, S. *J. Organomet. Chem.* **1992**, 428, 431.
- (2) Taube, R.; Sylvester, G. *Stereospecific Polymerization of Butadiene or Isoprene.*; Cornils, B., Herrmann, W. A. Eds.; VCH: Weinheim, Germany, 1996.
- (3) Taube, R.; Schmidt, U.; Gehrke, J. P.; Anacker, U. *J. Prakt. Chem.* **1984**, 326, 1.
- (4) Taube, R.; Langlotz, J.; Sieler, J.; Gelbrich, T.; Tittes, K. *J. Organomet. Chem.* **2000**, 597, 92.
- (5) Taube, R.; Gehrke, J. P.; Schmidt, U. *J. Organomet. Chem.* **1985**, 292, 287.
- (6) Taube, R.; Gehrke, J. P.; Bohme, P.; Scherzer, K. *J. Organomet. Chem.* **1991**, 410, 403.
- (7) Taube, R.; Gehrke, J. P.; Bohme, P.; Kottwitz, J. *J. Organomet. Chem.* **1990**, 395, 341.
- (8) Taube, R.; Gehrke, J. P. *J. Organomet. Chem.* **1987**, 328, 393.
- (9) Taube, R.; Gehrke, J. P. *J. Organomet. Chem.* **1985**, 291, 101.
- (10) Campora, P. J.; Carmona, G. E.; Conejo Argandona, M. M. 2004.
- (11) Campora, P. J.; Conejo, M. D. M.; Reyes, M. L.; Mereiter, K.; Passaglia, E. *Chem. Commun.* **2003**, 78.
- (12) O'Connor, A. R.; White, P. S.; Brookhart, M. *J. Am. Chem. Soc.* **2007**, 129, 4142.
- (13) O'Connor, A. R., University of North Carolina at Chapel Hill, 2008.
- (14) Yasuda, H.; Nakano, Y.; Natsukawa, K.; Tani, H. *Macromolecules* **1978**, 11, 586.
- (15) Tobisch, S.; Bogel, H.; Taube, R. *Organometallics* **1996**, 15, 3563.
- (16) Dahlmann, M.; Erker, G.; Froehlich, R.; Mayer, O. *Organometallics* **1999**, 18, 4459.
- (17) Kai, Y.; Kanehisa, N.; Miki, K.; Kasai, N.; Mashima, K.; Nagasuna, K.; Yasuda, H.; Nakamura, A. **1982**, 191.
- (18) Okamoto, T.; Yasuda, H.; Nakamura, A.; Kai, Y.; Kanehisa, N.; Kasai, N. *J. Am. Chem. Soc.* **1988**, 110, 5008.

- (19) Melendez, E.; Arif, A. M.; Rheingold, A. L.; Ernst, R. D. *J. Am. Chem. Soc.* **1988**, *110*, 8703.
- (20) Strauch, H. C.; Erker, G.; Froehlich, R. *Organometallics* **1998**, *17*, 5746.
- (21) Strauch, H. C.; Roesmann, R.; Pacheiner, S.; Erker, G.; Froehlich, R.; Wibbeling, B. *J. Organomet. Chem.* **1999**, *584*, 318.
- (22) Wang, L.-S.; Fettingner, J. C.; Poli, R. *J. Am. Chem. Soc.* **1997**, *119*, 4453.
- (23) Poli, R.; Wang, L.-S. *J. Am. Chem. Soc.* **1998**, *120*, 2831.
- (24) Hunter, A. D.; Legzdins, P.; Nurse, C. R.; Einstein, F. W. B.; Willis, A. C. *J. Am. Chem. Soc.* **1985**, *107*, 1791.
- (25) Christensen, N. J.; Hunter, A. D.; Legzdins, P. *Organometallics* **1989**, *8*, 930.
- (26) Benyunes, S. A.; Green, M.; Grimshire, M. J. *Organometallics* **1989**, *8*, 2268.
- (27) Debad, J. D.; Legzdins, P.; Young, M. A.; Batchelor, R. J.; Einstein, F. W. B. *J. Am. Chem. Soc.* **1993**, *115*, 2051.
- (28) Cheng, M.-H.; Ho, Y.-H.; Chen, C.-C.; Lee, G.-H.; Peng, S.-M.; Chu, S.-Y.; Liu, R.-S. *Organometallics* **1994**, *13*, 4082.
- (29) Herrmann, W. A.; Fischer, R. A.; Herdtweck, E. *Organometallics* **1989**, *8*, 2821.
- (30) Ernst, R. D.; Melendez, E.; Stahl, L.; Ziegler, M. L. *Organometallics* **1991**, *10*, 3635.
- (31) Melendez, E.; Ilarraza, R.; Yap, G. P. A.; Rheingold, A. L. *J. Organomet. Chem.* **1996**, *522*, 1.
- (32) Gemel, C.; Mereiter, K.; Schmid, R.; Kirchner, K. *Organometallics* **1997**, *16*, 2623.
- (33) Sugaya, T.; Tomita, A.; Sago, H.; Sano, M. *Inorg. Chem.* **1996**, *35*, 2692.
- (34) O'Connor, A. R.; Urbin, S. A.; Moorhouse, R. A.; White, P. S.; Brookhart, M. *Organometallics* **2009**, *28*, 2372.
- (35) Mabbott, D. J.; Mann, B. E.; Maitlis, P. M. *J. C. S. Dalton* **1977**, 294.
- (36) Alaimo, P. J.; Peters, D. W.; Arnold, J.; Bergman, R. *J. Chem. Educ.* **2001**, *78*, 64.

- (37) Pangborn, A. B.; Giardello, M. A.; Grubbs, R. H.; Rosen, R. K.; Timmers, F. J. *Organometallics* **1996**, *15*, 1518.
- (38) Siegel, J. S.; Anet, F. A. *J. Org. Chem.* **1988**, *53*, 2629.
- (39) Aranyos, A.; Szabo, K. J.; Castano, A. M.; Backvall, J.-E. *Organometallics* **1997**, *16*, 1058.
- (40) Auburn, P. R.; Mackenzie, P. B.; Bosnich, B. *J. Am. Chem. Soc.* **1985**, *107*, 2033.
- (41) Dent, W. T.; Long, R.; Wilkinson, A. J. *J. Chem. Soc.* **1964**, 1585.
- (42) Wilke, G.; Bogdanovic, B.; Heimbach, P.; Keim, W.; Kroner, M.; Oberkirch, W.; Tanaka, K.; Steinrucke, E.; Walter, D.; Zimmerman, H. *Angew. Chem. Int. Ed.* **1966**, *5*, 151.

CHAPTER FOUR

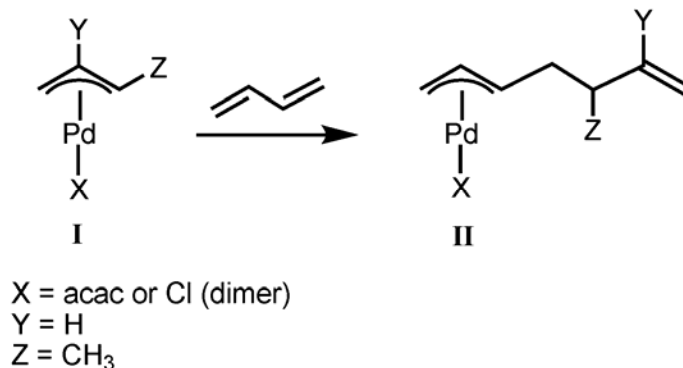
Synthesis, Characterization, and Reactivity of (π -Allyl)Palladium(II)

Wrap-Around Complexes with 1,3-Dienes

Introduction

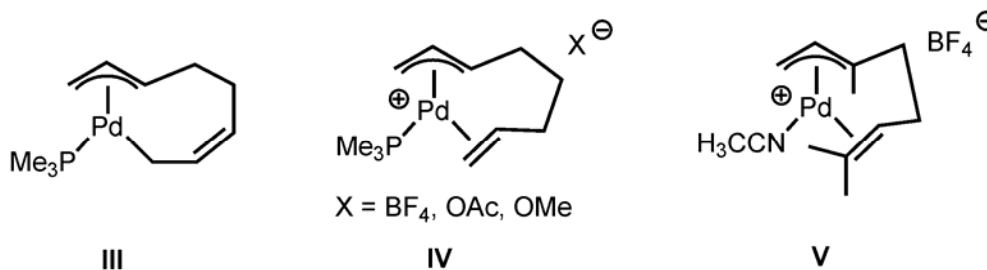
Insertion of 1,3-butadiene (BD) and isoprene (IP) into several different (π -allyl)palladium(II)-based complexes to form the corresponding η^3 “first insertion” products has been previously investigated (Scheme 4.1).¹⁻⁵ These palladium dimers are resistant to further insertion of 1,3-dienes and are not active for 1,3-diene polymerization. For several mononuclear complexes, the “first insertion” product can bind to the terminal olefin generated upon coupling and form “wrap-around” species. Direct evidence for wrap-around first insertion products that are η^3 and η^2 bound to the metal center has been limited until recently.⁶ The role and function of the wrap-around intermediate in the polymerization of 1,3-dienes is not well understood, and as such, a closer examination of these complexes is warranted.

Scheme 4.1. Insertion of 1,3-butadiene into allyl moiety of Pd(II) halide dimer.



Several wrap-around polymerization insertion intermediates, resulting from coordination and insertion of two 1,3-dienes to yield an eight-carbon chain, have been previously proposed by Jolly and Vitagliano (Scheme 4.2).⁷⁻⁹ Although these complexes have not been directly observed in polymerization reactions, the proposed model intermediates have been independently synthesized and then characterized by ^1H and ^{13}C NMR spectroscopy.

Scheme 4.2. Known wrap-around complexes.

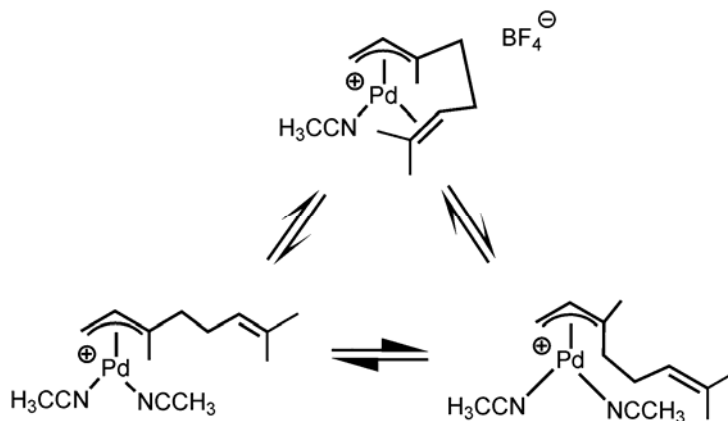


Jolly characterized two types of wrap-around intermediates; **III**, which is an $\eta^3\text{-}\eta^1$ bound neutral complex, and **IV**, an $\eta^3\text{-}\eta^2$ bound cationic complex prepared from **III** (Scheme 4.2). Complex **IV** is obtained by reaction of complex **III** with a proton source. Despite evidence for both complexes, Jolly proposes that the σ -bound complex **III** is the most likely insertion intermediate for the polymerization mechanism.

Vitagliano observes an η^3 - η^2 bound complex (**V**, Scheme 4.2) which has been characterized by X-ray crystallography.¹⁰ This wrap-around complex **V** is formed via reaction of complex **II** with AgBF_4 in the presence of acetonitrile, and is a useful model for the first insertion wrap-around product in the polymerization of 1,3-dienes.

Both groups have reported displacement of the η^2 -olefin by either acetic acid⁸ or acetonitrile.⁹ The tri-substituted, chelated olefin arm for complex **V** is not easily displaced by acetonitrile, and exists in equilibrium with the non-chelated species (Scheme 4.3). No further reactivity of these complexes with additional equivalents of 1,3-dienes has been reported.

Scheme 4.3. Displacement of η^2 -olefin chelate by nitrile.



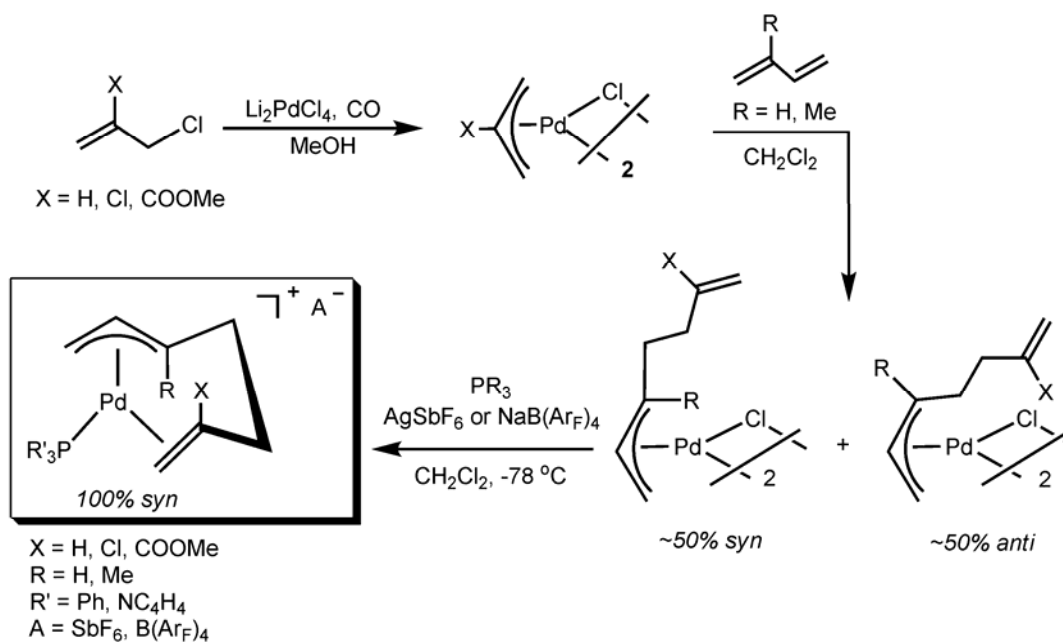
This chapter details the synthesis and characterization of cationic palladium wrap-around complexes bound in an η^3 - η^2 fashion. These complexes are stable models for the first insertion wrap-around species observed *in situ* and discussed in chapter 3. The nature of the binding of the η^2 -olefin arm is quantitatively analyzed and factors that influence the binding strength of the η^2 -olefin arm to the metal center are examined. A more labile olefin may be easier to displace by 1,3-dienes and therefore better able to

promote polymerization. As such, investigation of the palladium(II) wrap-around complexes as initiators for 1,3-diene polymerizations is explored.

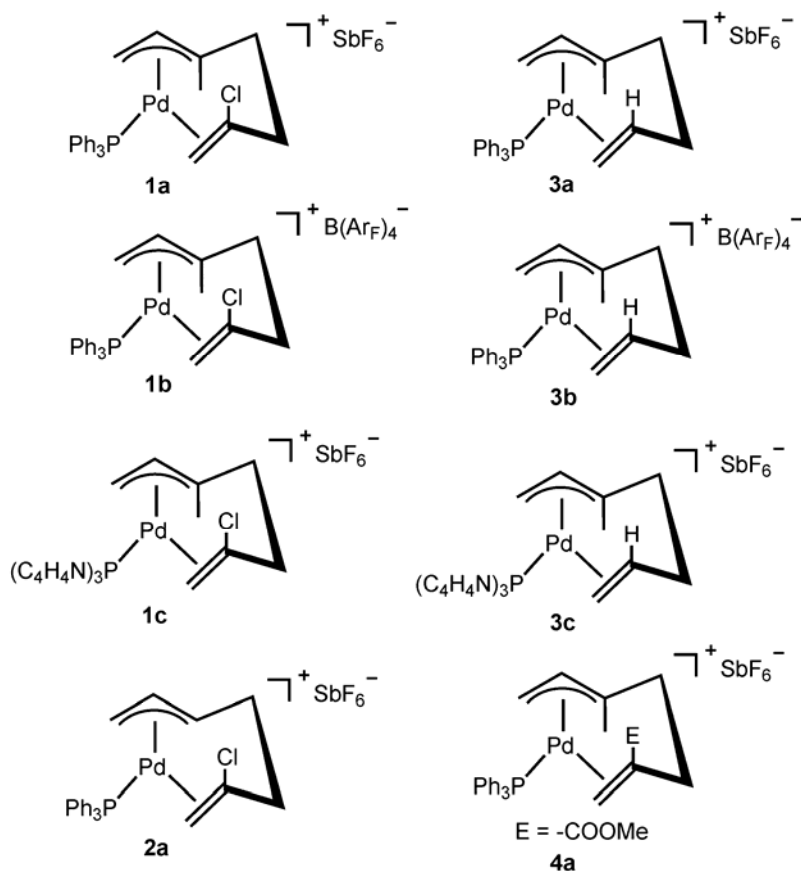
Results and Discussion

Synthesis of Wrap-Around Complexes. The wrap-around complexes **1a-4a** (see Scheme 4.5) were synthesized starting with the $[(\eta^3\text{-H}_2\text{CC(X)CH}_2)\text{PdCl}]_2$ dimer.¹¹ Functional groups in the 2-position of the allyl unit ($\text{X} = \text{H}, \text{Cl}, \text{COOMe}$) are readily incorporated by the use of the corresponding 2-substituted allyl chlorides. Selective insertion of a single diene unit forms the corresponding dimeric complexes as a 50:50 mixture of *syn* and *anti* isomers, and has been previously reported for $\text{X} = \text{H}$.^{1,3} Subsequent halide abstraction with $\text{NaB}(\text{Ar}_\text{F})_4$ or AgSbF_6 at -78°C and addition of a phosphine ligand affords the cationic *syn* wrap-around complexes in near quantitative yields (Scheme 4.4).

Scheme 4.4. General synthetic route for Pd(II) wrap-around complexes.



Scheme 4.5. Wrap-around Pd(II) complexes prepared.



The cationic, *syn* wrap-around complexes were characterized by multinuclear NMR spectroscopy and elemental analyses (see Experimental Section). The solid state structures of **1a** and **2a** were determined by X-ray crystallography. ORTEP drawings for **1a** and **2a** are shown in Figures 4.1 and 4.2, respectively. The crystallographic information is reported in Tables II.1 – II.3 of Appendix II. The X-ray structures confirm the *syn* geometry of the wrap-around complexes and the η^2 -binding of the chelating olefin arm.

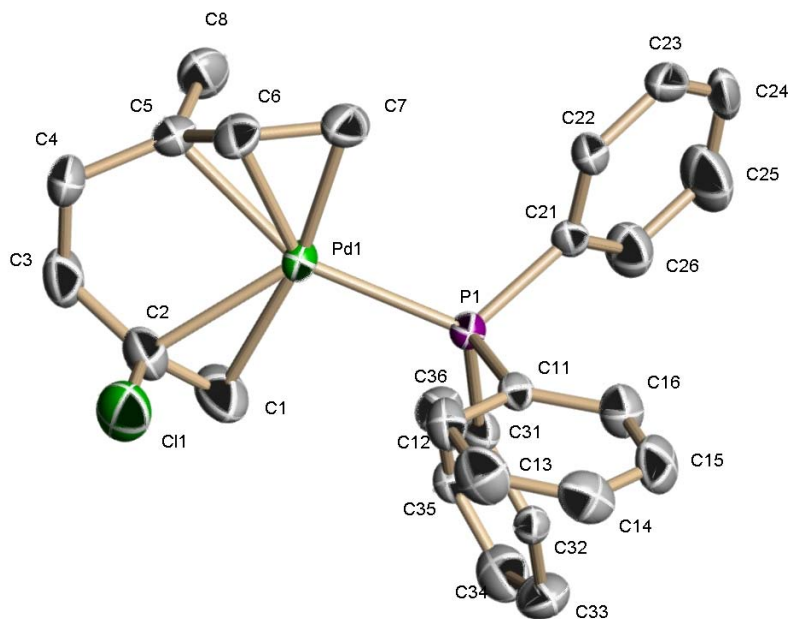


Figure 4.1. ORTEP diagram of **1a**. Thermal ellipsoids drawn at 50% probability, SbF_6^- and protons omitted for clarity. Selected bond lengths (Å): Pd(1)-C(7) 2.160(5), Pd(1)-C(6) 2.183(5), Pd(1)-C(5) 2.275(5), Pd(1)-C(1) 2.294(5), Pd(1)-C(2), 2.340(5), C(1)-C(2) 1.369(8), C(5)-C(6) 1.420(8), C(6)-C(7) 1.403(8).

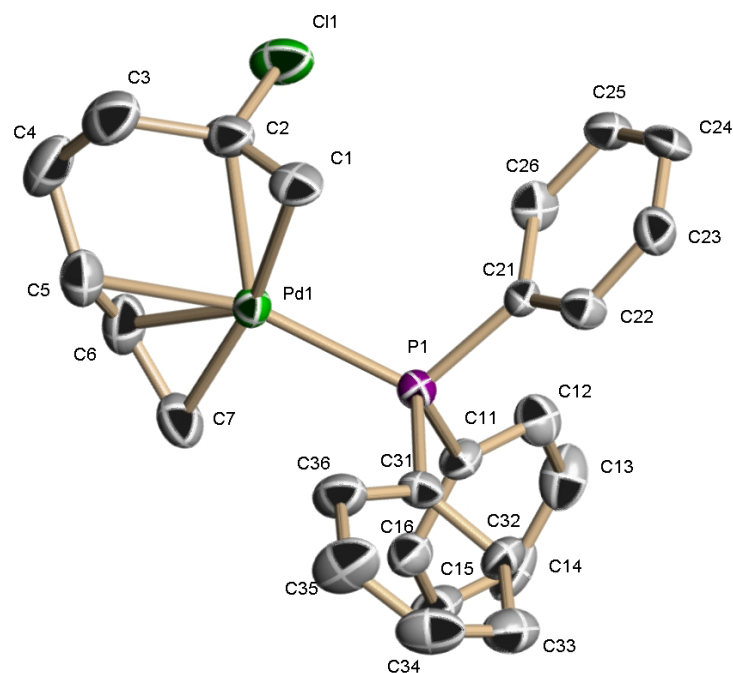


Figure 4.2. ORTEP diagram of **2a**. Thermal ellipsoids drawn at 50% probability, SbF_6^- and protons omitted for clarity. Selected bond lengths (Å): Pd(1)-C(7) 2.129(7), Pd(1)-C(6) 2.156(7), Pd(1)-C(5) 2.203(7), Pd(1)-C(1) 2.326(6), Pd(1)-C(2), 2.326(7), C(1)-C(2) 1.342(10), C(5)-C(6) 1.373(12), C(6)-C(7) 1.417(11).

Typical ^1H NMR spectra of the wrap-around complexes are shown in Figure 4.3. Signals assigned to the η^2 -bound olefinic protons appear upfield of the chemical shift of the corresponding free olefins, characteristic of alkene-metal interaction.¹²⁻¹⁴ Additionally, low temperature NMR studies ($-90\text{ }^\circ\text{C}$) of each complex verified that the structure and bonding properties were retained and did not undergo *syn/anti* isomerization or fluxional dissociation of the η^2 -olefin unit. The proton spectra are similar to a wrap-around complex reported by Echavarren and coworkers.¹⁵ Detailed peak assignments appear in the Experimental Section.

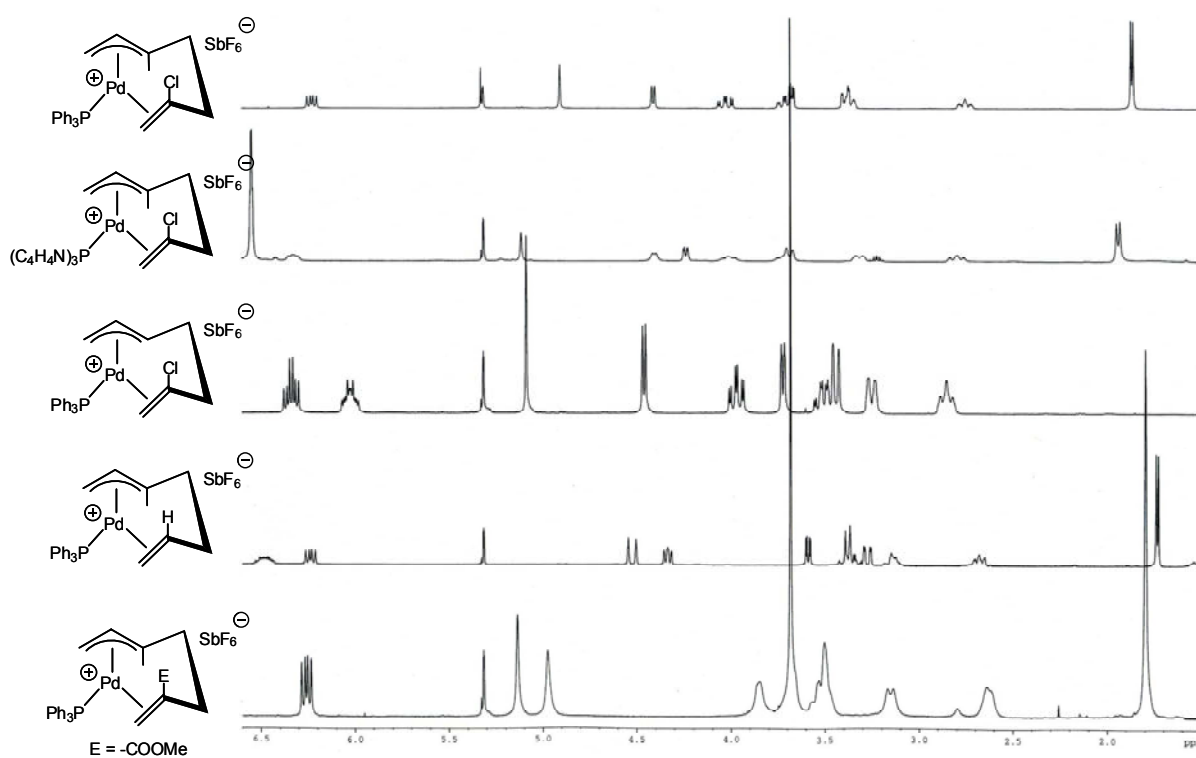
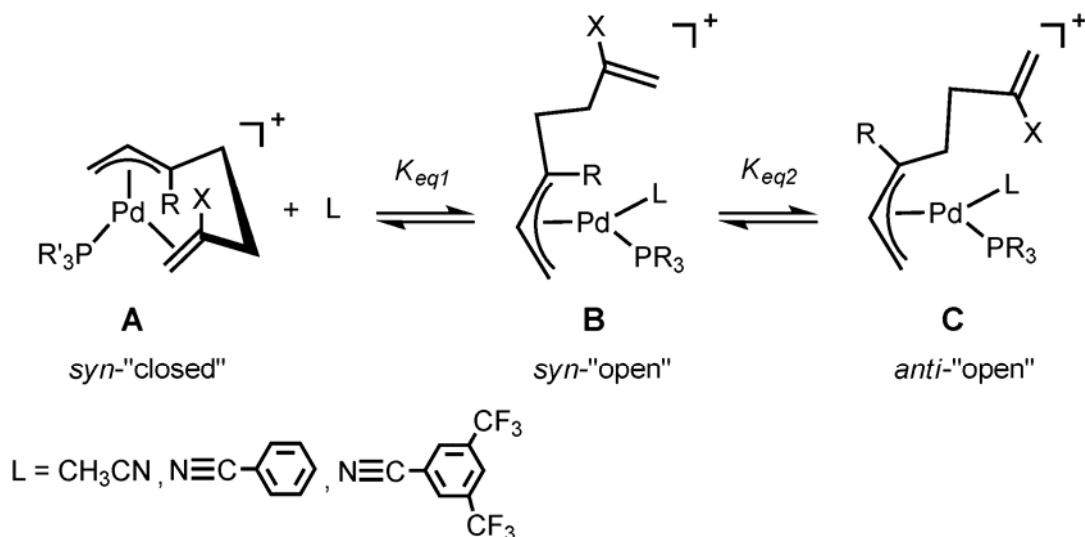


Figure 4.3. Sample ^1H NMR spectra of several *syn* wrap-around complexes.

Determination of Olefin Binding Affinities by Reaction of Wrap-Around Complexes with Nitriles. With the cationic palladium(II) wrap-around complexes in hand, titration experiments were performed using nitriles to displace the η^2 -olefin. A quantitative assessment of the equilibrium between the wrap-around complexes and their nitrile adducts provides relative binding strengths of the η^2 -olefins coordinated to the metal in the wrap-around complexes. The effect of varying the electronic properties of each η^2 -olefin, the phosphine ligand, and the counterion were examined. The equilibrium constants were quantified by monitoring the allylic, olefinic, and methyl ^1H NMR resonances and also the ^{31}P NMR resonances. These results reveal how readily the chelates open, and may offer insight as to the ability of these wrap-around complexes to serve as initiators for 1,3-diene polymerization.

Upon addition of nitrile to the wrap-around complex **A**, the nitrile may displace the η^2 -olefin to form the dechelated “open” complex **B**. Once the wrap-around complex is open, it can undergo *syn/anti* isomerization to form the open *anti* complex **C**, where the longer chain is *anti* to the allylic proton (H_c) (Scheme 4.6).

Scheme 4.6. Titration of wrap-around complexes with nitrile.



The opening/closing equilibria (interconversion of **A** and **B**) are fast on the NMR time scale and therefore only the time-averaged resonances are observed, whereas the *syn/anti* isomerization is slow on the NMR time scale. This is clearly shown by the olefinic, methyl, and allylic (H_c) resonances in the 1H NMR spectra in Figure 4.4, where 0, 1, 2, 3, and 5 equivalents of 3,5-bis(trifluoromethyl)benzonitrile have been added to **1b**. First, consider the allylic central 1H signal, H_c . At zero equivalents of nitrile, **1b** is completely closed and H_c resonates at 6.19 ppm. Upon addition of one equivalent of nitrile, the allylic resonance shifts upfield to 5.87 ppm, where this signal-averaged peak corresponds to 50:50 closed:open, or half **A** and half **B**. Subsequent additions of nitrile shift the allylic resonance further upfield until, at 5 equivalents of nitrile, **1b** has fully converted from closed (**A**) to open (**B**) and H_c resonates at 5.64 ppm. The equilibrium ratio of $[A]:[B]$ can be computed from the weighted average resonances (see below). The *syn/anti* isomerization from open *syn* complex **B** to *anti*-**C**, on the other hand, is slow on the NMR time scale, and *anti*-**C** has a separate, distinct H_c allylic resonance at 5.54 ppm. As more equivalents of nitrile are added, more of the open complex **B** is formed, which then in turn isomerizes to open complex **C**. At 1, 2, and 3 equivalents of nitrile, the allylic resonance for **C** grows as more open complex is formed and isomerized, until **1b** is fully opened at 5 equivalents of $(CF_3)_2$ -benzonitrile. At long times, the *syn/anti* ratio is constant and thermodynamically slightly favors the *syn* form.

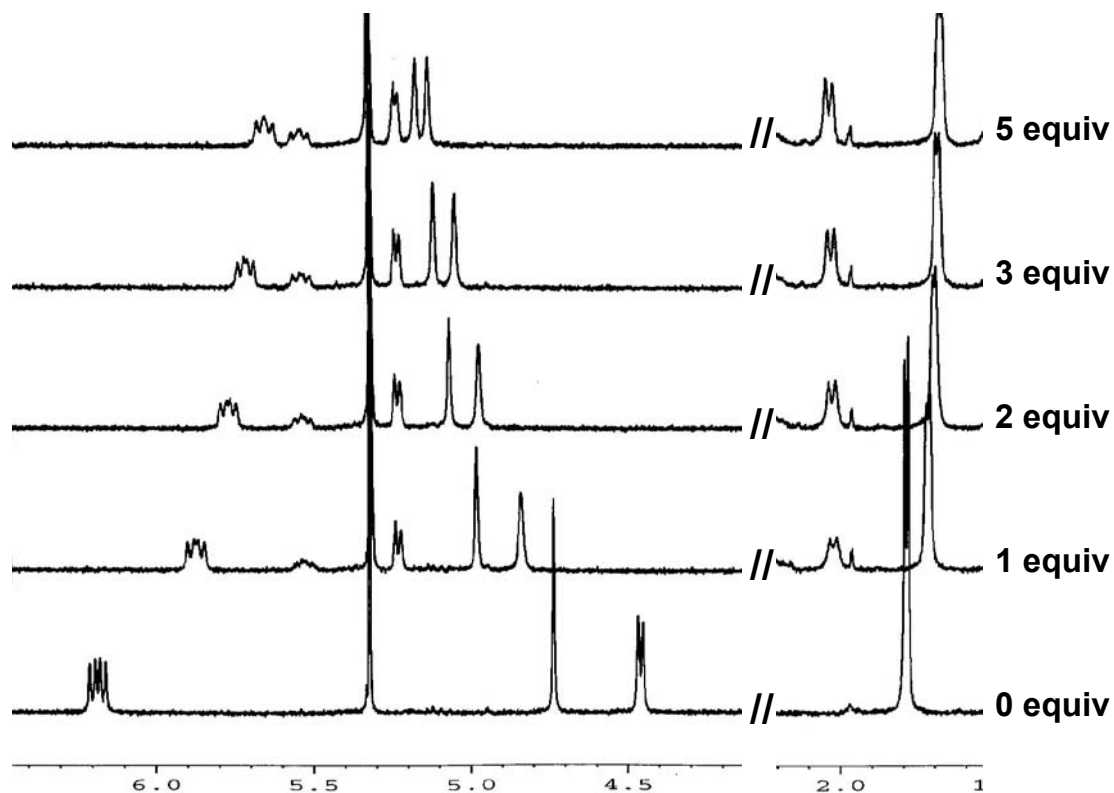


Figure 4.4. Allylic, olefinic, and methyl regions of the ^1H NMR spectra for the titration of **1b** with $(\text{CF}_3)_2$ -benzonitrile in $\text{CH}(\text{D})\text{Cl}_2$.

A similar phenomenon is observed with the olefinic resonances. The η^2 -bound olefinic protons in wrap-around complex **1b** resonate upfield at 4.73 and 4.46 ppm. Upon addition of nitrile, these olefinic protons shift downfield as the nitrile displaces the η^2 -olefin and resonate at 5.17 and 5.13 ppm when full conversion to **B** is achieved. The olefinic peaks for the *anti* open isomer, **C**, resonate at 5.24 and 5.23 ppm, characteristic of resonances for an unbound olefin. Finally, the methyl resonances exhibit the same behavior and resonate at 1.78 ppm for the completely closed complex **A**, 1.67 ppm for the completely open complex **B**, and 2.03 ppm for the *anti* open isomerized complex **C** for the 3,5-bis(trifluoromethyl)benzonitrile adduct.

Examination of the fast exchange between closed and open complexes **A** and **B** was possible through variable temperature ^{31}P NMR spectra upon addition of 5, 10, and 20 equivalents of benzonitrile to wrap-around complex **3a**. When five equivalents of benzonitrile were added to wrap-around complex **3a**, a roughly 50/50 mixture of open and closed species was generated (Figure 4.5). The phosphorus resonance at 28.1 ppm (23 °C), assigned to **C**, shifts upfield slightly to 27.6 ppm upon cooling to -80 °C. The second ^{31}P NMR peak at 27.1 ppm at room temperature, assigned to the time-averaged signal for **A** and **B**, broadens upon cooling, and decoalesces at temperatures lower than -70 °C into two separate peaks as the fast exchange between **A** and **B** is frozen out. At -80 °C, the resonance for the open complex of **3a**, or **B**, is shifted downfield to 28.0 ppm. Conversely, the resonance for the closed wrap-around complex **A** shifts upfield to 26.7 ppm towards the original phosphorus shift for the completely closed wrap-around **3a**, which resonates at 26.6 ppm. While the exchange between bound and free olefin is not completely frozen out at this temperature, as evidenced by the broad peaks, it is clear that the resonance at room temperature is indeed a time-averaged signal between open and closed complexes **A** and **B**.

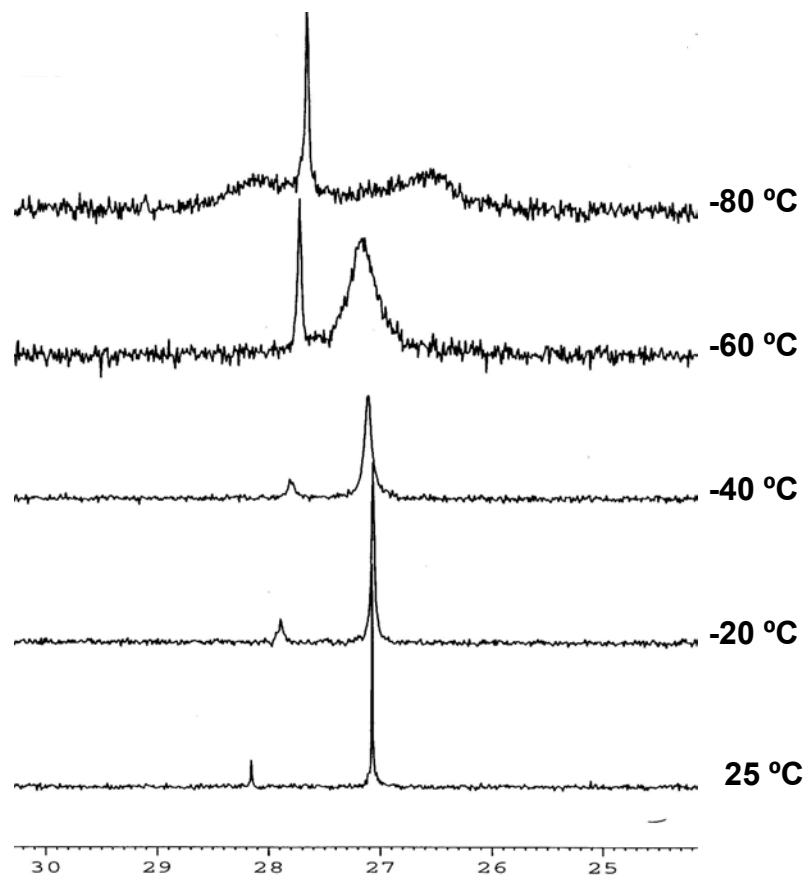


Figure 4.5. Variable temperature ^{31}P NMR spectra of **3a** with five equivalents of benzonitrile in CD_2Cl_2 .

The equilibrium constants determined by the titration experiments (K_{eq1} for the closed/open equilibrium and K_{eq2} for the *syn/anti* isomerization equilibrium) can be estimated by monitoring the resonances and integrations of the allylic, olefinic, and methyl peaks in the ^1H NMR and the phosphorus peaks in the ^{31}P NMR for the titration experiments. Since the resonances for **A** and **B** are averaged, a weighted distribution calculation is used to determine the relative amounts of **[A]** and **[B]** (see Experimental Section). The concentration of **C** is easily determined since its resonance is a distinct peak. From this information K_{eq1} and K_{eq2} were determined (eq. 4.1). Since K_{eq1} involves competitive binding between the η^2 -olefin and the nitrile, it is related to the binding

strength of the η^2 -olefin. If K_{eq1} is large, then η^2 -olefin coordination is weak and readily displaced by nitrile to form the open species **B**. However, if K_{eq1} is small, then the η^2 -olefin is bound more strongly to the metal and cannot be easily displaced by nitrile. K_{eq2} represents the thermodynamic ratio between the *syn* and *anti* isomers.

$$K_{eq1} = \frac{[B]}{[Nitrile][A]} \qquad K_{eq2} = \frac{[C]}{[B]} \qquad (4.1)$$

The titration experiments were repeated with two other nitriles, acetonitrile and benzonitrile, and the equilibrium constants for the opening of the wrap-around complex (K_{eq1}) as well as the *syn/anti* isomerization (K_{eq2}) were determined for all wrap-around complexes. With these two strongly coordinating nitriles, acetonitrile and benzonitrile, wrap-around complexes with electron-withdrawing groups (**1a-1c**, **2a**, **4a**) are completely opened after the addition of ≤ 2 equivalents of nitrile, whereas wrap-around complexes with electron-donating groups (**3a-3c**) exhibit a smaller K_{eq1} of 3 M^{-1} . The weakly coordinating 3,5-bis(trifluoromethyl)benzonitrile allows comparison of the equilibrium constants of all wrap-around complexes (Table 4.1). As explained previously (*vide supra*), a larger equilibrium constant (K_{eq1}) signifies a greater preference for the open complex **B**, with the η^2 -olefin being displaced by nitrile. Therefore, a large K_{eq1} is indicative of a more weakly bound η^2 -olefin. Likewise, a smaller K_{eq1} indicates a more strongly bound olefin to the metal center, and it is therefore more difficult to displace the olefin with the corresponding nitrile.

Scheme 4.7. Wrap-around equilibrium with 3,5-bis(trifluoromethyl)benzonitrile.

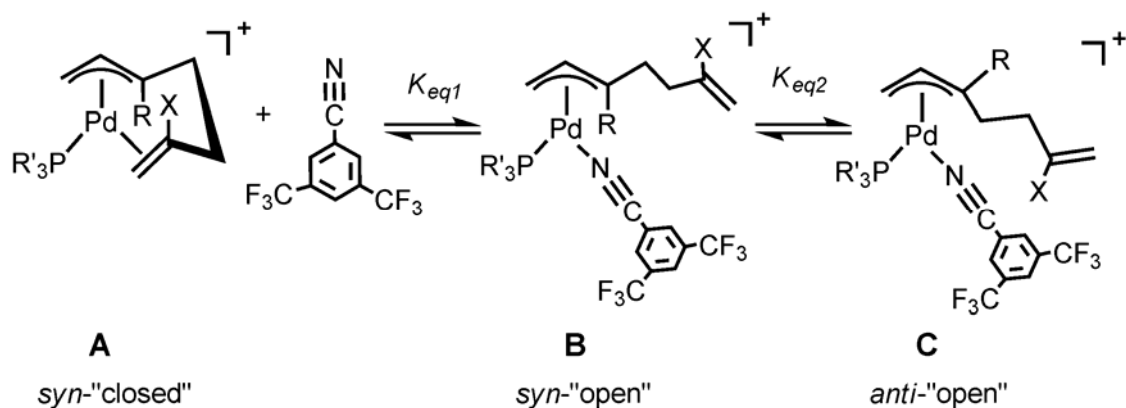


Table 4.1. Equilibrium constants for titration of wrap-around complexes with 3,5-bis(trifluoromethyl)benzonitrile.

Entry	Wrap-around complex	K_{eq1} (M^{-1}) ^a	K_{eq2} ^a
1	2a	230	< 0.05
2	4a	180	0.5
3	1a	120	0.4
4	1b	100	0.6
5	1c	150	0.5
6	3a	<3	N/A
7	3b	<3	N/A

^a Equilibrium constants were calculated at 25 °C.

The binding affinity of the olefin was studied as a function of substituent X, the phosphine ligand, and the counteranion. It was found that electron-withdrawing groups (X = CO₂Me, Cl, entries 1-5) weaken the binding affinity of the η^2 -wrap-around olefin, relative to the unsubstituted (X = H) systems (entries 6 and 7). Varying the phosphine ligand from PPh₃ to P(NC₄H₉)₃ also slightly influences the binding affinity of the olefin. Complex **1c** (entry 5) incorporates P(NC₄H₉)₃, which is a better π -acceptor than PPh₃, and shows a more weakly coordinated alkene arm relative to the analogous PPh₃ complex (entry 3). A small counterion effect was observed, with the more coordinating

counterion, SbF_6^- , having a slightly larger equilibrium constant than that of $\text{B}(\text{Ar}_\text{F})_4^-$ (compare entries 3 and 4).

Once the wrap-around is in the open form, **B**, σ - π isomerization yields the mixture of the *syn* and *anti* open chain products, **B** and **C**, respectively. The ratio of *syn* and *anti* isomers is nearly unaffected by the substituents on the olefin arm, the type of phosphine, or the counterion, and favors the less sterically hindered *syn* open isomer **B**. The *syn/anti* equilibrium (K_{eq2}) for all of the wrap-around complexes is essentially the same (*ca.* 0.5) with two exceptions. Wrap-around complex **2a** favors the *syn* species exclusively at room temperature and no isomerization is observed. This is attributed to the absence of a methyl group in the 3 position of the allyl unit and the large thermodynamic favorability of the *syn* open isomer **B** for **2a**. Additionally, the η^2 -olefin in wrap-around complexes **3a** and **3b** were never effectively displaced by excess $(\text{CF}_3)_2\text{-BN}$ as the olefin is very strongly bound to the metal, and because the open complex **B** was never formed for **3a** or **3b**, the *syn/anti* isomerization could not occur.

From these results, it is clear that substituents on the η^2 -olefin greatly impact its' binding affinity in the wrap-around complexes. Therefore, it is reasonable to believe that wrap-around complexes with electron-withdrawing groups on the η^2 -olefin, with their poor binding affinity to the metal center, would be readily displaced by 1,3-dienes and should be better catalysts for 1,3-diene polymerizations.

Polymerization of Isoprene and Butadiene by Wrap-Around Catalysts. The polymerization of 1,3-butadiene (BD) and isoprene (IP) was examined using wrap-around complexes **1a-1c**, **3a**, **3c**, and **4a** as catalysts in methylene chloride at room temperature and 50 °C for 20 hours (see Experimental Section for polymerization

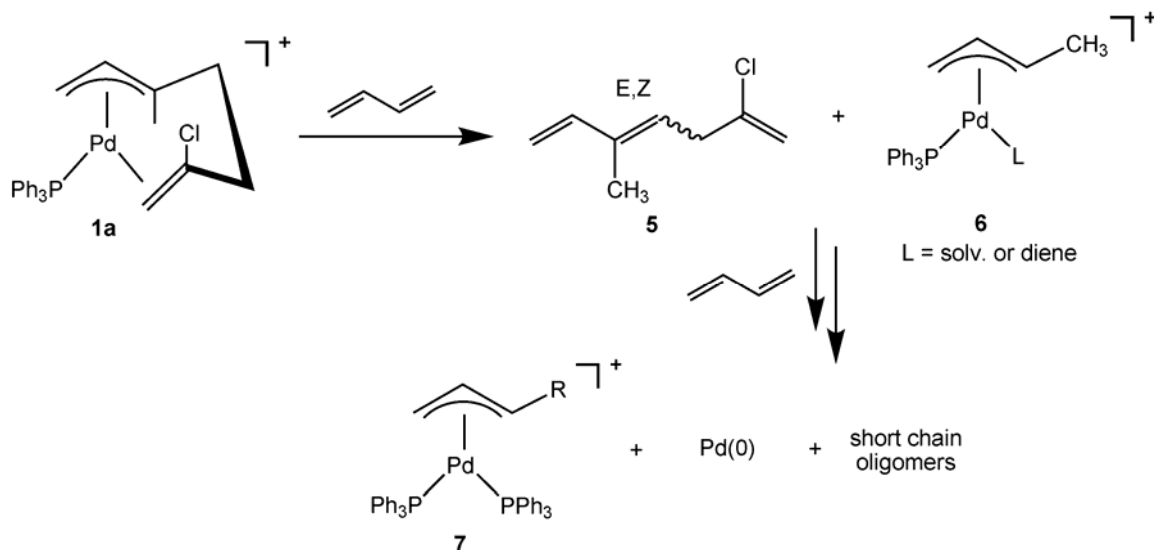
details). Unfortunately, these reactions proceeded with low conversions (2 – 12%) and little or no selectivity. ^{13}C NMR spectroscopy and GPC analyses showed formation of short chain oligomers with low molecular weights, indicating that the rate of chain transfer may be as fast or faster than the rate of propagation. Initial ^1H NMR spectroscopy investigations of the reactivity of wrap-around complexes with BD and IP showed decomposition of the catalyst via disproportionation to form a catalytically inactive bisphosphine species and palladium black after 20 hours. As such, a closer examination of the reactivity with 1,3-dienes and the mechanism of chain transfer was undertaken.

Chain Transfer with Wrap-Around Catalysts. Addition of BD to **1a** or **1b** in an *in situ* NMR experiment resulted in chain transfer and formation of the organic product **5** and subsequent insertion of one equivalent of BD to form a new crotyl π -allyl palladium(II) complex **6** at temperatures above $-55\text{ }^\circ\text{C}$ (Scheme 4.8). The crotyl complex **6** could not be isolated due to the labile nature of the solvent or diene in the fourth coordination site. However, trapping with triphenylphosphine yielded the bisphosphine complex **7**, which has been independently synthesized to confirm the ^1H and ^{31}P NMR spectral assignments of the *in situ* generated species. The organic product was isolated by vacuum removal of CD_2Cl_2 at $-30\text{ }^\circ\text{C}$, extraction of the nonpolar product from the residue by cyclohexane- d_{12} , and then independently characterized by NMR spectroscopy and mass spectrometry (see Experimental Section for details).

The chain transfer organic product, **5**, exists as a mixture of E and Z isomers in a 2:1 ratio, respectively. Two characteristic allylic peaks for each isomer resonate in the ^1H NMR spectrum at δ 6.65 and 5.48 for the E isomer, and at δ 6.33 and 5.39 for the Z

isomer. Additionally, each isomer has a distinct resonance for the methyl group, resonating at δ 1.72 and 1.83 for the E and Z isomers, respectively. These trienes are traditionally difficult to synthesize, and NMR spectra for these organic fragments are rarely reported.

Scheme 4.8. Chain transfer and trapping of the new Pd(II) complex.



The kinetics of this chain transfer process were studied by ^1H NMR spectroscopy. In a typical experiment, a screw-cap NMR tube was charged with a methylene chloride- d_2 solution of **1b** and 5-20 equivalents of BD at -45°C and monitored for 35 minutes. To determine the order in [BD], the observed rate constants for chain transfer were measured over several diene concentrations while holding the initial concentration of **1b** constant. The results of these experiments are summarized in Table 4.2. A clear first-order rate dependence on [BD] is observed for the chain transfer event. This is contrary to previous findings for π -allyl Ni(II) systems, where the rate of chain transfer is independent of the concentration of diene.¹⁶ These differences suggest that, while the π -allyl Ni(II) systems are highly active for BD and IP polymerization, the π -allyl Pd(II) systems suffer from a

fast rate of chain transfer relative to the rate of polymerization, resulting in mere oligomerization of BD and IP for the analogous Pd(II) systems.

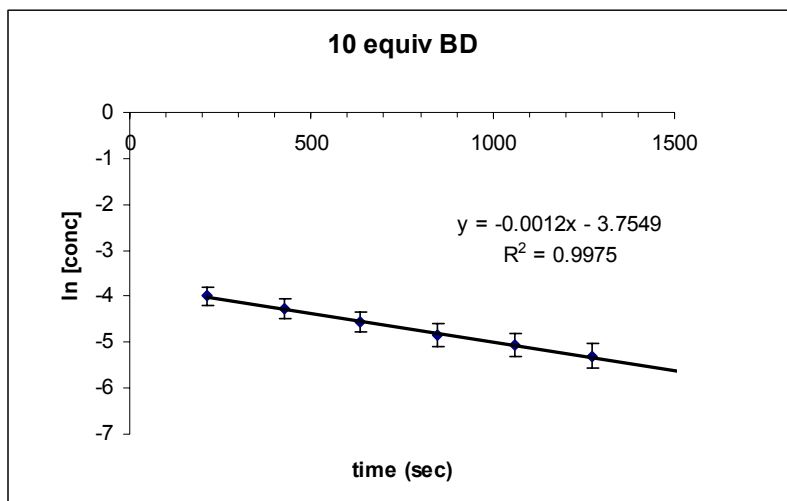


Figure 4.6. Kinetic plot of disappearance of the wrap-around complex **1b** over time upon addition of 10 equivalents of 1,3-butadiene.

Table 4.2. Influence of [BD] on the rate of chain transfer.

Equivalents	Temperature (°C)	Rate (s ⁻¹)
5	-45	0.8 x 10 ⁻³
10	-45	1.2 x 10 ⁻³
20	-45	2.9 x 10 ⁻³

Further *in situ* monitoring of the reaction of BD with Pd(II) wrap-around complexes via ¹H, ¹³P, and ¹³C NMR spectroscopy confirmed formation of short chain oligomers. Catalyst decomposition occurs upon disproportionation of the catalyst to form a π -allyl Pd(II) bisphosphine species (³¹P NMR) and palladium black (Scheme 4.8).

Summary

Syntheses and characterizations of several easily-tunable wrap-around complexes **1a-1-c**, **2a**, **3a-3c**, and **4a** have been described (see Scheme 4.5). Single crystal X-ray structural determinations of **1a** and **2a** reveal sixteen-electron π -allyl complexes with a chelating olefin arm. The η^2 -chelating olefin arm can be displaced by nitriles of varying strengths via titration of a solution of wrap-around complex with various equivalents of nitriles. These titration experiments lend insight into the relative binding affinity of the chelating olefin arm. Electron-withdrawing substituents on the olefin (X = -COOMe, -Cl) allowed for facile displacement of the η^2 -olefin by nitrile, whereas an unsubstituted vinyl group was much more strongly bound to the palladium center and could not be effectively displaced by nitrile. Counterion and phosphine substituent effects were relatively minor and had very little influence on the binding affinity of the olefin arm. Attempted catalytic polymerization of isoprene and 1,3-butadiene by wrap-around complexes yielded short chain oligomers with poor conversions and catalyst decomposition. The chain transfer mechanism of this process was examined, and it was found that the rate of chain transfer is first-order in [BD], contrary to the zero-order butadiene dependence of the chain transfer process found for polymerization of butadiene by ligand-free $(\pi\text{-allyl})\text{Ni(II)}$ complexes. The rate of chain transfer for these Pd(II) systems is much faster than the rate of propagation, which adequately explains the observed short chain oligomers seen in the polymerizations of BD and IP.

Experimental Section

General Considerations.

All reactions, unless otherwise stated, were conducted under an atmosphere of dry, oxygen free argon using standard high-vacuum, Schlenk, or drybox techniques. Argon was purified by passage through columns of BASF R3-11 catalyst (Chemalog) and 4Å molecular sieves. Palladium catalysts were stored in an MBraun glovebox at -35 °C to prevent thermal decomposition. ^1H , ^{31}P , and ^{13}C NMR spectra were recorded on a Bruker DRX 500 MHz or a Bruker DRX 400 MHz spectrometer. Chemical shifts were referenced relative to residual CHCl_3 (δ 7.24 for ^1H) and CH(D)Cl_2 (δ 5.32 for ^1H), CD_2Cl_2 (δ 53.8 for ^{13}C), CDCl_3 (δ 77.0 for ^{13}C). Assignments were supported by ^1H - ^{13}C HMQC, ^1H - ^1H COSY, and NOESY experiments. Elemental analyses were carried out by Atlantic Microlab, Inc., of Norcross, GA. GPC analyses were performed in HPLC grade tetrahydrofuran at 25 °C using a Waters Alliance HPLC equipped with Waters Styragel HR2, HR4, and HR5 columns and a Waters 410 refractive index detector. Molecular weights are reported relative to polystyrene standards. The crystallographic information for **1a** and **2a** is reported in Appendix IV. The data was obtained on a Bruker SMART APEX-2 X-ray diffractometer at -173 °C using Mo-K α radiation.

Materials.

All solvents were deoxygenated and dried by passage over columns of activated alumina.^{17,18} Isoprene and 1,3-butadiene were purchased from Aldrich and purified by vacuum transfer through 4Å molecular sieves and stored over 4 Å molecular sieves at -35 °C under argon. Methylene chloride- d_2 and chloroform- d were purchased from Cambridge Isotope Laboratories and stored over 4Å molecular sieves. $\text{NaB}(\text{Ar}_\text{F})_4$ was

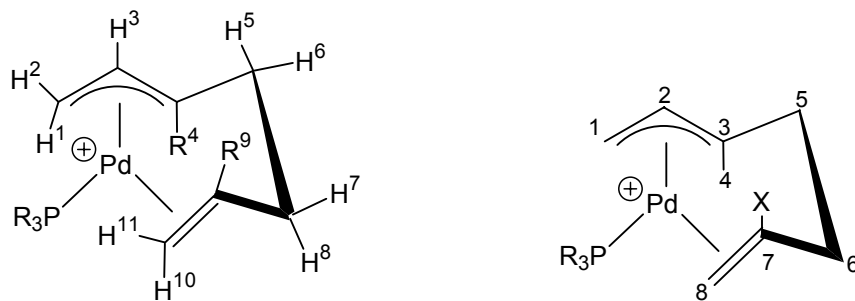
purchased from Boulder Scientific. Allyl chloride, allyl bromide, AgSbF₆, PdCl₂, LiCl, and tripyrrolidinylphosphine were purchased from Aldrich and used as received. Tripyrrolylphosphine was prepared according to literature methods.¹⁹ The π -allyl palladium halide dimers were synthesized according to literature procedures.¹¹

(Allyl)Pd(II) Complex Synthesis.

Synthesis of [(IP-2-Cl- π -allyl)PdCl]₂. Under an argon atmosphere, [(2-Cl- π -allyl)PdCl]₂ (0.600 g, 1.38 mmol) and excess isoprene (6.3mL, 69.0 mmol) were dissolved in dry methylene chloride (40 mL). The solution was allowed to stir for ca. 30 min at room temperature until one equivalent of diene had inserted into the palladium-allyl bond as determined by ¹H NMR analysis. The solvent was removed *in vacuo* to yield the dimer as a yellow oil. The product was washed with dry pentane (3 x 20 mL) to yield the product as an isolable powder. Yield: 0.702 g (89%).

General Procedure for the Synthesis of Complexes 1a – 1c. Under an argon atmosphere, [(IP-2-Cl- π -allyl)PdCl]₂ and two equivalents triphenylphosphine were dissolved in dry methylene chloride (20 mL) and the resulting yellow solution was stirred at room temperature for five minutes. A solution of two equivalents silver hexafluoroantimonate in 5 mL methylene chloride was then added via cannula at -78 °C and the mixture was stirred for an additional hour at this temperature before the solution was allowed to slowly warm to room temperature. The resulting solution was filtered through celite and the solvent evaporated *in vacuo*. The product was washed with 3x10 mL of dry pentane and dried under vacuum to yield a yellow powder.

General Numbering Scheme:



[Pd(IP-2Cl)PPh₃][SbF₆] (1a). The general procedure was employed using [(IP-2-Cl- π -allyl)PdCl]₂ (0.200 g, 0.460 mmol), triphenylphosphine (0.190 g, 0.74 mmol), and silver hexafluoroantimonate (0.250 g, 0.74 mmol). Yield: 0.365 g (64%). ¹H{³¹P} NMR (400 MHz, CD₂Cl₂, 25 °C): δ 7.40-7.70 (m, 15H, PPh₃), 6.24 (dd, ³J_{HHsyn} = 13 Hz, ³J_{HHanti} = 7.6 Hz, 1H, H₃), 4.93 (s, 1H, H₁₀), 4.41 (s, 1H, H₁₁), 4.04 (dd, ³J_{HH} = 16 Hz, ³J_{HH} = 12 Hz, ³J_{HH} = 4.0 Hz, 1H, H₈), 3.66-3.76 (m, 2H, H₆+H₂), 3.32-3.42 (m, 2H, H₁+H₇), 2.76 (m, 1H, H₅), 1.87 (s, 3H, R₄ = CH₃). ³¹P{¹H} NMR (160 MHz, CD₂Cl₂, 25 °C): δ 28.7. ¹³C{¹H} NMR (100 MHz, CD₂Cl₂, 25 °C): δ 20.8 (d, ³J_{CP} = 3.7 Hz, C₄), 45.2 (s, C₅), 49.3 (d, J = 5.0 Hz, C₆), 61.3 (s, C₁), 90.2 (s, C₈), 116.0 (d, J = 3.7 Hz, C₂), 130.3 (d, C₉), 129.9 (d, ³J_{CP} = 10.8 Hz, PPh₃), 132.1 (d, ⁴J_{CP} = 2.1 Hz, PPh₃), 133.8 (d, ²J_{CP} = 13.1 Hz, PPh₃), 139.3 (d, ²J_{CP} = 19.2 Hz, C₃), 145.2 (s, C₇). Anal. Calcd for C₂₆H₂₇PClPdSbF₆ (748.12): C, 41.74; H, 3.65. Found: C, 42.15; H, 3.67.

[Pd(IP-2Cl)PPh₃][B(Ar_F)₄] (1b). The general procedure was employed using [(IP-2-Cl- π -allyl)PdCl]₂ (0.200 g, 0.460 mmol), triphenylphosphine (0.190 g, 0.74 mmol), and NaB(Ar_F)₄ (0.620 g, 0.74 mmol). Yield: 0.698 g (72%). ¹H NMR (400 MHz, CD₂Cl₂, 25 °C): δ 7.4-7.6 (m, 15H, PPh₃), 6.18 (dd, ³J_{HHsyn} = 13.2 Hz, ³J_{HHanti} = 7.4 Hz, 1H, H₃), 1.79 (d, ⁴J_{HP} = 5.2 Hz, 3H, R₄ = CH₃), 4.73 (s, 1H, H₁₀), 4.46 (d, ³J_{HH} = 5.6 Hz, 1H, H₁₁), 3.86 (td, ³J_{HH} = 4.0 Hz, ³J_{HH} = 13.8 Hz, 1H, H₈), 3.70 (dd, 1H, H₂), 3.68 (m, 1H, H₇),

3.35 (dd, $^2J_{\text{HH}} = 2.4$ Hz, $^3J_{\text{HH}} = 13.2$ Hz, 1H, H₁), 3.34 (m, 1H, H₆), 2.73 (m, 1H, H₅), $^{31}\text{P}\{^1\text{H}\}$ NMR (160 MHz, CD₂Cl₂, 25 °C): δ 26.9. $^{13}\text{C}\{^1\text{H}\}$ NMR (126 MHz, CD₂Cl₂, 25 °C): δ 162.0 (q, $^1J_{\text{CB}} = 49.8$ Hz, B(Ar_F)₄ C_{ipso}), 145.2 (s, C₇), 138.2 (d, C₃), 135.2 (s, B(Ar_F)₄ C_o), 133.8 (d, $^2J_{\text{CP}} = 13.0$ Hz, Ph₃), 132.3 (d, $^4J_{\text{CP}} = 2.4$ Hz, Ph₃), 130.1 (d, C₉), 129.9 (d, $^3J_{\text{CP}} = 10.8$ Hz, Ph₃), 129.2 (q, $^2J_{\text{CF}} = 31.5$ Hz, B(Ar_F)₄ C_m), 128.3, 126.1, 123.9, 121.8 (q, $^1J_{\text{CF}} = 272.9$ Hz, B(Ar_F)₄ CF₃), 117.9 (B(Ar_F)₄ C_p), 116.1 (s, C₂), 90.3 (s, C₈), 61.2 (s, C₁), 49.2 (s, C₆), 45.0 (s, C₅), 20.8 (s, C₄). Anal. Calcd for C₅₈H₃₉PClPd(BAr_F)₄ (1375.62): C, 50.64; H, 2.86. Found: C, 50.61; H, 2.89.

[Pd(IP-2Cl)P(NC₄H₄)₃][SbF₆] (1c). The general procedure was employed using [(IP-2-Cl- π -allyl)PdCl]₂ (0.150 g, 0.26 mmol), tripyrrolylphosphine (0.120 g, 0.53 mmol), and silver hexafluoroantimonate (0.180 g, 0.53 mmol). Yield: 0.295 g (78%). ^1H NMR (400 MHz, CD₂Cl₂, 25 °C): δ 6.83 (s, 6H, P(NC₄H₄)₃), 6.54 (s, 4H, P(NC₄H₄)₃), 6.31 (m, 1H, H₃), 1.92 (d, $^4J_{\text{HP}} = 7.2$ Hz, 3H, R₄ = CH₃), 5.11 (s, 1H, H₁₀), 4.43 (d, $^3J_{\text{HH}} = 6.8$ Hz, 1H, H₁₁), 3.96 (td, $^3J_{\text{HH}} = 12.8$ Hz, $^3J_{\text{HH}} = 3.2$ Hz, 1H, H₈), 4.23 (dd, $^3J_{\text{HH}} = 7.6$ Hz, $^2J_{\text{HH}} = 2.4$ Hz, 1H, H₂), 3.68 (m, 1H, H₇), 3.67 (d, $^3J_{\text{HH}} = 12.8$ Hz, 1H, H₁), 3.28 (m, 1H, H₆), 2.78 (m, 1H, H₅), 1.96 (s, $^3J_{\text{HP}} = 7.2$ Hz, 3H, R₄ = CH₃). $^{31}\text{P}\{^1\text{H}\}$ NMR (160 MHz, CD₂Cl₂, 25 °C): δ 95.2. Anal. Calcd for C₂₀H₂₄PClN₃PdSbF₆ (714.79): C, 33.59; H, 3.39. Found: C, 33.66; H, 3.36.

[Pd(BD-2Cl)PPh₃][SbF₆] (2a). The general procedure was employed using [(2-Cl- π -allyl)PdCl]₂ (2.63 mmol) and excess butadiene (6.22 g, 0.115 mol) to form the isolable butadiene inserted palladium chloride dimer. For the second step, [Pd(BD-2Cl)Cl]₂ (0.100 g, 0.18 mmol), triphenylphosphine (0.097 g, 0.37 mmol) and AgSbF₆ (0.127 g, 0.37 mmol) were used. Yield: 0.214 g (79%). $^1\text{H}\{^{31}\text{P}\}$ NMR (400 MHz, CD₂Cl₂, 25 °C):

δ 7.4-7.6 (m, 15H, PPh₃), 6.34 (dt, $^3J_{\text{HHsyn}} = 12$ Hz, $^3J_{\text{HHanti}} = 6$ Hz, 1H, H₃), 6.04 (dt, $^3J_{\text{HH}} = 12$ Hz, $^3J_{\text{HH}} = 4.0$ Hz, 1H, R₄ = H), 5.11 (s, 1H, H₁₀), 4.48 (s, 1H, H₁₁), 4.00 (td, $^3J_{\text{HH}} = 13.6$ Hz, $^3J_{\text{HH}} = 4.4$ Hz, 1H, H₈), 3.73 (dd, $^3J_{\text{HH}} = 7.0$ Hz, $^2J_{\text{HH}} = 2.0$ Hz, 1H, H₂), 3.51 (m, 1H, H₇), 3.45 (d, $^3J_{\text{HH}} = 12.8$ Hz, 1H, H₁), 3.26 (m, 1H, H₆), 2.86 (m, 1H, H₅). $^{31}\text{P}\{^1\text{H}\}$ NMR (160 MHz, CD₂Cl₂, 25 °C): δ 26.4. Anal. Calcd for C₂₅H₂₄PClPdSbF₆ (733.08): C, 40.96; H, 3.31. Found: C, 41.01; H, 3.53.

General Procedure for the Synthesis of Complexes 3a – 3c and 4a. Under an argon atmosphere, $[(\pi\text{-allyl})\text{PdBr}]_2$ (0.200 g, 0.40 mmol) was dissolved in dry methylene chloride (20 mL) and then an excess of isoprene (2.3 mL, 23.0 mmol) was added. The solution was allowed to stir for 1-2 days until one equivalent of diene had inserted into the palladium-allyl bond as monitored by ^1H NMR spectroscopy. The solvent was removed *in vacuo* to yield the dimer as a yellow oil which was not isolated but was carried on directly to the next step. The dimer and triphenylphosphine (0.209 g, 0.80 mmol) were dissolved in dry methylene chloride (20 mL) and the resulting yellow solution was stirred at room temperature for five minutes. Next, two equivalents silver hexafluoroantimonate or NaB(Ar_F)₄ were added at -78°C and the mixture was stirred for an additional hour before the solution was allowed to slowly warm to room temperature. The resulting solution was filtered through Celite and the solvent evaporated *in vacuo*. The product was washed with 3x10 mL of dry pentane and dried under vacuum to yield a yellow powder.

[Pd(IP-2H)PPh₃][SbF₆] (3a). The general procedure was employed using AgSbF₆ (0.274 g, 0.80 mmol). Yield: 0.623 g (78%). ^1H NMR (400 MHz, CD₂Cl₂, 25 °C): δ 7.30-7.70 (m, 15H, PPh₃), 6.24 (dd, $^3J_{\text{HHsyn}} = 12.8$ Hz, $^3J_{\text{HHanti}} = 7.4$ Hz, 1H, H₃), 6.48 (m,

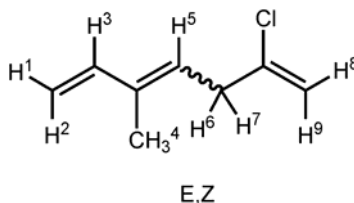
1H, R₉ = H), 4.52 (d, ³J_{HH} = 16.8, 1H, H₁₀), 4.34 (dd, ³J_{HH} = 7.6 Hz, ³J_{HH} = 7.7 Hz, 1H, H₁₁), 3.59 (d, ³J_{HH} = 7.4, 1H, H₂), 3.30 (d, ³J_{HH} = 12.8 Hz, 1H, H₁), 3.26-3.39 (m, 2H, H₇+H₆), 3.15 (m, 1H, H₈), 2.71 (pt, 1H, H₅), 1.73 (d, ³J_{HP} = 4.4 Hz, 3H, R₄ = CH₃). ³¹P{¹H} NMR (160 MHz, CD₂Cl₂, 25 °C): δ 26.6. ¹³C{¹H} NMR (126 MHz, CD₂Cl₂, 25 °C): δ 20.6 (s, C₄), 42.1 (d, *J* = 4.8 Hz, C₆), 46.2 (s, C₅), 61.1 (s, C₁), 92.3 (s, C₈), 116.4 (d, ²J_{CP} = 3.7 Hz, C₂), 129.8 (d, ³J_{CP} = 10.6 Hz, PPh₃), 130.6 (d, ¹J_{CP} = 43.8 Hz, PPh₃), 114.0 (d, ⁴J_{CP} = 2.4 Hz, PPh₃), 132.3 (s, C₇), 133.7 (d, ²J_{CP} = 13.0 Hz, PPh₃), 140.1 (d, ²J_{CP} = 19.9 Hz, C₃). Anal. Calcd for C₂₆H₂₈PPdSbF₆ (712.65): C, 43.75; H, 3.96. Found: C, 43.56; H, 4.00.

[Pd(IP-2H)PPh₃][B(Ar_F)₄] (3b). The general procedure was employed using NaB(Ar_F)₄ (0.706 g, 0.80 mmol). Yield: 0.936 g (64%). ¹H NMR (400 MHz, CD₂Cl₂, 25 °C): δ 7.30-7.70 (m, 15H, PPh₃), 7.63 & 7.52 (s & s, 12H, B(Ar_F)₄), 6.11 (dd, ³J_{HHsyn} = 14.8 Hz, ³J_{HHanti} = 7.4 Hz, 1H, H₃), 6.36 (m, 1H, R₉ = H), 4.49 (d, ³J_{HH} = 16.4 Hz, 1H, H₁₀), 4.35 (dd, ³J_{HH} = 7.6 Hz, 1H, H₁₁), 3.59 (dd, ²J_{HH} = 2.4 Hz, ³J_{HH} = 7.4 Hz, 1H, H₂), 3.3 (m, 3H, H₈+H₇+H₆), 3.11 (d, ³J_{HH} = 14.8 Hz, 1H, H₁), 2.64 (pt, 1H, H₅), 1.69 (d, ³J_{HP} = 4.4 Hz, 3H, R₄ = CH₃). ³¹P{¹H} NMR (160 MHz, CD₂Cl₂, 25 °C): δ 26.9. Anal. Calcd for C₅₈H₄₀PPdB(Ar_F)₄ (1339.75): C, 51.94; H, 3.01. Found: C, 51.35; H, 2.89.

[Pd(IP-2H)P(NC₄H₄)₃][SbF₆] (3c). The general procedure was employed using AgSbF₆ (0.274 g, 0.797 mmol). Yield: 0.360 g (66%). ¹H NMR (300 MHz, CD₂Cl₂, 25 °C): δ 6.83 (s, 6H, P(NC₄H₄)₃), 6.54 (s, 4H, P(NC₄H₄)₃), 6.71 (m, 1H, R⁹ = H), 6.48 (m, 1H, R₉ = H), 6.40 (dd, ³J_{HHsyn} = 16.8 Hz, ³J_{HHanti} = 7.5 Hz, 1H, H₃), 4.71 (d, ³J_{HH} = 16.8, 1H, H₁₀), 4.44 (dd, ³J_{HH} = 8.1 Hz, ³J_{HH} = 8.1 Hz, 1H, H₁₁), 4.12 (d, ³J_{HH} = 7.5, 1H, H₂), 3.53-

3.40 (m, peak overlap, 3H, H₁ + H₇ + H₈), 3.20 (m, 1H, H₆), 2.74 (pt, 1H, H₅), 1.82 (d, ³J_{HP} = 7.2 Hz, 3H, R₄ = CH₃). ³¹P{¹H} NMR (160 MHz, CD₂Cl₂, 25 °C): δ 95.7.

[Pd(IP-2COOMe)(PPh₃)] [SbF₆] (4a). The general procedure was employed using [(2-COOMe-π-allyl)PdCl]₂ (0.200 g, 0.83 mmol), triphenylphosphine (0.436 g, 1.66 mmol) and AgSbF₆ (0.571 g, 1.66 mmol). Yield: 0.795 g (62%). ¹H{³¹P} NMR (400 MHz, CD₂Cl₂, -40 °C): δ 7.30-7.70 (m, 15H, PPh₃), 6.28 (dd, ³J_{HHsyn} = 13 Hz, ³J_{HHanti} = 7.6 Hz, 1H, H₃), 5.11 (s, 1H, H₁₀), 4.85 (s, 1H, H₁₁), 3.84 (d, ³J_{HH} = 7.4 Hz, 1H, H₂), 3.66 (m, 1H, H₈), 3.57 (s, 3H, R₉ = COOCH₃), 3.40-3.55 (m, 2H, H₇+H₆), 3.12 (d, ³J_{HH} = 12.8 Hz, 1H, H₁), 2.61 (pt, ³J_{HH} = 11 Hz, 1H, H₅), 1.78 (s, 3H, R₄ = CH₃). ³¹P{¹H} NMR (160 MHz, CD₂Cl₂, 25 °C): δ 27.9. Anal. Calcd for C₂₈H₃₀O₂PPdSbF₆ · 2 CH₂Cl₂ (941.58): C, 38.26; H, 3.65. Found: C, 38.20; H, 3.68.



Characterization of the Organic Chain Transfer Product 5. Addition of 1,3-butadiene to **1a** or **1b** resulted in chain transfer and formation of the organic product and a new palladium(II) allyl complex (Scheme 4.8). The organic product was isolated by vacuum removal of the solvent at -30 °C, dissolved in cyclohexane-*d*₁₂, and characterized by NMR and ESI+ mass spectrometry. The ratio of E to Z isomers was 2:1. Characterization of E isomer: ¹H NMR (500 MHz, C₆D₁₂, 25 °C): δ 6.65 (dd, ³J_{H3-H1} = 10.5 Hz, ³J_{H3-H2} = 17.5 Hz, 1H, H³), 5.48 (dd, ³J_{HH} = 7.5 Hz, ³J_{HH} = 7.5 Hz, 1H, H⁵), 5.10 (d, ³J_{HH} = 17.5 Hz, 1H, H²), 5.08 (s, 1H, H⁸), 5.03 (s, 1H, H⁹), 4.94 (d, ³J_{HH} = 10.5 Hz, 1H, H¹), 3.11 (dd, ³J_{HH} = 9.5 Hz, ³J_{HH} = 9.5 Hz, 1H, H⁶ + H⁷), 1.72 (s, 3H, CH₃⁴).

Characterization of Z isomer: ^1H NMR (500 MHz, C_6D_{12} , 25 $^\circ\text{C}$): δ 6.33 (dd, $^3J_{\text{H}_3-\text{H}^1} = 10.5$ Hz, $^3J_{\text{H}_3-\text{H}^2} = 17.5$ Hz, 1H, H_3), 5.39 (dd, $^3J_{\text{HH}} = 7.5$ Hz, $^3J_{\text{HH}} = 7.5$ Hz, 1H, H^5), 5.21 (d, $^3J_{\text{HH}} = 17.5$ Hz, 1H, H^2), 5.08 (s, 1H, H^8), 5.03 (s, 1H, H^9), 5.00 (d, $^3J_{\text{HH}} = 10.5$ Hz, 1H, H^1), 3.11 (dd, $^3J_{\text{HH}} = 9.5$ Hz, $^3J_{\text{HH}} = 9.5$ Hz, 1H, $\text{H}^6 + \text{H}^7$), 1.83 (s, 3H, CH_3 ⁴). ESI-MS (methanol:cyclohexane (50:1), + ion scan, m/z): 142.1 Da (Expected: 142.055 Da).

***In situ* generated crotyl phosphine complex 6.** A screw-cap NMR tube was charged with **1b** (0.028 g, 0.021 mmol) dissolved in 500 μL CD_2Cl_2 . Two equivalents of 1,3-butadiene were then added at low temperature. The chain transfer reaction was monitored via ^1H NMR for 50 minutes, at which point all of the original starting wrap-around complex **1b** had undergone chain transfer and insertion of one equivalent of 1,3-butadiene formed the crotyl (π -allyl)Pd(triphenylphosphine)(solvent or diene) complex **6**. ^1H NMR (400 MHz, CD_2Cl_2 , -45 $^\circ\text{C}$): δ 7.50-7.30 (m, 15H, PPh_3), 5.72 (m, H_c , 1H), 4.42 (m, H^1 , 1H), 3.97 (d, $^3J_{\text{HH}} = 4.8$ Hz, H_{syn} , 1H), 2.83 (d, $^3J_{\text{HH}} = 12.4$ Hz, H_{anti} , 1H), 1.98 (bs, CH_3 , 3H). $^{31}\text{P}\{^1\text{H}\}$ NMR (160 MHz, CD_2Cl_2 , -45 $^\circ\text{C}$): δ 27.7 (bs, PPh_3).

***In situ* generated crotyl bisphosphine complex 7.** A screw-cap NMR tube was charged with **1b** (0.028 g, 0.021 mmol) dissolved in 500 μL CD_2Cl_2 . Two equivalents of 1,3-butadiene were added at low temperature, and the chain transfer reaction was monitored at -20 $^\circ\text{C}$ via ^1H NMR for 50 minutes, at which point all of the original starting wrap-around complex **1b** had undergone chain transfer and formed the crotyl (π -allyl)Pd(triphenylphosphine)(solvent or diene) complex **6**. Then, one equivalent of triphenylphosphine (5.5 mg, 0.021 mmol) was added via syringe to the solution to form the crotyl (π -allyl)Pd(PPh_3)₂ complex **7**. Only the major isomer was observed. ^1H NMR (400 MHz, CD_2Cl_2 , 25 $^\circ\text{C}$): δ 7.50-7.10 (m, 30H, PPh_3), 5.63 (m, H_c , 1H), 4.26 (m, H^1 ,

1H), 3.53 (dd, $^3J_{\text{HH}} = 6.4$ Hz, $J_{\text{HP}} = 6.4$ Hz, H_{syn} , 1H), 3.21 (dd, $^3J_{\text{HH}} = 10.4$ Hz, $J_{\text{HP}} = 10.4$ Hz, H_{anti} , 1H), 1.05 (m, CH_3 , 3H). $^{31}\text{P}\{^1\text{H}\}$ NMR (160 MHz, CD_2Cl_2 , 25 °C): δ 26.4 (d, $^2J_{\text{PP}} = 40.7$ Hz, PPh_3), 25.5 (d, $^2J_{\text{PP}} = 40.7$ Hz, PPh_3).

Synthesis of crotyl bisphosphine complex 7. In a Schenk tube under an argon atmosphere, $[(\pi\text{-allyl})\text{PdCl}]_2$ (0.100 g, 0.254 mmol) and four equivalents of triphenylphosphine (0.266 g, 1.02 mmol) were dissolved in dry methylene chloride (20 mL) and then cooled in a dry ice/isopropyl alcohol bath to -78 °C. A solution of two equivalents silver hexafluoroantimonate (0.150 g, 0.440 mmol) in 5 mL methylene chloride was then added dropwise at -78 °C and the mixture was stirred for ca. 30 min at low temperature before the solution was allowed to warm slowly to room temperature. The resulting solution was cannula filtered and the solvent evaporated in vacuo. The product was washed with 3 x 10 mL of pentane and dried under vacuum to yield the product as a yellow powder. Yield: 0.375 g (80%). The ratio of major (*syn*) to minor (*anti*) product was 12:1. Characterization of major (*syn* crotyl) isomer: ^1H NMR (400 MHz, CD_2Cl_2 , 25 °C): δ 7.50-7.10 (m, 30H, PPh_3), 5.63 (m, H_c , 1H), 4.26 (m, H^1 , 1H), 3.53 (dd, $^3J_{\text{HH}} = 6.4$ Hz, $J_{\text{HP}} = 6.4$ Hz, H_{syn} , 1H), 3.21 (dd, $^3J_{\text{HH}} = 10.4$ Hz, $J_{\text{HP}} = 10.4$ Hz, H_{anti} , 1H), 1.05 (m, CH_3 , 3H). Characterization of minor (*anti* crotyl) isomer: ^1H NMR (400 MHz, CD_2Cl_2 , 25 °C): δ 7.50-7.10 (m, 30H, PPh_3), 5.63 (m, H_c , 1H, overlap with major isomer), 4.79 (m, H^1 , 1H), 4.21 (dd, H_{syn} , 1H), 3.21 (dd, H_{anti} , 1H, overlap with major isomer), 1.05 (m, CH_3 , 3H, overlap with major isomer). $^{31}\text{P}\{^1\text{H}\}$ NMR (160 MHz, CD_2Cl_2 , 25 °C): δ 26.4 (d, $^2J_{\text{PP}} = 40.7$ Hz, PPh_3 , major isomer), 25.5 (d, $^2J_{\text{PP}} = 40.7$ Hz, PPh_3 , major isomer), 25.1 (d, $^2J_{\text{PP}} = 39.6$ Hz, PPh_3 , minor isomer), 24.2 (d, $^2J_{\text{PP}} = 39.6$ Hz, PPh_3 , minor isomer).

Polymerization Procedures

General Procedure for the Polymerization of Isoprene. Pd(II) wrap-around catalyst (1.50×10^{-5} mol) was dissolved in 2.25 mL of dry methylene chloride in a Kontes flask equipped with a stir bar in the dry box. 0.75 mL of isoprene ($[IP]/[cat] = 500$) was then added to the flask via syringe, the flask was sealed with a stopcock, removed from the dry box, and stirred for 20 hours at either room temperature or 50 °C. The reaction was terminated by addition of methanol and then removal of the solvent *in vacuo*. The polymer was dissolved in $CDCl_3$ for $^{13}C\{^1H\}$ NMR to analyze the microstructure and then dissolved in THF for GPC analysis.

General Procedure for the Polymerization of 1,3-Butadiene. Pd(II) wrap-around catalyst (1.50×10^{-5} mol) was dissolved 3.00 mL of a dry 2.3 M BD/ CH_2Cl_2 solution in a Kontes flask under argon atmosphere. The flask was stirred for 20 hours at 25 °C, after which the reaction was terminated by addition of methanol and removal of the solvent *in vacuo*. The polymer was dissolved in $CDCl_3$ for ^{13}C NMR to analyze the microstructure, and then dissolved in THF for GPC analysis.

General Procedure for Titration Experiments. A screw-cap NMR tube was charged with ca. 10.0 mg of the wrap-around complexes **1a – 1c**, **2a**, **3a – 3c**, and **4a** dissolved in 500 μ L of deuterated methylene chloride under inert atmosphere. NMR spectra were taken after 0, 1, 2, 3, 4, 5, 10, 15, 20, 25, 30, 35, and 40 equivalents of nitrile were added via a 10 μ L gas tight syringe at room temperature; a typical series of spectra are shown in the Results and Discussion section. Chemical shifts for H_3 , $R_4 = Me$, and the vinylic protons, H_{10} and H_{11} , were monitored and recorded. The first equilibrium (K_I , as described by text) was fast on the NMR time scale and thus the resonance monitored

(typically the allylic peak, H₃) was an average of that for A & B. Once the chemical shifts of the fully closed complex (**A**), the fully open complex (**B**), and the observed signal averaged peak (closed↔open) were recorded, equation 4.3 was employed to determine the fraction of the closed (**A**) and open (**B** + **C**) complexes. The concentration of closed and open was then determined by multiplying the respective fraction by the total palladium(II) concentration, calculated from the initial moles of palladium(II) wrap-around complex added over the total solution volume and taking into account the added nitrile. From the total open concentration, [**B** + **C**], the concentrations of **B** and **C** were calculated from their respective integrals. With all these known values, the equilibria constants K_{eq1} and K_{eq2} were determined.

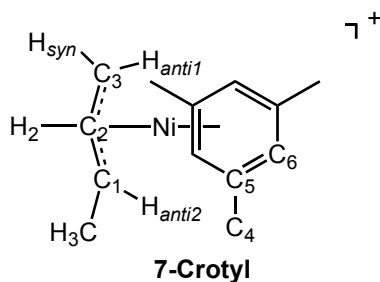
$$\begin{aligned}\delta_{\text{obs}} &= (1.00 - F_{\text{open}})A^{\text{closed}} + (F_{\text{open}})B^{\text{open}} \\ F_{\text{open}} &= [\delta_{\text{obs}} - A^{\text{closed}}]/[B^{\text{open}} - A^{\text{closed}}] \quad (4.3) \\ A^{\text{closed}} &= \delta \text{ for starting complex or } \delta \text{ when completely closed (olefin is } \eta^2 \text{ bound to} \\ &\quad \text{form the wrap-around)} \\ B^{\text{open}} &= \delta \text{ when the complex is completely "open"} \\ F_{\text{open}} &= \text{fraction of complex (out of 1.00 total) that is "open"}\end{aligned}$$

References and Notes

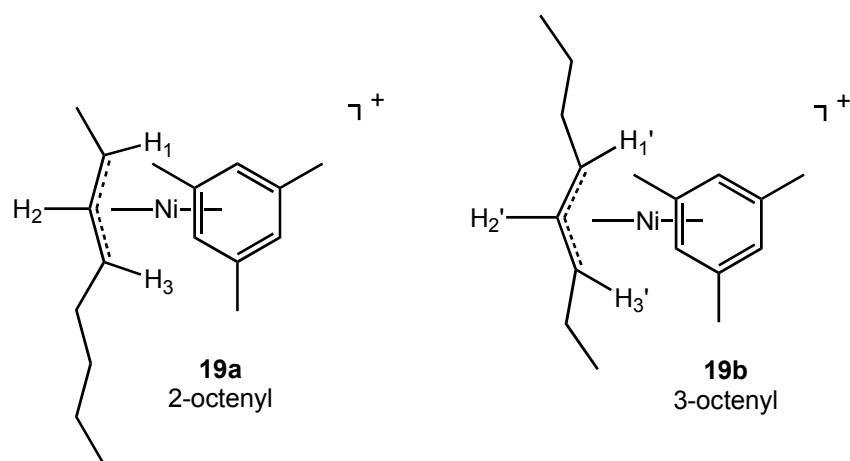
- (1) Takahashi, Y.; Sakai, S.; Ishii, Y. *J. Organometal. Chem.* **1969**, *16*, 177.
- (2) Medema, D.; van Helden, R.; Kohle, C. F. *Inorg. Chim. Acta.* **1969**, *3*, 255.
- (3) Medema, D.; van Helden, R. *Recl. Trav. Chim. Pays-Bas.* **1971**, *90*, 304.
- (4) Hughes, R. P.; Powell, J. *J. Am. Chem. Soc.* **1972**, 7723.
- (5) Hughes, R. P.; Jack, T.; Powell, J. *J. Organomet. Chem.* **1973**, *63*, 451-459.
- (6) See Chapter 3.
- (7) Jolly, P. W. *Angew. Chem. Int. Ed. Engl.* **1985**, *24*, 283.
- (8) Benn, R.; Jolly, P. W.; Mynott, R.; Raspel, B.; Schenker, G.; Schick, K.-P.; Schroth, G. *Organometallics* **1985**, *4*, 1945.
- (9) Akermark, B.; Vitagliano, A. *Organometallics* **1985**, *4*, 1275-1283.
- (10) Ciajolo, R.; Jama, M. A.; Tuzi, A.; Vitagliano, A. *J. Organomet. Chem.* **1985**, 233.
- (11) Aranyos, A.; Szabo, K. J.; Castano, A. M.; Backvall, J. E. *Organometallics* **1997**, 1058.
- (12) Crabtree, R. H. *The Organometallic Chemistry of the Transition Metals*; 3rd ed.; John Wiley and Sons: New York, 2001.
- (13) Dewar, M. J. S. *Bull. Soc. Chim. Fr.* **1951**, *18*, C71.
- (14) Chatt, J.; Duncanson, L. A. *J. Chem. Soc.* **1953**, 2939.
- (15) Gomez-Bengoa, E.; Cuerva, J. M.; Echavarren, A. M.; Martorell, G. *Angew. Chem. Int. Ed. Engl.* **1997**, 767.
- (16) Taube, R.; Wache, S.; Kehlen, H. *J. Mol. Cat. A.* **1995**, 21.
- (17) Alaimo, P. J.; Peters, D. W.; Arnold, J.; Bergman, R. G. *J. Chem. Educ.* **2001**, 64.
- (18) Pangborn, A. B.; Giardello, M. A.; Grubbs, R. H.; Rosen, R. K.; Timmers, F. J. *Organometallics* **1996**, 1518.

- (19) Atwood, J. L.; Cowley, A. H.; Hunter, W. E.; Mehrotra, S. K. *Inorg. Chem.* **1982**, *21*, 1354.

Appendix I



Synthesis of [(crotyl)Ni(Mes)][B(Ar_F)₄] (7-Crotyl). Under an atmosphere of argon, a Schlenk flask was charged with [(crotyl)NiBr]₂ (0.150 g, 0.39 mmol) and NaB(Ar_F)₄ (0.690 g, 0.78 mmol). Both components were dissolved in dry diethyl ether (10 mL) at -78 °C and an excess of mesitylene (350 μL, 2.52 mmol) was added. The reaction mixture was allowed to warm to 0 °C, stirred at this temperature for 1 h and filtered through Celite. The solvent was removed under dynamic vacuum and the red residue was washed with pentane (3 x 10 mL) to remove excess mesitylene. The red residue was redissolved in CH₂Cl₂ (10 mL), filtered via Celite to remove residual alkali metal salts and crystallized via slow diffusion of pentane into a saturated CH₂Cl₂ solution at -25 °C to yield dark red blocks (0.45 g, 0.40 mmol, 51 %). Only one isomer (*syn*) is visible by ¹H and ¹³C NMR spectroscopy. ¹H NMR (400 MHz, CD₂Cl₂, 25 °C): δ 6.55 (s, 3H, mes_{Ar}), 5.65 (ddd, ³J_{HH}= 6.4 Hz, ³J_{H-H}= 6.4 Hz, ³J_{H-H}= 12.0 Hz, 1H, H₂), 3.44 (d, ³J_{H-H}= 6.4 Hz, 2H, H_{syn}), 3.34 (dq, ³J_{HH}= 6.4 Hz, ³J_{H-H}= 12.0 Hz, 1H, H_{anti2}), 2.33 (s, 9H, mesCH₃), 2.20 (d, ³J_{H-H}= 12.0 Hz, H_{anti1}), 1.10 (d, ³J_{H-H}= 6.4 Hz, 3H, crotyl-CH₃). ¹³C{¹H} NMR (126 MHz, CD₂Cl₂, 25 °C): δ 124.1 (C₅), 109.4 (C₆), 107.0 (crotyl, C₂), 80.6 (crotyl, C₁), 56.1 (crotyl, C₃), 20.2 (C₆), 19.5 (crotyl, CH₃). Anal. Calcd for C₄₅H₃₁BF₂₄Ni•(CH₂Cl₂)_{0.5} C, 47.95; H, 2.83. Found: C, 47.97; H, 2.54.



In situ generation of (2/3-octenyl)Ni(mes)[B(Ar_F)₄] (19a/19b). A J-Young tube was charged with **7-H** (0.011 g, 0.010 mmol) and dissolved in CD₂Cl₂ (600 mL). The solution was mixed to ensure the catalyst was completely dissolved. 1-Octene (8.0 μ L, 0.051 mmol) was then added and the NMR tube was inverted to mix the sample. The reaction was monitored by ¹H NMR spectroscopy and complete conversion to complex **19** was obtained within an hour at 25 °C. There appears to be two isomers in approximately 50/50 mixture in solution. These are tentatively assigned as the 2- and 3-octenyl positional isomers of complex **19**. ¹H NMR (400 MHz, CD₂Cl₂, 25 °C): δ 6.43 (s, 3H, mes_{Ar}), 5.45 (t, 1H, overlapping H₂ and H_{2'}), 3.12 (m, 2H, overlapping H_{1&3} and H_{1'&3'}), 2.31 (s, 9H, mes_{CH₃}), the methylene groups appear in a range from 1.60-1.29 ppm and the methyl groups appear in a range from 1.10-0.88 ppm for both isomers.

Table I.1. X-Ray crystallographic data for complexes **7-H** and **8-Me**.

	7-H	8-Me
Formula	C ₄₄ H ₂₉ BF ₂₄ Ni	C ₄₈ H ₃₇ BF ₂₄ Ni
Formula Weight	1083.19	1139.30
Temperature (°C)	-173	-173
Wavelength (Å)	0.71073	1.54178
Crystal System	Orthorhombic	Monoclinic
Space Group	P2 ₁ 2 ₁ 2 ₁	P2(1)/c
Unit Cell Dimensions	a = 13.3171(3)Å α = 90° b = 14.5598(19)Å β = 90° c = 16.336(2)Å γ = 90°	a = 12.4231(10)Å α = 90° b = 19.4054(16)Å β = 104.801(4)° c = 20.6838(17)Å γ = 90°
Volume	4544.34(17)Å ³	4820.9(7)Å ³
Z	4	4
D _{calcd} , mg/m ⁻³	1.583	1.570
Abs coeff, mm ⁻¹	0.558	1.750
F(000)	2168	2296
Crystal size (mm ³)	0.25 x 0.20 x 0.10	0.30 x 0.30 x 0.05
Theta range (°)	1.62-27.00	3.17-69.60
Index range	-17≤h≤17, -19≤k≤19, -28≤l≤28	-14≤h≤, -22≤k≤23, -24≤l≤24
Reflections collected	78781	34611
Independent Reflections	9927[(R(int) 0.0314]	8776[R(int) 0.0239]
Absorption Correction	SADABS	Numerical
Refinement Method	Full-matrix least squared on F ²	Full-matrix least squared on F ²
Data/restraints/parameters	9927/0/742	8776/33/834
Goodness-of-fit on F ²	1.044	1.046
Final R indices [I>2σ(I)]	R1 = 0.0555, wR2 = 0.1176	R1 = 0.0377, wR2 = 0.0923
Largest diff peak and hole	1.983; -1.740e/Å ⁻³	0.548; -0.428e/Å ⁻³

Table I.1. Selected bond lengths (Å) for complex **7-H**.

Ni(1)-C(2)	1.962(4)	Ni(1)-C(7)	2.192(4)
Ni(1)-C(1)	1.994(4)	C(1)-C(2)	1.414(8)
Ni(1)-C(3)	2.061(6)	C(2)-C(3)	1.401(10)
Ni(1)-C(6)	2.121(4)	C(4)-C(9)	1.383(5)
Ni(1)-C(8)	2.130(4)	C(4)-C(5)	1.402(5)
Ni(1)-C(5)	2.142(4)	C(5)-C(6)	1.432(6)
Ni(1)-C(9)	2.157(3)	C(5)-C(10)	1.528(6)
Ni(1)-C(4)	2.176(4)	C(6)-C(7)	1.392(5)

C(7)-C(8)	1.402(5)	C(38)-F(35)	1.314(6)
C(7)-C(11)	1.504(5)	C(38)-F(36)	1.326(5)
C(8)-C(9)	1.419(5)	C(38)-F(34)	1.326(5)
C(9)-C(12)	1.512(5)	C(41)-C(42)	1.400(4)
B(20)-C(41)	1.641(5)	C(41)-C(46)	1.403(4)
B(20)-C(51)	1.642(4)	C(42)-C(43)	1.401(5)
B(20)-C(31)	1.646(5)	C(43)-C(44)	1.392(5)
B(20)-C(21)	1.653(5)	C(43)-C(47)	1.501(5)
C(21)-C(26)	1.394(4)	C(44)-C(45)	1.384(5)
C(21)-C(22)	1.399(5)	C(45)-C(46)	1.384(5)
C(22)-C(23)	1.402(5)	C(45)-C(48)	1.505(5)
C(23)-C(24)	1.379(5)	C(47)-F(41)	1.334(4)
C(23)-C(27)	1.504(6)	C(47)-F(43)	1.338(4)
C(24)-C(25)	1.393(5)	C(47)-F(42)	1.341(4)
C(25)-C(26)	1.390(5)	C(48)-F(45)	1.251(9)
C(25)-C(28)	1.501(5)	C(48)-F(146)	1.256(10)
C(27)-F(23)	1.274(12)	C(48)-F(145)	1.259(11)
C(27)-F(122)	1.28(2)	C(48)-F(44)	1.316(9)
C(27)-F(21)	1.297(18)	C(48)-F(46)	1.388(10)
C(27)-F(123)	1.319(13)	C(48)-F(144)	1.399(10)
C(27)-F(121)	1.32(2)	C(51)-C(52)	1.397(5)
C(27)-F(22)	1.355(18)	C(51)-C(56)	1.403(5)
C(28)-F(26)	1.317(5)	C(52)-C(53)	1.393(5)
C(28)-F(25)	1.329(5)	C(53)-C(54)	1.389(6)
C(28)-F(24)	1.334(4)	C(53)-C(57)	1.498(5)
C(31)-C(32)	1.395(5)	C(54)-C(55)	1.377(5)
C(31)-C(36)	1.401(5)	C(55)-C(56)	1.402(4)
C(32)-C(33)	1.395(5)	C(55)-C(58)	1.504(6)
C(33)-C(34)	1.378(5)	C(57)-F(151)	1.27(3)
C(33)-C(37)	1.493(5)	C(57)-F(52)	1.309(14)
C(34)-C(35)	1.379(5)	C(57)-F(152)	1.309(16)
C(35)-C(36)	1.387(5)	C(57)-F(53)	1.342(13)
C(35)-C(38)	1.497(6)	C(57)-F(153)	1.374(15)
C(37)-F(32)	1.335(5)	C(57)-F(51)	1.38(3)
C(37)-F(31)	1.340(5)	C(58)-F(156)	1.224(15)
C(37)-F(33)	1.351(4)	C(58)-F(155)	1.246(14)

C(58)-F(54)	1.284(8)	F(45)-F(146)	1.367(15)
C(58)-F(56)	1.316(10)	F(46)-F(146)	0.914(15)
C(58)-F(55)	1.326(11)	F(46)-F(145)	1.754(18)
C(58)-F(154)	1.331(15)	F(54)-F(154)	0.61(3)
F(21)-F(121)	0.54(4)	F(54)-F(156)	1.57(3)
F(22)-F(122)	0.75(3)	F(55)-F(155)	0.62(3)
F(22)-F(121)	1.76(3)	F(56)-F(156)	0.63(3)
F(23)-F(122)	1.67(3)	F(56)-F(155)	1.67(2)
F(45)-F(144)	0.825(13)		

Table I.2. Selected bond angles (°) for complex **7-H**.

		C(9)-Ni(1)-C(7)	69.37(14)
C(2)-Ni(1)-C(1)	41.9(2)	C(4)-Ni(1)-C(7)	80.99(14)
C(2)-Ni(1)-C(3)	40.7(3)	C(2)-C(1)-Ni(1)	67.8(3)
C(1)-Ni(1)-C(3)	70.7(3)	C(3)-C(2)-C(1)	113.0(6)
C(2)-Ni(1)-C(6)	123.3(2)	C(3)-C(2)-Ni(1)	73.5(3)
C(1)-Ni(1)-C(6)	160.72(19)	C(1)-C(2)-Ni(1)	70.3(3)
C(3)-Ni(1)-C(6)	105.3(2)	C(2)-C(3)-Ni(1)	65.9(3)
C(2)-Ni(1)-C(8)	134.5(3)	C(9)-C(4)-C(5)	120.9(3)
C(1)-Ni(1)-C(8)	112.1(3)	C(9)-C(4)-Ni(1)	70.7(2)
C(3)-Ni(1)-C(8)	168.8(2)	C(5)-C(4)-Ni(1)	69.7(2)
C(6)-Ni(1)-C(8)	68.26(15)	C(4)-C(5)-C(6)	118.9(4)
C(2)-Ni(1)-C(5)	137.9(2)	C(4)-C(5)-C(10)	121.7(4)
C(1)-Ni(1)-C(5)	158.3(2)	C(6)-C(5)-C(10)	119.4(4)
C(3)-Ni(1)-C(5)	99.5(3)	C(4)-C(5)-Ni(1)	72.4(2)
C(6)-Ni(1)-C(5)	39.24(16)	C(6)-C(5)-Ni(1)	69.6(2)
C(8)-Ni(1)-C(5)	81.34(15)	C(10)-C(5)-Ni(1)	131.8(4)
C(2)-Ni(1)-C(9)	152.2(2)	C(7)-C(6)-C(5)	121.5(4)
C(1)-Ni(1)-C(9)	110.7(2)	C(7)-C(6)-Ni(1)	73.9(2)
C(3)-Ni(1)-C(9)	151.8(3)	C(5)-C(6)-Ni(1)	71.2(2)
C(6)-Ni(1)-C(9)	81.96(15)	C(6)-C(7)-C(8)	117.2(3)
C(8)-Ni(1)-C(9)	38.66(15)	C(6)-C(7)-C(11)	120.9(4)
C(5)-Ni(1)-C(9)	68.62(14)	C(8)-C(7)-C(11)	121.9(4)
C(2)-Ni(1)-C(4)	155.6(2)	C(6)-C(7)-Ni(1)	68.5(2)
C(1)-Ni(1)-C(4)	129.65(18)	C(8)-C(7)-Ni(1)	68.7(2)
C(3)-Ni(1)-C(4)	119.2(3)	C(11)-C(7)-Ni(1)	132.7(3)
C(6)-Ni(1)-C(4)	69.19(15)	C(7)-C(8)-C(9)	122.6(4)
C(8)-Ni(1)-C(4)	68.03(15)	C(7)-C(8)-Ni(1)	73.5(2)
C(5)-Ni(1)-C(4)	37.89(15)	C(9)-C(8)-Ni(1)	71.7(2)
C(9)-Ni(1)-C(4)	37.21(14)	C(4)-C(9)-C(8)	118.6(3)
C(2)-Ni(1)-C(7)	122.1(2)	C(4)-C(9)-C(12)	121.4(3)
C(1)-Ni(1)-C(7)	131.8(2)	C(8)-C(9)-C(12)	120.0(3)
C(3)-Ni(1)-C(7)	132.0(2)	C(4)-C(9)-Ni(1)	72.1(2)
C(6)-Ni(1)-C(7)	37.60(14)	C(8)-C(9)-Ni(1)	69.6(2)
C(8)-Ni(1)-C(7)	37.83(15)	C(12)-C(9)-Ni(1)	131.5(2)
C(5)-Ni(1)-C(7)	69.28(15)	C(41)-B(20)-C(51)	109.6(3)

C(41)-B(20)-C(31)	109.4(3)	F(121)-C(27)-C(23)	114.9(11)
C(51)-B(20)-C(31)	107.7(2)	F(22)-C(27)-C(23)	110.8(7)
C(41)-B(20)-C(21)	111.7(2)	F(26)-C(28)-F(25)	106.9(4)
C(51)-B(20)-C(21)	107.5(3)	F(26)-C(28)-F(24)	106.8(3)
C(31)-B(20)-C(21)	110.8(3)	F(25)-C(28)-F(24)	104.8(3)
C(26)-C(21)-C(22)	115.4(3)	F(26)-C(28)-C(25)	113.1(3)
C(26)-C(21)-B(20)	123.2(3)	F(25)-C(28)-C(25)	112.4(3)
C(22)-C(21)-B(20)	121.1(3)	F(24)-C(28)-C(25)	112.2(3)
C(21)-C(22)-C(23)	122.1(3)	C(32)-C(31)-C(36)	115.7(3)
C(24)-C(23)-C(22)	121.0(3)	C(32)-C(31)-B(20)	122.3(3)
C(24)-C(23)-C(27)	120.6(3)	C(36)-C(31)-B(20)	121.9(3)
C(22)-C(23)-C(27)	118.4(4)	C(31)-C(32)-C(33)	122.0(3)
C(23)-C(24)-C(25)	117.9(3)	C(34)-C(33)-C(32)	121.1(3)
C(26)-C(25)-C(24)	120.5(3)	C(34)-C(33)-C(37)	118.5(3)
C(26)-C(25)-C(28)	121.3(3)	C(32)-C(33)-C(37)	120.5(3)
C(24)-C(25)-C(28)	118.2(3)	C(33)-C(34)-C(35)	118.0(3)
C(25)-C(26)-C(21)	123.0(3)	C(34)-C(35)-C(36)	121.1(3)
F(23)-C(27)-F(122)	81.4(13)	C(34)-C(35)-C(38)	120.0(3)
F(23)-C(27)-F(21)	106.7(14)	C(36)-C(35)-C(38)	118.9(3)
F(122)-C(27)-F(21)	129.0(13)	C(35)-C(36)-C(31)	122.2(3)
F(23)-C(27)-F(123)	19.7(15)	F(32)-C(37)-F(31)	106.5(3)
F(122)-C(27)-F(123)	98.1(12)	F(32)-C(37)-F(33)	105.0(3)
F(21)-C(27)-F(123)	88.1(12)	F(31)-C(37)-F(33)	105.8(3)
F(23)-C(27)-F(121)	121.6(12)	F(32)-C(37)-C(33)	113.3(4)
F(122)-C(27)-F(121)	109.8(15)	F(31)-C(37)-C(33)	114.0(3)
F(21)-C(27)-F(121)	23.6(16)	F(33)-C(37)-C(33)	111.5(3)
F(123)-C(27)-F(121)	105.8(12)	F(35)-C(38)-F(36)	105.4(5)
F(23)-C(27)-F(22)	111.3(13)	F(35)-C(38)-F(34)	107.6(4)
F(122)-C(27)-F(22)	32.9(12)	F(36)-C(38)-F(34)	104.9(4)
F(21)-C(27)-F(22)	105.3(12)	F(35)-C(38)-C(35)	112.7(4)
F(123)-C(27)-F(22)	124.1(10)	F(36)-C(38)-C(35)	112.1(4)
F(121)-C(27)-F(22)	82.4(13)	F(34)-C(38)-C(35)	113.4(4)
F(23)-C(27)-C(23)	111.9(8)	C(42)-C(41)-C(46)	115.7(3)
F(122)-C(27)-C(23)	112.4(9)	C(42)-C(41)-B(20)	123.0(3)
F(21)-C(27)-C(23)	110.5(11)	C(46)-C(41)-B(20)	121.3(3)
F(123)-C(27)-C(23)	114.4(8)	C(41)-C(42)-C(43)	122.1(3)

C(44)-C(43)-C(42)	120.7(3)	C(52)-C(51)-B(20)	122.6(3)
C(44)-C(43)-C(47)	120.7(3)	C(56)-C(51)-B(20)	121.5(3)
C(42)-C(43)-C(47)	118.6(3)	C(53)-C(52)-C(51)	122.3(3)
C(45)-C(44)-C(43)	117.6(3)	C(54)-C(53)-C(52)	120.8(3)
C(46)-C(45)-C(44)	121.5(3)	C(54)-C(53)-C(57)	120.4(3)
C(46)-C(45)-C(48)	119.2(3)	C(52)-C(53)-C(57)	118.8(4)
C(44)-C(45)-C(48)	119.3(3)	C(55)-C(54)-C(53)	118.4(3)
C(45)-C(46)-C(41)	122.2(3)	C(54)-C(55)-C(56)	120.6(3)
F(41)-C(47)-F(43)	106.7(3)	C(54)-C(55)-C(58)	120.6(3)
F(41)-C(47)-F(42)	106.0(3)	C(56)-C(55)-C(58)	118.8(3)
F(43)-C(47)-F(42)	106.1(3)	C(55)-C(56)-C(51)	122.2(3)
F(41)-C(47)-C(43)	112.4(3)	F(151)-C(57)-F(52)	112.5(13)
F(43)-C(47)-C(43)	112.9(3)	F(151)-C(57)-F(152)	110.9(17)
F(42)-C(47)-C(43)	112.3(3)	F(52)-C(57)-F(152)	89.7(11)
F(45)-C(48)-F(146)	66.1(8)	F(151)-C(57)-F(53)	101.5(17)
F(45)-C(48)-F(145)	123.6(8)	F(52)-C(57)-F(53)	105.7(11)
F(146)-C(48)-F(145)	108.9(10)	F(152)-C(57)-F(53)	16.2(16)
F(45)-C(48)-F(44)	113.8(8)	F(151)-C(57)-F(153)	106.6(13)
F(146)-C(48)-F(44)	123.5(7)	F(52)-C(57)-F(153)	13.2(13)
F(145)-C(48)-F(44)	20.1(10)	F(152)-C(57)-F(153)	103.0(12)
F(45)-C(48)-F(46)	105.8(8)	F(53)-C(57)-F(153)	118.9(12)
F(146)-C(48)-F(46)	40.1(7)	F(151)-C(57)-F(51)	8(2)
F(145)-C(48)-F(46)	82.8(9)	F(52)-C(57)-F(51)	104.8(11)
F(44)-C(48)-F(46)	102.6(6)	F(152)-C(57)-F(51)	110.6(14)
F(45)-C(48)-F(144)	35.7(6)	F(53)-C(57)-F(51)	103.3(14)
F(146)-C(48)-F(144)	99.2(8)	F(153)-C(57)-F(51)	99.3(11)
F(145)-C(48)-F(144)	101.3(9)	F(151)-C(57)-C(53)	110.6(15)
F(44)-C(48)-F(144)	84.9(7)	F(52)-C(57)-C(53)	115.6(7)
F(46)-C(48)-F(144)	135.2(6)	F(152)-C(57)-C(53)	116.0(7)
F(45)-C(48)-C(45)	112.7(5)	F(53)-C(57)-C(53)	109.7(8)
F(146)-C(48)-C(45)	118.2(5)	F(153)-C(57)-C(53)	109.1(8)
F(145)-C(48)-C(45)	117.0(6)	F(51)-C(57)-C(53)	116.6(13)
F(44)-C(48)-C(45)	112.9(5)	F(156)-C(58)-F(155)	103.5(14)
F(46)-C(48)-C(45)	108.0(5)	F(156)-C(58)-F(54)	77.6(14)
F(144)-C(48)-C(45)	109.3(6)	F(155)-C(58)-F(54)	120.1(9)
C(52)-C(51)-C(56)	115.7(3)	F(156)-C(58)-F(56)	28.5(15)

F(155)-C(58)-F(56)	81.3(11)	C(27)-F(122)-F(23)	49.0(9)
F(54)-C(58)-F(56)	104.0(7)	F(144)-F(45)-C(48)	82.0(12)
F(156)-C(58)-F(55)	127.1(12)	F(144)-F(45)-F(146)	133.3(16)
F(155)-C(58)-F(55)	27.7(14)	C(48)-F(45)-F(146)	57.1(6)
F(54)-C(58)-F(55)	107.1(8)	F(146)-F(46)-C(48)	62.2(9)
F(56)-C(58)-F(55)	108.4(9)	F(146)-F(46)-F(145)	95.0(12)
F(156)-C(58)-F(154)	103.4(14)	C(48)-F(46)-F(145)	45.4(5)
F(155)-C(58)-F(154)	106.3(12)	F(45)-F(144)-C(48)	62.3(10)
F(54)-C(58)-F(154)	26.9(11)	C(48)-F(145)-F(46)	51.8(6)
F(56)-C(58)-F(154)	127.3(9)	F(46)-F(146)-C(48)	77.8(13)
F(55)-C(58)-F(154)	85.5(12)	F(46)-F(146)-F(45)	133.8(16)
F(156)-C(58)-C(55)	115.1(8)	C(48)-F(146)-F(45)	56.8(6)
F(155)-C(58)-C(55)	117.5(7)	F(154)-F(54)-C(58)	80.9(18)
F(54)-C(58)-C(55)	114.9(6)	F(154)-F(54)-F(156)	128(2)
F(56)-C(58)-C(55)	112.0(5)	C(58)-F(54)-F(156)	49.5(7)
F(55)-C(58)-C(55)	110.0(7)	F(155)-F(55)-C(58)	69.0(18)
F(154)-C(58)-C(55)	109.7(8)	F(156)-F(56)-C(58)	67.7(19)
F(121)-F(21)-C(27)	81(4)	F(156)-F(56)-F(155)	106(2)
F(122)-F(22)-C(27)	68(2)	C(58)-F(56)-F(155)	47.6(7)
F(122)-F(22)-F(121)	109(3)	F(54)-F(154)-C(58)	72.2(18)
C(27)-F(22)-F(121)	48.0(10)	F(55)-F(155)-C(58)	83(3)
C(27)-F(23)-F(122)	49.6(9)	F(55)-F(155)-F(56)	133(3)
F(21)-F(121)-C(27)	76(4)	C(58)-F(155)-F(56)	51.2(7)
F(21)-F(121)-F(22)	124(5)	F(56)-F(156)-C(58)	84(2)
C(27)-F(121)-F(22)	49.6(9)	F(56)-F(156)-F(54)	132(3)
F(22)-F(122)-C(27)	79(3)	C(58)-F(156)-F(54)	52.9(10)
F(22)-F(122)-F(23)	123(4)		

Table I.3. Selected bond lengths (Å) for complex **8-Me**.

Ni(1)-C(2)	1.978(2)	C(25)-C(26)	1.404(3)
Ni(1)-C(1)	2.001(2)	C(25)-C(28)	1.503(3)
Ni(1)-C(3)	2.007(2)	C(27)-F(21)	1.343(3)
Ni(1)-C(8)	2.1205(19)	C(27)-F(22)	1.347(2)
Ni(1)-C(5)	2.1392(18)	C(27)-F(23)	1.351(2)
Ni(1)-C(10)	2.1426(18)	C(28)-F(26)	1.327(3)
Ni(1)-C(7)	2.1857(19)	C(28)-F(24)	1.339(3)
Ni(1)-C(9)	2.1901(19)	C(28)-F(25)	1.343(2)
Ni(1)-C(6)	2.2563(18)	C(31)-C(32)	1.400(2)
C(1)-C(2)	1.405(3)	C(31)-C(36)	1.412(2)
C(2)-C(3)	1.402(4)	C(32)-C(33)	1.406(2)
C(2)-C(4)	1.498(3)	C(33)-C(34)	1.386(3)
C(5)-C(6)	1.427(3)	C(33)-C(37)	1.502(2)
C(5)-C(10)	1.433(3)	C(34)-C(35)	1.397(3)
C(5)-C(11)	1.514(3)	C(35)-C(36)	1.392(2)
C(6)-C(7)	1.414(3)	C(35)-C(38)	1.501(2)
C(6)-C(12)	1.516(3)	C(37)-F(31)	1.333(2)
C(7)-C(8)	1.435(3)	C(37)-F(32)	1.337(2)
C(7)-C(13)	1.514(3)	C(37)-F(33)	1.341(2)
C(8)-C(9)	1.418(3)	C(38)-F(36)	1.335(2)
C(8)-C(14)	1.520(3)	C(38)-F(34)	1.346(2)
C(9)-C(10)	1.417(3)	C(38)-F(35)	1.351(2)
C(9)-C(15)	1.513(3)	C(41)-C(42)	1.402(2)
C(10)-C(16)	1.512(3)	C(41)-C(46)	1.408(3)
B(20)-C(51)	1.644(3)	C(42)-C(43)	1.401(3)
B(20)-C(41)	1.646(3)	C(43)-C(44)	1.390(3)
B(20)-C(21)	1.648(3)	C(43)-C(47)	1.507(3)
B(20)-C(31)	1.656(2)	C(44)-C(45)	1.394(3)
C(21)-C(26)	1.400(3)	C(45)-C(46)	1.394(3)
C(21)-C(22)	1.408(3)	C(45)-C(48)	1.505(3)
C(22)-C(23)	1.394(3)	C(47)-F(41)	1.341(2)
C(23)-C(24)	1.396(3)	C(47)-F(43)	1.342(2)
C(23)-C(27)	1.500(3)	C(47)-F(42)	1.349(2)
C(24)-C(25)	1.382(3)	C(48)-F(44)	1.321(2)

C(48)-F(46)	1.342(2)	C(57)-F(53)	1.339(2)
C(48)-F(45)	1.349(3)	C(57)-F(52)	1.346(2)
C(51)-C(52)	1.399(2)	C(57)-F(51)	1.350(2)
C(51)-C(56)	1.412(2)	C(58)-F(57)	1.255(10)
C(52)-C(53)	1.403(3)	C(58)-F(54)	1.293(3)
C(53)-C(54)	1.386(3)	C(58)-F(59)	1.300(8)
C(53)-C(57)	1.504(2)	C(58)-F(55)	1.336(3)
C(54)-C(55)	1.396(3)	C(58)-F(56)	1.351(3)
C(55)-C(56)	1.392(3)	C(58)-F(58)	1.420(10)
C(55)-C(58)	1.505(3)		

Table I.4. Selected bond angles (°) for complex **8-Me**.

C(2)-Ni(1)-C(1)	41.33(10)	C(9)-Ni(1)-C(6)	80.06(7)
C(2)-Ni(1)-C(3)	41.19(10)	C(2)-C(1)-Ni(1)	68.46(13)
C(1)-Ni(1)-C(3)	71.62(11)	C(3)-C(2)-C(1)	113.3(2)
C(2)-Ni(1)-C(8)	142.10(9)	C(3)-C(2)-C(4)	122.2(3)
C(1)-Ni(1)-C(8)	161.76(12)	C(1)-C(2)-C(4)	123.5(3)
C(3)-Ni(1)-C(8)	103.43(9)	C(3)-C(2)-Ni(1)	70.50(13)
C(2)-Ni(1)-C(5)	129.31(8)	C(1)-C(2)-Ni(1)	70.20(13)
C(1)-Ni(1)-C(5)	105.04(10)	C(4)-C(2)-Ni(1)	118.71(16)
C(3)-Ni(1)-C(5)	168.11(11)	C(2)-C(3)-Ni(1)	68.31(12)
C(8)-Ni(1)-C(5)	83.18(7)	C(6)-C(5)-C(10)	120.27(17)
C(2)-Ni(1)-C(10)	146.91(8)	C(6)-C(5)-C(11)	119.55(18)
C(1)-Ni(1)-C(10)	105.93(9)	C(10)-C(5)-C(11)	120.12(18)
C(3)-Ni(1)-C(10)	152.47(11)	C(6)-C(5)-Ni(1)	75.57(10)
C(8)-Ni(1)-C(10)	70.01(7)	C(10)-C(5)-Ni(1)	70.57(10)
C(5)-Ni(1)-C(10)	39.12(7)	C(11)-C(5)-Ni(1)	128.09(14)
C(2)-Ni(1)-C(7)	126.74(8)	C(7)-C(6)-C(5)	118.97(17)
C(1)-Ni(1)-C(7)	159.30(12)	C(7)-C(6)-C(12)	120.41(19)
C(3)-Ni(1)-C(7)	110.02(10)	C(5)-C(6)-C(12)	120.53(19)
C(8)-Ni(1)-C(7)	38.90(8)	C(7)-C(6)-Ni(1)	68.74(10)
C(5)-Ni(1)-C(7)	68.92(7)	C(5)-C(6)-Ni(1)	66.66(10)
C(10)-Ni(1)-C(7)	82.12(7)	C(12)-C(6)-Ni(1)	135.41(15)
C(2)-Ni(1)-C(9)	157.07(8)	C(6)-C(7)-C(8)	120.04(17)
C(1)-Ni(1)-C(9)	128.87(10)	C(6)-C(7)-C(13)	120.9(2)
C(3)-Ni(1)-C(9)	121.75(10)	C(8)-C(7)-C(13)	119.08(19)
C(8)-Ni(1)-C(9)	38.36(8)	C(6)-C(7)-Ni(1)	74.17(11)
C(5)-Ni(1)-C(9)	69.47(7)	C(8)-C(7)-Ni(1)	68.10(10)
C(10)-Ni(1)-C(9)	38.15(7)	C(13)-C(7)-Ni(1)	131.20(15)
C(7)-Ni(1)-C(9)	68.89(7)	C(9)-C(8)-C(7)	120.34(17)
C(2)-Ni(1)-C(6)	122.73(8)	C(9)-C(8)-C(14)	119.77(19)
C(1)-Ni(1)-C(6)	127.55(12)	C(7)-C(8)-C(14)	119.86(19)
C(3)-Ni(1)-C(6)	135.44(11)	C(9)-C(8)-Ni(1)	73.48(11)
C(8)-Ni(1)-C(6)	68.57(7)	C(7)-C(8)-Ni(1)	73.01(11)
C(5)-Ni(1)-C(6)	37.77(7)	C(14)-C(8)-Ni(1)	126.94(15)
C(10)-Ni(1)-C(6)	68.59(7)	C(10)-C(9)-C(8)	119.26(17)
C(7)-Ni(1)-C(6)	37.08(7)	C(10)-C(9)-C(15)	120.04(19)

C(8)-C(9)-C(15)	120.62(19)	F(24)-C(28)-F(25)	105.27(17)
C(10)-C(9)-Ni(1)	69.11(10)	F(26)-C(28)-C(25)	112.64(17)
C(8)-C(9)-Ni(1)	68.16(11)	F(24)-C(28)-C(25)	112.61(18)
C(15)-C(9)-Ni(1)	133.49(16)	F(25)-C(28)-C(25)	112.77(17)
C(9)-C(10)-C(5)	119.90(17)	C(32)-C(31)-C(36)	115.93(15)
C(9)-C(10)-C(16)	118.83(18)	C(32)-C(31)-B(20)	125.60(15)
C(5)-C(10)-C(16)	121.27(17)	C(36)-C(31)-B(20)	118.39(15)
C(9)-C(10)-Ni(1)	72.74(11)	C(31)-C(32)-C(33)	121.85(16)
C(5)-C(10)-Ni(1)	70.31(10)	C(34)-C(33)-C(32)	121.17(16)
C(16)-C(10)-Ni(1)	129.65(14)	C(34)-C(33)-C(37)	119.46(16)
C(51)-B(20)-C(41)	106.44(14)	C(32)-C(33)-C(37)	119.31(16)
C(51)-B(20)-C(21)	110.63(14)	C(33)-C(34)-C(35)	117.90(16)
C(41)-B(20)-C(21)	113.17(14)	C(36)-C(35)-C(34)	120.94(16)
C(51)-B(20)-C(31)	111.59(14)	C(36)-C(35)-C(38)	121.49(16)
C(41)-B(20)-C(31)	111.39(14)	C(34)-C(35)-C(38)	117.57(16)
C(21)-B(20)-C(31)	103.74(13)	C(35)-C(36)-C(31)	122.19(16)
C(26)-C(21)-C(22)	116.00(16)	F(31)-C(37)-F(32)	106.19(16)
C(26)-C(21)-B(20)	124.22(16)	F(31)-C(37)-F(33)	106.19(17)
C(22)-C(21)-B(20)	119.30(15)	F(32)-C(37)-F(33)	106.08(17)
C(23)-C(22)-C(21)	121.94(17)	F(31)-C(37)-C(33)	112.78(15)
C(22)-C(23)-C(24)	120.91(17)	F(32)-C(37)-C(33)	112.01(16)
C(22)-C(23)-C(27)	121.12(18)	F(33)-C(37)-C(33)	113.04(16)
C(24)-C(23)-C(27)	117.97(17)	F(36)-C(38)-F(34)	106.85(16)
C(25)-C(24)-C(23)	118.23(17)	F(36)-C(38)-F(35)	106.34(15)
C(24)-C(25)-C(26)	120.76(17)	F(34)-C(38)-F(35)	105.90(15)
C(24)-C(25)-C(28)	119.61(17)	F(36)-C(38)-C(35)	113.81(15)
C(26)-C(25)-C(28)	119.58(17)	F(34)-C(38)-C(35)	111.54(15)
C(21)-C(26)-C(25)	122.15(17)	F(35)-C(38)-C(35)	111.90(15)
F(21)-C(27)-F(22)	106.51(17)	C(42)-C(41)-C(46)	115.57(16)
F(21)-C(27)-F(23)	106.87(17)	C(42)-C(41)-B(20)	125.32(16)
F(22)-C(27)-F(23)	106.24(16)	C(46)-C(41)-B(20)	119.06(15)
F(21)-C(27)-C(23)	113.37(16)	C(43)-C(42)-C(41)	121.92(17)
F(22)-C(27)-C(23)	111.57(16)	C(44)-C(43)-C(42)	121.32(17)
F(23)-C(27)-C(23)	111.84(17)	C(44)-C(43)-C(47)	119.96(17)
F(26)-C(28)-F(24)	106.0(2)	C(42)-C(43)-C(47)	118.69(16)
F(26)-C(28)-F(25)	107.01(19)	C(43)-C(44)-C(45)	117.86(17)

C(46)-C(45)-C(44)	120.50(17)	F(53)-C(57)-F(52)	106.78(15)
C(46)-C(45)-C(48)	118.92(17)	F(53)-C(57)-F(51)	106.56(15)
C(44)-C(45)-C(48)	120.56(17)	F(52)-C(57)-F(51)	105.19(15)
C(45)-C(46)-C(41)	122.78(17)	F(53)-C(57)-C(53)	112.85(15)
F(41)-C(47)-F(43)	106.94(17)	F(52)-C(57)-C(53)	112.06(15)
F(41)-C(47)-F(42)	105.40(16)	F(51)-C(57)-C(53)	112.86(15)
F(43)-C(47)-F(42)	106.12(16)	F(57)-C(58)-F(54)	125.1(6)
F(41)-C(47)-C(43)	112.82(16)	F(57)-C(58)-F(59)	110.7(6)
F(43)-C(47)-C(43)	112.89(16)	F(54)-C(58)-F(59)	64.0(6)
F(42)-C(47)-C(43)	112.11(16)	F(57)-C(58)-F(55)	32.0(7)
F(44)-C(48)-F(46)	106.92(17)	F(54)-C(58)-F(55)	108.1(3)
F(44)-C(48)-F(45)	107.67(18)	F(59)-C(58)-F(55)	131.9(5)
F(46)-C(48)-F(45)	104.14(16)	F(57)-C(58)-F(56)	73.2(7)
F(44)-C(48)-C(45)	113.65(16)	F(54)-C(58)-F(56)	105.4(3)
F(46)-C(48)-C(45)	112.56(17)	F(59)-C(58)-F(56)	44.9(7)
F(45)-C(48)-C(45)	111.31(17)	F(55)-C(58)-F(56)	103.8(2)
C(52)-C(51)-C(56)	115.94(16)	F(57)-C(58)-F(58)	105.2(7)
C(52)-C(51)-B(20)	125.42(15)	F(54)-C(58)-F(58)	38.8(6)
C(56)-C(51)-B(20)	118.65(15)	F(59)-C(58)-F(58)	101.9(5)
C(51)-C(52)-C(53)	121.86(16)	F(55)-C(58)-F(58)	76.9(7)
C(54)-C(53)-C(52)	121.32(16)	F(56)-C(58)-F(58)	136.3(5)
C(54)-C(53)-C(57)	119.76(16)	F(57)-C(58)-C(55)	116.2(6)
C(52)-C(53)-C(57)	118.83(16)	F(54)-C(58)-C(55)	114.8(2)
C(53)-C(54)-C(55)	117.70(17)	F(59)-C(58)-C(55)	113.5(4)
C(56)-C(55)-C(54)	121.02(17)	F(55)-C(58)-C(55)	112.3(2)
C(56)-C(55)-C(58)	118.95(17)	F(56)-C(58)-C(55)	111.65(19)
C(54)-C(55)-C(58)	120.03(17)	F(558)-C(58)-C(55)	107.9(5)
C(55)-C(56)-C(51)	122.12(17)		

Appendix II

Table II.1. X-ray crystallographic data for complexes **1a** and **2a**.

	1a	2a
Formula	C ₂₇ H ₂₉ Cl ₃ PSbF ₆ Pd	C ₂₅ H ₂₅ ClPSbF ₆ Pd
Formula Weight	832.97	734.02
Temperature (K)	173(2)	173(2)
Wavelength (Å)	0.71073	0.71073
Crystal System	Triclinic	Monoclinic
Space Group	P1	Cc
Unit Cell Dimensions	a = 11.0152(18)Å α = 107.230° b = 11.5158(19)Å β = 100.549(3)° c = 13.805(2)Å γ = 106.336(3)°	a = 20.7243(14)Å α = 90° b = 9.7381(7)Å β = 115.671(4)° c = 14.4872(10)Å γ = 90°
Volume	4544.34(17)Å ³	2635.2(3)Å ³
Z	2	4
D _{calcd} , mg/m ⁻³	1.801	1.850
Abs coeff, mm ⁻¹	1.831	1.925
F(000)	816	1432
Crystal size (mm ³)	0.15 x 0.15 x 0.10	0.20 x 0.15 x 0.10
Theta range (°)	1.61-28.01	2.18-28.10
Index range	-14 ≤ h ≤ 14, -15 ≤ k ≤ 15, -18 ≤ l ≤ 18	-27 ≤ h ≤ 27, -12 ≤ k ≤ 12, -18 ≤ l ≤ 19
Reflections collected	16512	20402
Independent Reflections	7370 [R(int) 0.0473]	6328 [R(int) 0.0615]
Completeness to theta = 28.01°	99.4%	99.5%
Absorption Correction	SADABS	SADABS
Refinement Method	Full-matrix least squared on F ²	Full-matrix least squared on F ²
Data/restraints/parameters	7370/0/353	6328/2/316
Goodness-of-fit on F ²	1.034	1.141
Final R indices [I > 2σ(I)]	R1 = 0.0457, wR2 = 0.1011	R1 = 0.0454, wR2 = 0.0945
R indices (all data)	R1 = 0.0763, wR2 = 0.1121	R1 = 0.0491, wR2 = 0.0959
Largest diff peak and hole	1.587; -1.105 e/Å ⁻³	1.051; -1.616 e/Å ⁻³

Table II.2. Selected bond lengths (Å) and angles (°) for complex **1a**.

Pd(1)-C(7)	2.160(5)	C(7)-Pd(1)-C(5)	67.0(2)
Pd(1)-C(6)	2.183(5)	C(6)-Pd(1)-C(5)	37.1(2)
Pd(1)-C(5)	2.275(5)	C(7)-Pd(1)-C(1)	169.7(2)
Pd(1)-C(1)	2.294(5)	C(6)-Pd(1)-C(1)	132.2(2)
Pd(1)-C(2)	2.340(5)	C(5)-Pd(1)-C(1)	103.2(2)
Pd(1)-P(1)	2.3506(12)	C(7)-Pd(1)-C(2)	135.9(2)
P(1)-C(31)	1.817(4)	C(6)-Pd(1)-C(2)	98.4(2)
P(1)-C(11)	1.821(4)	C(5)-Pd(1)-C(2)	76.2(2)
P(1)-C(21)	1.830(5)	C(1)-Pd(1)-C(2)	34.35(19)
Cl(1)-C(2)	1.741(6)	C(7)-Pd(1)-P(1)	96.33(16)
C(1)-C(2)	1.369(8)	C(6)-Pd(1)-P(1)	132.59(16)
C(2)-C(3)	1.493(8)	C(5)-Pd(1)-P(1)	157.45(15)
C(3)-C(4)	1.527(8)	C(1)-Pd(1)-P(1)	93.97(15)
C(4)-C(5)	1.503(8)	C(2)-Pd(1)-P(1)	124.75(14)
C(5)-C(6)	1.420(8)	C(31)-P(1)-C(11)	104.6(2)
C(5)-C(8)	1.497(8)	C(31)-P(1)-C(21)	102.6(2)
C(6)-C(7)	1.403(8)	C(11)-P(1)-C(21)	104.1(2)
C(11)-C(12)	1.388(6)	C(31)-P(1)-Pd(1)	114.82(14)
C(11)-C(16)	1.389(6)	C(11)-P(1)-Pd(1)	112.99(14)
C(12)-C(13)	1.382(7)	C(21)-P(1)-Pd(1)	116.24(15)
C(13)-C(14)	1.377(7)	C(2)-C(1)-Pd(1)	74.7(3)
C(14)-C(15)	1.382(7)	C(1)-C(2)-C(3)	126.0(6)
C(15)-C(16)	1.391(6)	C(1)-C(2)-Cl(1)	119.1(5)
C(21)-C(26)	1.385(7)	C(3)-C(2)-Cl(1)	113.9(4)
C(21)-C(22)	1.388(7)	C(1)-C(2)-Pd(1)	71.0(3)
C(22)-C(23)	1.386(8)	C(3)-C(2)-Pd(1)	107.9(4)
C(23)-C(24)	1.376(10)	Cl(1)-C(2)-Pd(1)	102.4(3)
C(24)-C(25)	1.369(9)	C(2)-C(3)-C(4)	110.8(5)
C(25)-C(26)	1.392(7)	C(5)-C(4)-C(3)	108.2(5)
C(31)-C(32)	1.389(6)	C(6)-C(5)-C(8)	121.6(5)
C(31)-C(36)	1.400(6)	C(6)-C(5)-C(4)	119.5(5)
C(32)-C(33)	1.381(6)	C(8)-C(5)-C(4)	117.7(5)
C(33)-C(34)	1.394(7)	C(6)-C(5)-Pd(1)	67.9(3)
C(34)-C(35)	1.368(7)	C(8)-C(5)-Pd(1)	99.8(4)
C(35)-C(36)	1.385(6)	C(4)-C(5)-Pd(1)	112.7(4)
Sb(1)-F(6)	1.850(4)	C(7)-C(6)-C(5)	120.4(6)
Sb(1)-F(3)	1.861(3)	C(7)-C(6)-Pd(1)	70.3(3)
Sb(1)-F(2)	1.863(3)	C(5)-C(6)-Pd(1)	75.0(3)
Sb(1)-F(5)	1.866(3)	C(6)-C(7)-Pd(1)	72.0(3)
Sb(1)-F(4)	1.869(4)	C(12)-C(11)-C(16)	119.1(4)
Sb(1)-F(1)	1.875(3)	C(12)-C(11)-P(1)	119.7(3)
C(41)-Cl(3)	1.727(7)	C(16)-C(11)-P(1)	121.1(3)
C(41)-Cl(2)	1.734(8)	C(13)-C(12)-C(11)	120.0(4)
C(7)-Pd(1)-C(6)	37.7(2)	C(14)-C(13)-C(12)	121.0(5)

C(13)-C(14)-C(15)	119.5(5)	C(35)-C(36)-C(31)	120.5(4)
C(14)-C(15)-C(16)	119.9(4)	F(6)-Sb(1)-F(3)	91.5(2)
C(11)-C(16)-C(15)	120.5(4)	F(6)-Sb(1)-F(2)	89.8(2)
C(26)-C(21)-C(22)	118.5(5)	F(3)-Sb(1)-F(2)	89.62(17)
C(26)-C(21)-P(1)	122.5(4)	F(6)-Sb(1)-F(5)	90.7(2)
C(22)-C(21)-P(1)	119.1(4)	F(3)-Sb(1)-F(5)	91.52(17)
C(23)-C(22)-C(21)	120.4(6)	F(2)-Sb(1)-F(5)	178.74(19)
C(24)-C(23)-C(22)	120.5(6)	F(6)-Sb(1)-F(4)	178.1(2)
C(25)-C(24)-C(23)	119.7(6)	F(3)-Sb(1)-F(4)	90.28(18)
C(24)-C(25)-C(26)	120.1(6)	F(2)-Sb(1)-F(4)	89.5(2)
C(21)-C(26)-C(25)	120.7(5)	F(5)-Sb(1)-F(4)	89.9(2)
C(32)-C(31)-C(36)	118.3(4)	F(6)-Sb(1)-F(1)	90.4(2)
C(32)-C(31)-P(1)	123.9(3)	F(3)-Sb(1)-F(1)	178.13(18)
C(36)-C(31)-P(1)	117.8(3)	F(2)-Sb(1)-F(1)	90.16(17)
C(33)-C(32)-C(31)	120.9(4)	F(5)-Sb(1)-F(1)	88.68(16)
C(32)-C(33)-C(34)	120.1(4)	F(4)-Sb(1)-F(1)	87.86(17)
C(35)-C(34)-C(33)	119.5(4)	Cl(3)-C(41)-Cl(2)	115.6(4)
C(34)-C(35)-C(36)	120.6(5)		

Table II.3. Selected bond lengths (Å) and angles (°) for complex **2a**.

Pd(1)-C(7)	2.129(7)	C(6)-Pd(1)-C(2)	102.9(3)
Pd(1)-C(6)	2.156(7)	C(5)-Pd(1)-C(2)	76.5(3)
Pd(1)-C(5)	2.203(7)	C(7)-Pd(1)-C(1)	167.8(3)
Pd(1)-C(2)	2.326(7)	C(6)-Pd(1)-C(1)	135.0(3)
Pd(1)-C(1)	2.326(6)	C(5)-Pd(1)-C(1)	102.4(3)
Pd(1)-P(1)	2.3429(16)	C(2)-Pd(1)-C(1)	33.5(3)
Cl(1)-C(2)	1.758(7)	C(7)-Pd(1)-P(1)	96.3(2)
P(1)-C(11)	1.818(6)	C(6)-Pd(1)-P(1)	131.2(2)
P(1)-C(31)	1.817(5)	C(5)-Pd(1)-P(1)	162.5(2)
P(1)-C(21)	1.825(5)	C(2)-Pd(1)-P(1)	120.83(18)
C(1)-C(2)	1.342(10)	C(1)-Pd(1)-P(1)	92.80(18)
C(2)-C(3)	1.524(10)	C(11)-P(1)-C(31)	103.5(3)
C(3)-C(4)	1.532(12)	C(11)-P(1)-C(21)	106.1(3)
C(4)-C(5)	1.490(11)	C(31)-P(1)-C(21)	105.1(3)
C(5)-C(6)	1.373(12)	C(11)-P(1)-Pd(1)	116.77(19)
C(6)-C(7)	1.417(11)	C(31)-P(1)-Pd(1)	112.1(2)
C(11)-C(12)	1.392(9)	C(21)-P(1)-Pd(1)	112.22(19)
C(11)-C(16)	1.410(8)	C(2)-C(1)-Pd(1)	73.2(4)
C(12)-C(13)	1.403(10)	C(1)-C(2)-C(3)	127.8(7)
C(13)-C(14)	1.369(11)	C(1)-C(2)-Cl(1)	118.1(5)
C(14)-C(15)	1.389(12)	C(3)-C(2)-Cl(1)	112.7(5)
C(15)-C(16)	1.358(10)	C(1)-C(2)-Pd(1)	73.2(4)
C(21)-C(22)	1.395(8)	C(3)-C(2)-Pd(1)	108.0(5)
C(21)-C(26)	1.411(8)	Cl(1)-C(2)-Pd(1)	101.5(3)
C(22)-C(23)	1.393(8)	C(2)-C(3)-C(4)	110.4(7)
C(23)-C(24)	1.372(9)	C(5)-C(4)-C(3)	106.9(6)
C(24)-C(25)	1.381(10)	C(6)-C(5)-C(4)	125.5(7)
C(25)-C(26)	1.383(9)	C(6)-C(5)-Pd(1)	69.8(4)
C(31)-C(32)	1.363(9)	C(4)-C(5)-Pd(1)	115.3(5)
C(31)-C(36)	1.382(9)	C(5)-C(6)-C(7)	119.2(7)
C(32)-C(33)	1.410(9)	C(5)-C(6)-Pd(1)	73.5(4)
C(33)-C(34)	1.377(12)	C(7)-C(6)-Pd(1)	69.6(4)
C(34)-C(35)	1.358(12)	C(6)-C(7)-Pd(1)	71.7(4)
C(35)-C(36)	1.389(9)	C(12)-C(11)-C(16)	118.5(6)
Sb(1)-F(2)	1.837(5)	C(12)-C(11)-P(1)	123.3(5)
Sb(1)-F(3)	1.856(5)	C(16)-C(11)-P(1)	118.1(5)
Sb(1)-F(6)	1.857(5)	C(11)-C(12)-C(13)	119.4(6)
Sb(1)-F(5)	1.863(5)	C(14)-C(13)-C(12)	120.9(7)
Sb(1)-F(1)	1.865(4)	C(13)-C(14)-C(15)	119.5(7)
Sb(1)-F(4)	1.869(5)	C(16)-C(15)-C(14)	120.6(7)
C(7)-Pd(1)-C(6)	38.6(3)	C(15)-C(16)-C(11)	121.0(6)
C(7)-Pd(1)-C(5)	67.5(3)	C(22)-C(21)-C(26)	118.5(5)
C(6)-Pd(1)-C(5)	36.7(3)	C(22)-C(21)-P(1)	122.4(4)
C(7)-Pd(1)-C(2)	141.4(3)	C(26)-C(21)-P(1)	118.8(4)

C(23)-C(22)-C(21)	120.2(5)	F(3)-Sb(1)-F(6)	90.8(3)
C(24)-C(23)-C(22)	120.5(6)	F(2)-Sb(1)-F(5)	92.0(3)
C(23)-C(24)-C(25)	120.1(6)	F(3)-Sb(1)-F(5)	91.0(3)
C(24)-C(25)-C(26)	120.4(6)	F(6)-Sb(1)-F(5)	176.4(4)
C(25)-C(26)-C(21)	120.3(5)	F(2)-Sb(1)-F(1)	88.9(3)
C(32)-C(31)-C(36)	118.5(6)	F(3)-Sb(1)-F(1)	179.4(3)
C(32)-C(31)-P(1)	121.8(5)	F(6)-Sb(1)-F(1)	89.1(3)
C(36)-C(31)-P(1)	119.7(5)	F(5)-Sb(1)-F(1)	89.1(3)
C(31)-C(32)-C(33)	122.0(7)	F(2)-Sb(1)-F(4)	178.8(3)
C(34)-C(33)-C(32)	117.4(7)	F(3)-Sb(1)-F(4)	88.1(3)
C(35)-C(34)-C(33)	121.6(7)	F(6)-Sb(1)-F(4)	87.7(3)
C(34)-C(35)-C(36)	119.8(8)	F(5)-Sb(1)-F(4)	89.2(3)
C(31)-C(36)-C(35)	120.5(7)	F(1)-Sb(1)-F(4)	91.4(3)
F(2)-Sb(1)-F(3)	91.7(3)		
F(2)-Sb(1)-F(6)	91.1(3)		